Order Number 1339234

Finite element analysis of continuous prestressed composite girders

Tong, Wenxia, M.S.

The University of Arizona, 1989

U·M·I
300 N. Zeeb Rd.
Ann Arbor, MI 48106

FINITE ELEMENT ANALYSIS OF CONTINUOUS PRESTRESSED COMPOSITE GIRDERS

by

Wenxia Tong

A Thesis Submitted to the Faculty of the
DEPARTMENT OF CIVIL ENGINEERING AND ENGINEERING MECHANICS
In Partial Fulfillment of the Requirements
For the Degree of
MASTER OF SCIENCE
WITH A MAJOR IN CIVIL ENGINEERING
In the Graduate College
THE UNIVERSITY OF ARIZONA

1990

STATEMENT BY AUTHOR

This thesis has been submitted in partial fulfillment of requirements for an advanced degree at The University of Arizona and is deposited in the University Library to be made available to borrowers under rules of the library.

Brief quotations from this thesis are allowable without special permission, provided that accurate acknowledgement of source is made. Requests for permission for extended quotation from or reproduction of this manuscript in whole or in part may be granted by the head of the major department or the Dean of the Graduate College when in his or her judgment the proposed use of the material is in the interests of scholarship. In all other instances, however, permission must be obtained from the author.

SIGNED: Wenxia Tong

APPROVAL BY THESIS DIRECTOR

This thesis has been approved on the date shown below:

Hamid Saadatmanesh

January 12, 1990

Hamid Saadatmanesh
Assistant Professor of Civil Engineering
and Engineering Mechanics

Date

Acknowledgements

I wish to express my sincere gratitude to my advisor Dr. Hamid Saadatmanesh for his encouragement, guidance and help throughout the length of my graduate studies.

Special thanks are also extended to the committee members Dr. Mohammad Ehsani and Dr. Panos Kiousis for their review and comments regarding this work.

TABLE OF CONTENTS

TABLE OF CONTENTS (Continued)

LIST OF FIGURES

LIST OF FIGURES (Continued)

LIST OF TABLES

ABSTRACT

Prestressing a steel girder reduces the required structural steel weight, limits tension stresses in the section, increases the ultimate strength, and increases the fatigue resistance. The technique of prestressing with tendons can be used for strengthening of existing bridges as well as for construction of new bridges.

This thesis presents an analytical study of the behavior of simply–supported and continuous prestressed composite girders and describes the benefits of prestressing steel in composite construction. Analytical models are developed and used as a basis for a computer program that calculates the stresses and displacements in the cables and the girder at discrete number of nodes along the length of the girder.

The effects of design variables such as prestress force, tendon profile, eccentricity and tendon length are studied. The results indicate that prestressing is an effective means of increasing the load carrying capacity of simple–span as well as continuous composite girders.

CHAPTER 1 — INTRODUCTION

1.1 Basic Concept

The concept of prestressed steel offers an effective solution for strengthening of existing composite steel–concrete girders, and an economical alternative for the design of new steel girders. Prestressing is accomplished by means of high–strength cables or bars anchored to the steel beam. Prestressing can be applied to single–span as well as continuous girders. Figs 1.1 and 1.2 show typical continuous prestressed composite steel–composite girders with straight, discontinuous and draped, continuous tendon profiles, respectively. In the positive moment region, the cables are located above the bottom (tension) flange; in the negative moment region, the cables are placed below the top (tension) flange.

The use of prestressing in steel structures is not to overcome tensile deficiencies of material, as is the case in prestressed concrete structures, but to induce initial stresses into the member that oppose the stresses caused by external loads. It may be said, in effect, that favorable residual stresses have been induced in the member, so that it can carry greater loads than its conventional counterpart.

Prestressing can be accomplished "externally", for example, by jacking the structure against the abutments or piers, or "internally", for example, by means of high-strength steel cables tensioned to induce initial stresses into the structure. The later case will be considered in this study.

Prestressing of steel structures by means of high–strength steel involves two basic phenomena. First, it introduces desirable internal stresses by tensioning the high–strength steel tendons against other parts of the structure; second, the initial tensioning in effect "prestrains" the high–strength steel so that it can be used at high levels of stress without excessive deformation.

The analysis of prestressed composite steel girders is different from that of the conventional, non-prestressed girders. The following additional factors must be considered in the analysis of prestressed composite girders: (1) because of the cable force prestressed steel girders have a higher degree of indeterminacy, for example, a simple–supported prestressed composite girder is internally statically indeterminate to the first degree; (2) the eccentric tendon force induces moments along the girder that changes in accordance to the eccentricity of the cable from the centroidal axis; (3) the force in the tendon increases proportionally with applied gravity loads and (4) the negative bending moments at the interior supports are reduced due to the increase in the tendon force.

The static analysis of prestressed composite girders presented in this study covers the elastic range of behavior of materials, and therefore, the principles of linear stress distribution and superposition are assumed to be valid. The analysis is based on the stiffness method and the mixed method, i.e., the combination of the stiffness and flexibility methods. The girders are modeled by a series of discrete plane–frame elements. The stiffness method is used to analyze girders with discontinuous tendons, as shown in Fig. 1.1. For this type of construction, The tendon is modeled with eccentric truss elements connected to nodes on the centroidal axis of the composite beam through rigid links at the ends of tendon segments. The degree of static indeterminacy is given by the number of reaction components plus the number of pairs of tendons on both sides of the web less the number of equations of static equilibrium. The mixed method is used to analyze girders with continuous cables, as shown in Fig.1.2. Neglecting the effect of friction between the girder and the cable at saddle points, the force in the cable remains constant throughout its length for this type of construction. The degree of static indeterminacy, in this case, is given by the number of reaction components plus one for the cable force minus the number of equations of static equilibrium.

It is noted that in both types of prestressed composite construction no shear is transfered between the cables and the girder along the girder length except at the anchorage points.

A computer program 'BRIDGE' was developed in FORTRAN for the VAX computer system to carry out the numerical calculations in the analysis. The solution gives the moment, shear, axial force and the corresponding strains and stresses along the girder at the nodal points. The method has been made general so that it can provide solutions to a wide variety of prestressed continuous composite girders.

Two design examples are also presented to demonstrate the benefits of prestressing for strengthening of existing bridges. A parametric study is performed to determine the most favorable tendon profile and stress distribution in the girders.

1.2 Review of Previous Analytical Studies

The concept of prestressed steel has been around for about 40 years. But, relatively few applications of this technique have been reported for strengthening of existing bridges and for construction of new structures.

Szilard (1959) developed equations for calculating the stresses in a simply supported composite girder prestressed with draped, high–strength cables, using the virtual work method. He considered prestressing the composite section after the concrete reached its prescribed cylinder strength. However, prestressing a composite section after the concrete has been cast produces undesirable tensile cracks in concrete. A better method would be to prestress the steel girder before the concrete is cast to prevent the concrete from going into tension. Therefore, a different approach to calculation of stresses is imperative.

Hoadley (1963) derived an expression for the increase in tendon force with applied load using the strain energy method for a simple–supported steel girder prestressed with two tendons of constant eccentricity. The behavior of single–span, conventional composite girders and prestressed composite girders were compared. The study of the numerical values revealed that the yield and ultimate moment ratios $M_{y'}/M_y$ and $M_{p'}/M_p$, in which $M_{y'}$ and $M_{p'}$ are the yield and ultimate moment capacities of the prestressed structure, respectively, and M_y and M_p are the yield and ultimate moment capacities of the conventional structure, respectively,

are not affected significantly by a change in slab dimensions or material properties. A comparison between linear versus draped prestressing tendons was made and it was concluded that the moment produced by the variable eccentric prestressing force more nearly canceled the moment produced by the applied load. A brief qualitative discussion of prestressed continuous composite girders was made through an example of a three span continuous girder with only the center span prestressed.

Regan and Krahl (1965) analyzed a series of simple–span composite sections, prestressed with tendons running below the tension flange with a constant eccentricity. A numerical analysis scheme, based upon the equilibrium of forces and compatibility of deformations for the entire range of loading up to failure was presented. This method was used to study the structural behavior of three groups of prestressed and conventional composite girders: (a) fourteen girders of configuration which might be found in a highway bridge; (b) eleven girders of configuration which might be found in a building; (c) three girders for which unpublished experimental results were available (Stras 1968). The following conclusions were drawn: (1) The effect of prestressing on the behavior of a composite girder is markedly different in some respects from the effect of the addition of a cover plate. Both significantly increase the following: the load producing the allowable steel stress, the load producing the yield stress, and the ultimate load. Prestressing only slightly increases the load producing the allowable concrete stress and the load producing the allowable live load deflection, while the addition of a cover plate increase both these loads to a much greater degree; (2) Large amounts of prestress force caused yielding over the support in some of the prestressed composite girders. This is undesirable and can be prevented by limiting the magnitude of prestressing force; (3) Prestressed composite girders behave nearly linearly until after the yielding of the steel girder. (4) The method of analysis reasonably approximates the behavior of conventional and prestressed composite girders throughout the entire range of loading up to failure.

Klaiber, Dunker, and Sanders (1982) discussed the feasibility of using post-tensioning to increase the strength of simple–span highway bridges made of steel girders and concrete slabs. A test was performed on a half–scale model of a 15.3

m (50 ft) long by 9.1 m (30 ft) wide four–beam bridge. Orthotropic plate theory and SAP IV were used to predict the behavior of the post–tensioned bridge. The analytical results correlated well with the experimental observations.

Troitsky, et al. (1988) introduced a method for the static analysis of continuous steel girders prestressed with continuous, high–strength steel cables. Their analysis was based on the flexibility and virtual work methods. The indeterminate structure was converted to determinate by assuming the redundants as the increase in tendon force caused by gravity loads and the negative bending moments at the interior supports. The simultaneous equations in terms of the unknown redundants were written as following:

$$\begin{bmatrix} d_{11} & d_{12} & \dots & d_{1j} \\ d_{21} & d_{22} & \dots & d_{2j} \\ \vdots & \vdots & \ddots & \vdots \\ d_{i1} & d_{i2} & \dots & d_{ij} \\ d_{x1} & d_{x2} & \dots & d_{xj} \end{bmatrix} \begin{Bmatrix} M_1 \\ M_2 \\ \vdots \\ M_i \\ X \end{Bmatrix} = \begin{Bmatrix} D_{1L} \\ D_{2L} \\ \vdots \\ D_{iL} \\ D_{x_L} \end{Bmatrix} \tag{1.1}$$

Where d_{ij} = displacement at support i caused by a unit couple at support j; D_{iL} = displacement at support i corresponding to applied service loads, M_i = bending moment at supports; d_{xj} = displacement in tendons caused by a unit couple at support j; D_{xL} = displacement in tendons corresponding to applied service loads; X = increase of tendon force.

The displacement coefficients were calculated by the virtual work method. Because the expressions for the displacements D_{iL} and D_{xL}, and the flexibility coefficients d_{ij} and d_{xj} depend on the applied loads and the cable layout, the equations presented in their method of analysis is restricted to only certain loadings and tendon profile. Therefore, it will be cumbersome to use this method for general cases.

They studied several examples of three–span prestressed composite steel girders of equal spans and unequal spans. It was concluded that a decrease in

negative bending moment results at the interior supports due to the effect of prestressing. The reduction in the negative moment varies with the number of spans, span length, cross sectional properties, etc.. Reductions of up to 20% in negative bending moments was achieved as a result of prestressing. The larger the span, the greater will be the reduction in negative bending moment and the higher the increase in the prestressing force due to the application of gravity loads.

Saadatmanesh, et al. (1989) developed analytical models and design methodologies for prestressed composite steel girders subjected to positive and/or negative bending moment based on the working stress and ultimate strength design methods. The proposed analytical models were verified with the test results of two girders, one subjected to positive bending moment and the other subjected to negative bending moment.

1.3 Objectives

The objectives of the present study are the following:

1. Formulate general analytical models for the elastic analysis of continuous, prestressed, composite girders based on the Finite Element Method.
2. Calculate the stresses and deflections at any desired sections of girders.
3. Investigate the advantages of prestressing by comparing the behavior of prestressed composite girders and coventional composite girders.
4. Examine the effects of design variables, such as prestress force, eccentricity, tendon profile, and the tendon length on the distribution of stresses in the girder.

An extensive literature search revealed several experimental studies of prestressed composite girders. In addition, a number of analytical studies of single span, prestressed composite girders were reported in the literature. However, only one study considered the behavior of multi-span, prestressed composite girders with draped continuous tendons. This study was restricted to certain tendon profiles and loading conditions and therefore, it can not be generalized. No study was

found on the behavior of prestressed continuous composite girders with straight discontinuous tendons (Fig.1.1).

CHAPTER 2—ANALYSIS

2.1 Finite Element Formulation

The elastic behavior of continuous prestressed composite girders is examined with the Finite Element Method. The girder is analyzed by considering it as a series of plane frame elements connected at their nodal points on the centroidal axis of the transformed composite section. The nodal points are located at the following positions: (1) supports; (2) anchorages or saddles; (3) concentrated loads (optional); (4) any other locations where stresses or deflections are desired.

In prestressed composite girders, the tendon force increases as a result of application of gravity loads. Therefore, in the analysis of this type of girders, the increase in the tendon force must be calculated and added to the initial prestressing force to obtain the total force in the tendon. Each pair of tendons in girders with discontinuous tendons is modeled with a plane truss element connected at its ends to the the nodal points on the centroidal axis of the transformed composite section through two rigid links, as shown in Fig.2.1. In this case, the degree of freedom of the system is given by the number of reaction components plus the number of pairs of tendons.

In girders with continuous tendons, the tendon is anchored at the girder's ends and can roll freely on the intermediate saddle points, for example, no shear is transfered between the tendon and the girder at saddle points (Fig.2.2). The tendon is modeled with continuous cable element, ie., an element that can resist axial tension force only. The cable is connected to the centroidal axis of the transformed composite section at the girder's ends through two rigid links. At each saddle point, the cable is supported by a rigid plane frame element (rigid link) that is fixed at one end to the centroidal axis and the other end connected to a roller (Fig.2.3). This will ensure that no shear is transfered between the girder and the cable at

saddle points, and that the force in the cable will remain constant throughout its length. In this case, the degree of freedom of the system is given by the number of reation components plus one for the cable force.

The following assumptions were made in the analysis: (1) materials obey Hook's law; (2) small deformations; (3) full composite action, ie., no slip between concrete slab and steel beam; (4) no shear deformations; (5) zero friction at saddle points.

2.2 Element Stiffness Matrix

Two types of elements are used in the analysis: plane frame element and plane truss element. The stiffness matrices of these elements are given in the following.

2.2.1 Plane Frame Element

The prestressed composite girder is modeled with a series of plane frame elements. The 6×6 stiffness matrix of the element is given by

$$[k_f] = \begin{bmatrix} \frac{EA}{L} & 0 & 0 & -\frac{EA}{L} & 0 & 0 \\ 0 & \frac{12EI}{L^3} & \frac{6EI}{L^2} & 0 & -\frac{12EI}{L^3} & \frac{6EI}{L^2} \\ 0 & \frac{6EI}{L^2} & \frac{4EI}{L} & 0 & -\frac{6EI}{L^2} & \frac{2EI}{L} \\ -\frac{EA}{L} & 0 & 0 & \frac{EA}{L} & 0 & 0 \\ 0 & -\frac{12EI}{L^3} & -\frac{6EI}{L^2} & 0 & \frac{12EI}{L^3} & -\frac{6EI}{L^2} \\ 0 & \frac{6EI}{L^2} & \frac{2EI}{L} & 0 & -\frac{6EI}{L^2} & \frac{4EI}{L} \end{bmatrix} \tag{2.1}$$

where A = area of element; L = length of element; and E = modulus of elasticity of element. The stiffness matrix, $[k_f]$, operates on nodal d.o.f. in the order listed in Fig.2.4a. The rigid plane frame member (rigid link) used to support and connect the cable to the centroidal axis of the girder has the same stiffness

matrix as the one given by Equation 2.1. The effect of high rigidity is incorporated by assuming large values for the axial rigidity EA and flexural rigidity EI.

2.2.2 Plane Truss Element

The cable in the girder with discontinuous tendons are modeled with plane truss elements. The corresponding 6×6 stiffness matrix in local coordinate is given by

$$[k_t] = \begin{bmatrix} \frac{EA}{L} & 0 & 0 & -\frac{EA}{L} & 0 & 0 \\ 0 & 0 & 0 & 0 & 0 & 0 \\ 0 & 0 & 0 & 0 & 0 & 0 \\ -\frac{EA}{L} & 0 & 0 & \frac{EA}{L} & 0 & 0 \\ 0 & 0 & 0 & 0 & 0 & 0 \\ 0 & 0 & 0 & 0 & 0 & 0 \end{bmatrix} \tag{2.2}$$

The stiffness matrix is then transformed into global coordinate system. The d.o.f. at nodes i and j of the truss element are made "slave" to the "master" d.o.f. at nodes 1 and 2 of the frame element respectively, as shown in Fig.2.4b. The d.o.f. at the nodes i and j of the truss element are related to the d.o.f. at the nodes 1 and 2 of the plane frame on the centroidal axis of the transformed composite section through the following equations.

$$\begin{Bmatrix} u_i \\ w_i \\ \theta_i \end{Bmatrix} = [\Lambda_1] \begin{Bmatrix} u_1 \\ w_1 \\ \theta_1 \end{Bmatrix} \tag{2.3}$$

$$\begin{Bmatrix} u_j \\ w_j \\ \theta_j \end{Bmatrix} = [\Lambda_2] \begin{Bmatrix} u_2 \\ w_2 \\ \theta_2 \end{Bmatrix} \tag{2.4}$$

where

$$[\Lambda_1] = \begin{bmatrix} 1 & 0 & -e_1 \\ 0 & 1 & 0 \\ 0 & 0 & 1 \end{bmatrix} \tag{2.5}$$

$$[\Lambda_2] = \begin{bmatrix} 1 & 0 & -e_2 \\ 0 & 1 & 0 \\ 0 & 0 & 1 \end{bmatrix} \tag{2.6}$$

e_1 and e_2 = eccentricities of cable at nodes i and j, respectively, measured from centroidal axis of transformed composite section.

The stiffness matrix $[k_t]$ is transformed into global coordinates by premultiplying it by $[\Gamma]^T$ and postmultiplying it by $[\Gamma]$, where

$$[\Gamma] = \begin{bmatrix} \Lambda_1 & 0 \\ 0 & \Lambda_2 \end{bmatrix} \tag{2.7}$$

therefore, the stiffness matrix of a plane truss element in global coordinates is given by

$$[k_T] = [\Gamma]^T [k_t] [\Gamma] \tag{2.8}$$

2.3 Force Displacement Relationship

The forces and displacements at the nodal points are calculated for girders with discontinuous tendons and girders with continuous tendons as explained in the following.

2.3.1 Discontinuous Cable

Once the stiffness matrix for each elements is formed, it is assembled into a global stiffness matrix $[K]$. The forces and displacements at the nodal points are then calculated with the following equation:

$$[K]\{D\} = \{R\} \tag{2.9}$$

where $[K]$ = assembled structure stiffness matrix; $\{D\}$ = nodal displacement vector; and $\{R\}$ = vector of external nodal forces.

The vector of nodal displacement $\{D\}$ is found accordingly from

$$\{D\} = [K]^{-1}\{R\} \tag{2.10}$$

2.3.2 Continuous Cable

In this case, the tension force in the cable is transfered to the girder only at the two anchorages. No shear force is transferred between the cable and the girder at saddle points. Therefore, neglecting the friction between the cable and the girder, the force in the cable will remain constant throughout its length during prestressing as well as when the external loads are applied. Also, during the prestressing opperation, or when the external loads are applied, there will be a relative sliding motion between the cable and the girder at saddle points. In other words, the deformations of the rigid links and the cable are not compatible at saddle points. Hence, due to the incompatibility of deformations, the cable can not be modeled as series of plane truss elements connectted to the girder at anchorages and saddle points.

Two approaches are presented for analyzing prestressed composite girders with continuous cables.

<u>Mixed Method:</u> In this method a compatibility equation is derived for the elongation of the tendon and a girder fiber at the level of the tendon. The girder fiber can be visualized as the shadow of the cable on the girder. The procedure is as follows: First, as shown in Fig.2.5a, the girder is transformed into a conventional continuous composite girder by cutting the tendon; Second, the relative displacement of the tendon ends at the cut due to the applied load is calculated. For the convenence of calculations, the ralative displacements of the ends of successive rigid links are calculated and added to obtain the total relative displacement at the location of the cut(Fig.2.5b). Third, a tendon force increment, due to applied gravity

load, ΔT, is applied to the cable nodes to close the gap, as shown in Fig.2.5c. The compatibility condition between the girder and cable requires that

$$\delta_P - \delta_1 \Delta T = \frac{L}{EA} \Delta T \tag{2.11}$$

or

$$\Delta T = \frac{\delta_P}{\delta_1 + \frac{L}{EA}} \tag{2.12}$$

where ΔT = increase in tendon force caused by external loads and; δ_P = total elongation of girder fiber at level of tendon due to applied loads; δ_1 = total elongation of girder fiber at level of tendon due to pairs of unit increment in tendon force (Fig.2.5c).

The elongations, δ_P and δ_1 are calculated from the analysis of the conventional girder as follows.

$$\delta_{P_i} = \sqrt{{L'_{ix}}^2 + {L'_{iy}}^2} - L_i \tag{11}$$

where

$$L'_{ix} = x_k - x_j + u_j + u_k \tag{12}$$

$$L'_{iy} = y_k - y_j + v_j + v_k \tag{13}$$

L_i = initial length of girder fibe between node j and k; L'_{ix} = horizontal projection of deformed girder fiber between nodes j and k; L'_{iy} = vertical projection of deformed girder fiber between nodes j and k; x_j and x_k = initial horizontal coordinates of nodes j and k; y_j and y_k = initial vertical coordinates nodes j and k; u_j and u_k = horizontal displacements of nodes j and k due to applied loads; v_j and v_k = vertical displacements of nodes j and k.

The total elongation of the girder fiber at the level of the tendon due to applied loads is calculated by adding the elongations of all cable segments.

$$\delta_P = \sum_{i=1}^{n} \delta_{P_i} \tag{2.16}$$

where n= number of cable segments; and δ_{P_i} = elongation of cable segment i due to applied load.

Similarly, δ_1 is calculated as

$$\delta_1 = \sum_{i=1}^{n} \delta_{1_i} \tag{2.17}$$

where δ_{1_i} = elongation of cable segment i due to pairs of unit increment in tendon force applied at all saddle points and anchorages.

The final solution is obtained by superimposing the solution of the conventional composite girder subjected to the external loads and the same composite girder subjected to the initial prestress force, T_i. The initial prestress force ia applied at all anchorages and saddle points as shown in Fig.2.5c.
where $T - i$ = initial prestress force.

Iterative Solution: Another approach for the analysis of girders with continuous cable involves an iterative finite element technique. In this method, the entire structure is analyzed in one step. The structure stiffness equation is given by

$$[K_b]\{U_b\} + [K_c]\{U_c\} = \{R\} \tag{2.18}$$

where $[K_b]$ = assembled stiffness matrix for plane frame elements, including rigid links connecting cable and girder; $[K_c]$ = stiffness matrix of cable; $\{U_b\}$ = displacement vector of girder and rigid links; $\{U_c\}$ = displacement vector of cable; and $\{R\}$ = vector of applied external loads.

The displacements of the girder and cable due to applied loads are decoupled to allow different displacements of cable and girder at saddle points.

Equation 2.18 can be written in the following way:

$$[K_b]\{U_b\} = \{R\} - [K_c]\{U_c\} \tag{2.19}$$

or

$$[K_b]\{U_b\} = \{R\} - \{R_c\} \tag{2.20}$$

$$\{R_c\} = \{1\}R_c \tag{2.21}$$

where $\{R_c\}$ = cable force, constant throughout.

Equations 2.20 is solved by an iterative scheme. Similar to the mixed method, a conventional continuous composite girder is considered here to find the elongation of the girder fiber at the cable level due to applied load and prestress force. The extended length of the cable is assumed to equal to this elongation. Its corresponding cable force is then calculated. A new stiffness equition 2.20 is setup based on the external loads and cable force. Therefore, a new displacement vector $\{U_b\}$ is calculated accordingly. This process is continued until tendon force $\{R\}$ converge to a specified tolerance value. The method and error criteria are described below.

(1) Iterate Equation 2.20 by first assuming a zero force in the cable $R_{c1} = 0$

$$[K_b]\{U_b\} = \{R\} \tag{2.22}$$

(2) From the displacement vector $\{U_b\}$, therefore, calculate strains for the girder fiber segments along the tendon profile and add them to find the total strain, ϵ_1, along the tendon's length

$$\epsilon_1 = \frac{1}{L}\sum_{i=1}^{n} \Delta L_i \tag{2.23}$$

where n = number of segments along tendon profile.

(3) Calculate a trial value for the force in the cable using the total strain, ϵ_1

$$R_{c1} = E\epsilon_1 A_c \tag{2.24}$$

(4) Substitute Equation 2.21 into 2.19 and an updated displacement vector calculated.

$$[K_b]\{U_b\}_1 = \{R\} - \{1\}R_{c1} \tag{2.25}$$

(5) The new vector $\{U_b\}_1$ is used to calculate a new cable force R_{c2}. Steps (2) to (5) are repeated untill the difference between successive cable forces becomes smaller than the specified to a tolerance value, ie.,

$$[K_b]\{U_b\} = \{R\} - \{1\}R_{ci-1} \tag{2.26}$$

$$|R_{cn} - R_{cn-1}| \leq \delta \tag{2.27}$$

where E = modulus of elasticity of cable; ϵ = strain of girder fiber at level of tendon; A_c = area of cable; δ = tolerance value; n = iterative number.

This approach has been used to check the previous method. And the results are same when the tolerance value is set appropriately.

2.4 Formation of Load Vector

After finding the joint stiffness matrix, the next step in the analysis is to consider the loads on the structure. The joint loads are placed into the vector $\{R\}$ directely, while the loads on the members are taken into account by calculating the fixed end actions that they produce. These fixed end actions may then be transfored into equivalent joint loads and combined with the actual joint loads on the structure. The support reactions for the structure subject to the combined loads $\{R\}$ are the same as the support reactions caused by the actual loads.

2.5 Element Stiffness Eqation

For an element, the stiffness equation is given by:

$$[k]\{d\} = \{r\} \tag{2.28}$$

where $[k]$ = element stiffness matrix; $\{d\}$ = vector of nodal displacements, known from the last step; and $\{r\}$ = vector of element nodal forces.

The forces at the nodes of an element can then be calculated by solving Equation 2.28

$$\{r\} = [k]^{-1}\{d\} \tag{2.29}$$

. In contrast to the support reactions for the structure, the member end-actions caused by the combined joint loads acting on the structure are not usually the same as those caused by the actual loads. Instead, the end-actions due to the actual loads

must be obtained by superimposing the equivalent joint loads and nodal forces $\{r\}$, from Equation 2.28, ie.,

$$[k]\{d\} = \{r\} - \{r_q\} \tag{2.30}$$

where $\{r_q\}$ = vector of equivalent joint loads.

2.6 Evaluation of Element Properties

As was stated in Chapter 1, it is better to prestress a steel beam before the concrete slab is cast to prevent the concrete from cracking under tension due to the negative moment induced by prestressing. Therefore, the stresses are calculated for this type of construction in this study. On the other hand, if a beam is prestressed after the concrete slab has been cast, the formulas can be used as well. The stresses at each node location are calculated from the following general equations:

Stresses in bars

$$f_b = \frac{T_s}{A_{bs}} \tag{2.31}$$

Stresses at the extreme fiber of top flange of steel beam

$$f_{st} = -\frac{M}{I}y - \frac{T_s}{A} \tag{2.32}$$

Stresses at the extreme fiber of bottom flange of steel beam

$$f_{sb} = \frac{M}{I}y - \frac{T_s}{A} \tag{2.33}$$

Stresses in concrete slab

$$f_{ct} = \frac{\alpha}{n}\left(\frac{M}{I_{tr}}y - \frac{T_s}{A_{tr}}\right) \tag{2.34}$$

where:

T_s = force in prestressing bars; M = effective moment resisted by composite section, this moment is equal to the moment due to applied load minus the counter acting moment produced by the prestressing force and/or the increment in the tendon force; $A = A_s$ = area of the steel beam when the steel beam alone carries loads; $A = A_{tr}$ = area of transformed composite

section when the composite section carries loads; A_{bs} = total bar area in steel beam; $I = I_s$ = moment of inertia of beam when the steel beam alone carries loads; $I = I_{tr}$ = moment of inertia of transformed composite section when composite section carries loads; $n = \frac{E_s}{E_c}$, modular ratio; $\alpha = 0$ when steel beam alone carries loads; $\alpha = 1$ when composite section carries loads.

As far as the sign convention is concerned the following has been adopted: (+) denotes tension, (-) compression; (+) moment causing tension in the bottom fiber, and (-) in the top fiber of the section.

CHAPTER 3 — COMPUTER PROGRAM

3.1 Programe and Main Flow Chart

Based on the theoretical analysis discussed in Chapter 2, two programs were developed in FORTRAN for the VAX computer system. The program BRIDGE analyzes prestressed composite girders with discontinuous cables using the stiffness method as well as prestressed composite girders with continuous cables using the mixed method. The program CONVER uses the iterative scheme discussed in Section 2.2 to check the program BRIDGE. The program BRIDGE can analyze prestressed composite girders with a wide variety of loading conditions and tendon profiles. The solution gives the moment, shear and axial force and the corresponding strains and stresses along the beam at node sections. The complete listings of the program BRIDGE are given in Appendix A.

The flow chart for the program BRIDGE is shown in Fig.3.1. The following section describes the function performed in each box in the flow chart.

1. The dimensions of the structure, number and type of elements, material properties and support restrain conditions are read and printed.
2. The applied forces, including prestress force, dead load and live load plus impact, are read and printed.
3. The stiffnesses of the frame elements and/or plane truss elements are formed. Structure nodes are located and assigned numbers, such as 1, 2, 3, etc., as shown in Fig.2.1. The nodes on each element are tagged with a structure node number to show where they are to be placed. One by one, elements are attached to the appropriate structure nodes. This is accomplished by subroutine STORE, for example, for girders with discontinuous tendons, i.e., NN = 1, where NN =1 defines calculation of girders with discontinuous tendons, and NN = any number other than one indicates calculation of

girders with discontinuous tendons. This step will carry out plane truss and frame element stiffness calculations and transfer the stiffness matrices of plane truss elements $[k_t]$ into $[k_T]$ associated with d.o.f. in the global coordinate system. The stiffness of plane truss element is then added up to the coresponding plane frame element stiffness to obtain the entire structure stiffness.

4. The structure stiffness Equation 2.9 is generated. The displacements vector $\{D\}$ contains only the unknowns and the load vector $\{R\}$ contains only the knowns. Subroutine EQSOLV applies the Gauss elimination method solving the equation $[K]\{D\} = \{R\}$.
5. The elongations of the girder fiber along the tendon due to applied load (N = 1) and the tendon unit force (N = 2) are calculated, respectively.
6. The components of the unit increment in tendon force in x and y direction in the right-hand system are calculated based on the geometry of the cable elements.
7. The increase in cable force is calculated according to Equation 2.12.
8. The structure displacements and reactions caused by applied loads and the increment in tendon force are combined. It is assumed that all calculations are within elastic range and the superposition principle is valid.
9. The stresses and strains in the composite girder are found based on the equations in section 2.4 and 2.5.
10. Displacements, stresses and strains at nodal points and tendon forces increment are printed.

The program BRIDGE for analyzing prestressed composite girders with discontinuous cables can also be used to analyze conventional composite girders simply by inputing zeros for variables pertaining to cables.

3.2 Program Evaluation

The program was used to analyze two girders for which experimental results were available. The results from the program are compared to the experimental results in the following.

The first girder was 4.57 m (15 ft) long. It had a 915 mm (36 in.) wide by 75 mm (3 in.) thick concrete slab, and was compositely connected to a $W360 \times 44.8$ ($W14 \times 30$) rolled girder of ASTM A588 high-strength low alloy steel. The beam was subjected to a positive bending moment, and was prestressed with two straight, 16 mm (5/8 in.) diameter Grade 150 DYWIDAG thread bars running 57 mm (2.25 in.) below the tension flange along the full beam length. Each bar was prestressed to 50% of its tensile strength or 152 MPa. Fig.3.2 shows the design details of the girder.

The second girder was 4.57 m (15 ft) long, had a 1070 mm (42 in.) wide by 90 mm (3.5 in.) in thick concrete slab connected compositely to the steel beam $W360 \times 44.8$ ($W14 \times 30$). The steel beam was prestressed with two 16 mm (0.63 in) diameter Grade 270 low relaxation 7-wire strands with a draped tendon profile. The strands were anchored in both ends at the centroidal axis of the composite section, 30 mm (1.2 in.) in below the top flange and 30 mm (1.2 in.) above the bottom flange between the loading points. The cable were anchored at the girder's ends and were also loaded with two concentrated loads placed symmetrically about the midpan 915 mm (36 in). The details of the girder are shown in Fig.3.3 (Ayyub et al. 1988).

The program BRIDGE was used to calculate the midspan deflection, stresses, strains in the girder and the increment of the tendon force of the girders. The girder with straight tendon was used to validate the program for analysis of girders with discontinuous tendons (stiffness method applied); and the girder with draped tendon was used to validated the program for analysis of girders with draped, continuous tendons (mixed method applied). The results are explained in the following.

Fig.3.4 shows the measured and calculated load vs. deflection at midspan of the test girder with straight tendon. The calculated curve correlated reasonably

well with the measured curve in the elastic region. The smaller slope of the measured curve can be attributed to imperfect composite action of the concrete slab and steel beam in the test girder. The larger difference between the two curves at higher values of the load is due to the yielding of the steel beam in the test girder which occured at a load of about 400 kN (90 kips). The sharp drop, shown on the measured curve, was due to a sudden slip at the concrete steel beam interface.

Fig.3.5 shows the calculated and measured load vs. strain in the tendon of the girder with straight tendon. The calculated and measured values are correlated well in the elastic region. The smaller strain, observed in the measured results, could partly be attributed to the decrease in the eccentricity of the tendon as the test girder deflected downward and the clearence between the tension flange and cable reduced.

Fig.3.6 shows with solid line the calculated load vs. strain curves in the tension flanges of the girder with straight tendon at midspan, while the curve with dashed line is the measured load vs. strain values in the tension flanges of the girder at midspan. The program solution of strain correlated well with the measured values in the elastic range.

Fig.3.7 shows the measured and calculated load vs. deflection at midspan of the test girder with draped tendon. The two curves correlated reasonably well in the elastic region. The smaller slope of the measured curve is due to imperfect composite action between the concrete slab and steel beam. At a load of about 450 kN (101 kips), the steel beam yielded. This resulted in a larger difference between the two curves.

Fig.3.8 shows the load–force curves in the strands of the girder with draped tendon. The force in the tendon was measured by means of a load cell at the anchorage. In this case, the measured values are slightly less than the calculated values. This could be due to several reasons, i.e. setting of anchorage chucks, slipage of strands in the cable, and the friction between the cable and the steel beam at saddle points in the test girder. The cable and the steel beam was ignored in the analytical models.

Fig.3.9 shows the measured and calculated load vs. strain in the tension flange at midspan of the test girder with straight tendon. The measured strains are smaller than the calculated values. This could be also related to the friction at saddle points which results in higher force in the mid–segment of the cable and smaller force in the outer segments. Higher prestressing force in the mid–segments of the cable results in lower stresses in the same segment of the tension flange.

The comparison of calculated results and experimental results of two girders with straight and draped tendon profiles indicated that the models of analytical methods predict the behavior of the girders with a reasonable accuracy.

CHAPTER 4 — PARAMETRIC STUDY

In this chapter, the behavior of two continuous, prestressed composite girders (girders A and B) are studied to examine the effects of design variables such as prestress force, eccentricity, and tendon length on the working load, tendon force and deflection. The effect of pattern loading is also studied in this chapter.

4.1 Example Girders

Girder A: This is a continuous girder with two equal spans of 19.5 m (64 ft) each. It consists of a $W775 \times 145$ ($W30 \times 90$) steel beam compositely connected to a 165 mm (6–1/2 in.) thick and 2.1 m (6 ft 11 in.) wide concrete deck. In the positive moment region, the deck is cast in place; in the negative moment region, precast, prestressed concrete deck panels are used. The steel beam is prestressed in the positive moment regions with two 25 mm (1 in.) diameter high–strength bars with constant eccentricity located above the tension flange in the positive moment regions. Fig.4.1 shows the cross section of the girder in the positive moment region. Fig.4.2a shows the model of girder A that was used in the analysis. The yield stress of the steel beam is $F_y = 345$ MPa (50 ksi); its allowable stress is $F_s = 190.3$ MPa (27.6 ksi). The yield stress of the prestressing bar is $F_y = 1034$ MPa (150 ksi) and its allowable stress is $F_s = 723.9$ MPa (105 ksi). Concrete with compressive strength $f'_c = 27.6$ MPa (4 ksi) is used for the deck. The allowable compressive stress of concrete is $F_c = 11.0$ MPa (1.6 ksi).The allowable stresses are calculated according to AASHTO Specifications (Standard 1983).

It is assumed that prestressing operation is performed after the concrete deck in the positive moment regions and precast, prestressed, concrete panels in the negative moment region are placed and compositely connected to the steel beam.

For the convenience of discussion, a uniformly distributed live load of 25 N/mm (1.7 k/ft) is considered acting on the girders through its length. This load is the largest load that can be applied to the girder without exceeding the allowable stresses before prestressing. Specifications in girder A before prestressing. It is noted that girder A is originally designed for the maximum moment at the interior support caused by this load. The load is applied through the entire length of girder A.

Girder B: This is a three span continuous girder with equal span lengths of 21.3 m (70 ft). The cross section and design details of this girder are same as those for girder A. Fig.4.2b shows the model of girder B which was used in the analysis. It is also assumed that the prestressing operation is performed after the concrete deck and the precast prestressed concrete panels are placed and compositely connected to the steel beam.

The uniformly distributed live load of 25 N/mm (1.7 k/ft), which produces the allowable steel stress at the interior supports of girder B before prestressing, is considered in the example. The load is applied to girder B over the first span and middle span to obtain the maximum negative moment.

4.2 Results and Discussion

The method of analysis and program BRIDGE explained in Chapter 2 are used in the study of the effects of prestress force, eccentricity, and tendon length on the behavior of girders A and B. These variables are explained in the following.

1. Prestress force: This force is assumed to vary from 0 to the allowable working load for the tendon. The following equation is used to calculate the maximum allowable tendon force.

$$T_{max} = (0.7F_y)A_s \tag{4.1}$$

where F_y = yield stress of tendon; A_s = area of steel bar.
Accordingly, T_{max} = 794 kN (178.5 kip).

2. Eccentricity: The eccentricity is measured from the centroidal axis of the transformed composite section. It is assumed to vary from 0 to 1.17h, where h is the height of the steel beam, within a practical limit, e_{max} = 89 mm (35 in.).
3. Length of prestressing tendon: The length varies from 12% to the full length of the span in each girder.
4. Load pattern: The load patterns shown in Table 4.1 and 4.2 are used for girders with discontinuous and continuous tendons, respectively.

In both girders, the stresses are calculated at the first interior support. The maximum deflection is calculated at the middle of the first span. Only the positive moment regions of the composite girders are prestressed.

The results of the parametric study are explained in the following sections.

4.2.1 Girder A

Prestress Force: The two high-strength bars are located symmetrically about the web, 50 mm (2 in.) below the bottom flange of the steel beam. The eccentricity is 762 mm (30 in.). The length of each bar is 9.75 m (32 ft), that is 1/2 of the span. The bars are anchored at points 4.9 m (16 ft) length from span ends.

The effect of variation of prestress force, expressed in the form of T/T_{max} (%), where T is the applied prestress force and T_{max} is the allowable force in tendon, is shown in Figs.4.3 and 4.4.

Fig.4.3 shows the increase in allowable load vs. the variation of prestress force. On the absissca T/T_{max} (%), the ratio of the applied prestress force to the maximum allowable prestress force is plotted. On the ordinate the increase in allowable load is plotted. The increase in allowable load is defined as $(w - w_0)/w_0$ (%), where w_0 is the maximum load that produces the allowable stress in the steel beam at the loaction of maximum moment (interior support)in the conventional girder and w is the maximum load that produces the allowable steel stress in the prestressed girder. When the girder is not prestressed, i.e. $T = 0.0$, the allowable load in the girder is increased by 4%. This is the result of the bars anchored to

the girder but not prestressed them. As the initial prestressing force increases, th allowable load increases linearly by up to 34.8%. The stresses in the concrete remain below thier allowable values when the uniform load w is applied.

Fig.4.4 shows the relationship between initial prestressing force and deflection at the center of span of girder A. The deflection ratio is given by δ/δ_0 (%), where δ is the deflection in the prestressed girder due to the live load; and δ_0 is the deflection of the conventional girder due to the applied load. When the girder is not prestressed, i.e. $T = 0.0$, the deflection is reduced by 5% as a result of the bars anchored to beam but not prestressed. As the magnitude of prestress force increase, the deflection reduces linearly. This reduction is due to camber induced by prestressing. The deflection is significantly reduced by up to 50%.

Eccentricity: In this case, the length of the tendon is 9.75 m (32 ft), 1/2 of the span; and the prestress force is held constant at 794 kN (178.5 kip), the allowable force of the tendon.

The effect of the variation of eccentricity, expressed in the form of e/h, where e is the eccentricity of the tendon measured from the centroidal axis of the transformed composite section, and h is the height of steel beam, appears in Figs.4.5, 4.6, and 4.7.

Fig.4.5, similar to Fig.4.3, shows the increase in the allowable load vs. increase in the eccentricity. Again, the increase in allowable load is defined by the ratio $(w - w_0)/w_0$ (%), where w_0 and w have the same definition as in Fig.4.3. Fig.4.5 shows that the increases in the allowable load is directly proportional to the increase in the eccentricity. The maximum increase of the allowable load is about 35.8%.

Fig.4.6 shows the curve of the increase in tendon force, $\Delta T/T_{max}$ (%), vs. the increase in the eccentricity. It is seen that there is a nonlinear relationship between these variables. This nonlinear relationship has also been observed for a single–span (Hoadly 1963). The relationship of ΔT and e for a single–span prestressed composite girder with straight tendons is given by

$$\Delta T = \frac{\frac{e}{L}\int_0^L M_x dx}{e^2 + \frac{EL}{E_t A_t} + \frac{I}{A}} \tag{4.2}$$

where M_x = moment due to applied load; e = eccentricity of tendon measured from the centroidal axis of transformed composite section; E = modulus of elasticity of steel beam; E_t = modulus of elasticity of tendon; L = length of tenon; I = moment of inertia of transformed composite section; A = area of transformed composite section; and A_t = area of tendon. The integral is the area under the moment diagram over the length of the tendon.

The maximum increase in the tendon force is 11.5% of the allowable force of the tendon. The uniform load of 25 kN/mm (1.7 k/ft) was applied on the girder when calculating the tendon force. However, depending on the magnitude of external loads and the geometry of the girde the ratio of $\Delta T/T_{max}$ could reach as higher values (Saadatmanesh et al. 1989). Therefore, for design purpose, considerations should be given to this effect, when selecting the magnitude of initial prestress force.

Fig.4.7 shows the eccentricity versus deflection curve for girder A. The deflection ratio is given by δ/δ_0 (%) again. The curve shows that the maximum deflection is significantly reduced by up to 56% in the girder when the eccentricity e reaches 1.17 times of the height of the steel beam.

Tendon Length : In this case, the prestress force equals its allowable value of 794 kN (178.5 kip). The eccentricity is held at 762 mm (30 in.). The length of the tendon is varied from 2.4 m (8.0 ft) to 19.5 m (64 ft), the full length of the span. The uniform load of 25 kN/mm (1.7 k/ft) was applied to the girder. The variation of the tendon length is the same for each span. The changing of of the length of the tendon is made for all span at the same time.

Figs.4.8, 4.9 and 4.10 summarize the effects of variation of tendon length, expressed in terms of L_t/L, where L_t is the length of the tendon and L is the span of the girder, on the increase in the allowable load, tendon force, and the reduction of the deflection for girder C, respectively.

Fig.4.8 shows the increase, in the ratio of $(w - w_0)/w_0$ (%) vs. L_t/L. Here the increase in the allowable load is plotted from a value of $L_t/L = 12\%$. Note that the increase in the allowable load is proportional to the increase in tendon length. Also, the maximum increase in the allowable load ratio is about 40% higher than those from changing the prestress force or the eccentricity.

Fig.4.9 is the plot of the increase in the tendon force, $\Delta T/T_{max}$ vs. the change of the length of the tendons. A nonlinear relationship exists between these variables. This nonlinear relationship can also be varified qualitatively with the expression obtained by Hoadly for single–span prestressed girders Eq.4.2. The maximum value of 9.2% is reached when the length of the tendon equals the full length of the span.

Fig.4.10 shows the deflection at the center of each span vs. the change in the tendon length. As the tendon length increases, the deflection decreases. The maximum reduction in the deflection reaches when the ratio of L_t/L is about 60%. For higher values of L_t/L, the reduction in the deflection is not as significant. Further studies of girders with different number of spans are needed to establish a relationship between the tendon length and span length for an optimum deflection control.

4.2.2 Girder B

Same aspects of the effect of variations of the prestress force, eccentricity and tendon length are studied for the three span continuous girder B. Same definations as those used for girder A are used in the discussion of girder B.

Prestress Force: The two prestress bars are located symmetrically about the web, 50 mm (2 in.) below the bottom flange of the steel beam in each span of the girder. The length of each bar is 10.7 m (35 ft), 1/2 of the span, anchored at 1/4 L from the span ends.

The effect of variation of the prestress force, again, expressed in the terms of T/T_{max} (%), is shown on Figs.4.11 and 4.12.

Fig.4.11 shows the increase in the allowable load defined by the ratio, $(w - w_0)/w_0$ (%), vs. the prestress force ratio. It is seen that the increase in the ratio of the allowable load can reach as high as 23.5% for this girder. The maximum increase in the allowable load is lower than that for the two span continuous girder A. Fig.4.12 shows the deflection vs. the initial prestress force ratio. It is seen from the curve that the deflection is also greatly reduced to about the same magnitude as the one in girder A.

Eccentricity: The length of the tendon is 10.7 m (35 ft). The prestress force is held constant at 794 kN (178.5 kip), the allowable force of the tendon. The effect of the variation of the eccentricity ratio, e/h, is summaried in Figs.4.13, 4.14, and 4.15.

Fig.4.13, similar to Fig.4.5 for girder A, presents the increase ratio in the allowable load, $(w - w_0)/w_0$ (%), vs. the eccentricity. It shows that changing the eccentricity produces an increase as high as 28.9% in the allowable load. It also shows a less increase in the allowable load than that for girder A due to changing the eccentricity. For instance, when e is at its maximum value, the increase in the allowable load for girder D is 28.9% and 35.8% for girder A.

Fig.4.14, similar to Fig.4.6, shows the relationship between the increase in the tendon force and the variation of the eccentricity. It is seen that the increase in the tendon force for girder B is higher than the one for girder C. When e/h is at its maximum, the increase in the tendon force, $\Delta T/T_{max}$ (%), is 14.9% for girder B and 11.5% for girder A.

Fig.4.15, similar to Fig.4.7, shows the relationship between eccentricity and deflection for girder B. The curve shows that the maximum deflection is significantly reduced by up to 47%, slightly less than the magnitude for girder A.

Length of Tendon: In this case, the prestressing force equals the allowable force in the tendon, and the eccentricity is held at 50 mm below the bottom flange of the steel beam in each span. The length of the tendon is varied from 2.6 m (8.5 ft) to 20.3 m (70 ft), the full length of span.

Figs.4.16, 4.17 and 4.18 summarize the effect of the variation of the tendon length on the change of the allowable load, tendon force, and the reduction of the deflection, respectively.

Fig.4.16 shows the plot of $(w-w_0)/w_0$ (%) vs.the length of the tendon. The maximum increase in the ratio of the allowable load is 49.5%. This is lower than 61.7% for girder A. However, this value (49.5%) is higher than those from changing the prestress force and the eccentricity.

Similar observations as those in Figs.4.9 and 4.10 for girder A can be made for increase in the tendon force and the decrease in the deflection for girder B in Figs.4.17 and 4.18, respectively.

4.2.3 Load Pattern

The effects of load pattern on the tendon force are also studied for girder A and D. Straight, discontinuous as well as draped, continuous tendon profiles are considered. A uniformly distributed live load of 25 kN/mm (1.7 k/ft) is assumed in the study.

Straight Tendon:

Fig.4.19 shows the models of girders A and B with straight, discontinuous tendons. The two 25 mm (1 in.) diameter bars are located 62 mm (2.5 in.) below the bottom flange of the steel beam in each span. The eccentricity, measured from the centroidal axis of the transformed composite girder, is 762 mm (30 in.). The tendon length equals 1/2 of the span in girders A and B.

Table 4.1 summarizes the change in the tendon force of girders A and B due to various load patterns. The change in the tendon force is expressed by the ratio, $\Delta T/T_{max}$. In girder A, when both spans are loaded the force in the tendons fo both spans increases by 10.2% of the allowable tendon force. However, when only one span is loaded, the force in the tendon of the loaded span increases by a higher percentage, 15.9%, while a prestress loss of 5.6% occures in the unloaded span. This phenomenon is due to the negative moment induced in the unloaded span as a result of the load on the adjacent span. The negative moment, causes an upward

deflections of the span which, in turn, results in inward moment of anchorages, and therefore, a loss of prestress force.

Load pattern 1, shown for girder B, results in equal increases of 14.9% in the exterior spans and a smaller increase of 4% in the middle span. The smaller increase in the tendon force in the middle span is due to the negative moment induced in the middle span by loads on the exterior spans. Load pattern 2 causes the highest increase (20.4%) in the tendon force of the exterior spans and the largest prestress loss in the middle span (–11%). Load pattern 3 results in the largest increase of the tendon force in the middle span. Pattern 4 increases the tendon forces in the first two spans and reduces the tendon force in the third span.

Draped Tendon: Fig.4.20 shows models of girders A and B with draped, continuous tendons. Neglecting the friction at saddle points, the force in the tendon remains constant throughout its length. The two 25 mm (1 in.) diameter bars are located 62 mm (2.5 in.) below the bottom flange of the steel beam in the positive moment region and 13 mm (0.5 in.) below of the top flange of the steel beam in the negative moment region. The maximum eccentricity, measured from the centroidal of the transformed composite girder, is 762 mm (30 in.) in the positive moment region, and 51 mm (2 in.) in the negative moment region. The tendon is continued within the top and bottom flanges of the steel beam.

Table 4.2 summarizes the change in the tendon force due to various load patterns. Load pattern 1 for girder A results in an increase of 9.2% in the tendon force, slightly less than that for straight tendon profile. Load pattern 2 causes an increase of 4.6% in the tendon force, significantly less than the 15.9% for the same girder with straight tendon. Also, due to continuity of the tendon, no loss of prestress occures in this case. A comparison of load patterns 1 through 4 for girder B indicates that the change in the tendon force is not as critically dependent on the load pattern as that for girder with straight, discontinuous tendons, but, it depends generally on the amount of load on the spans.

4.3 Prestressing Sequence

The effect of prestressing sequence is shown in Fig.4.21. The girder has the same number of spans and cross sectional properties as those for girder B. However, to show the effect of prestressing the negative moment regions, this girder is also prestressed over the interior supports, as shown in Fig.4.21a. A constant prestress force of 667 kN (150 kip) was used for all tendons.

Fig.4.21b shows the moments produced in the girder as a result of prestressing the positive moment region of the first span. Prestressing the positive moment region, induces negative moment in the girder between anchorages and positive moment over the first interior support. These moments oppose moments induced by gravity loads. The small, positive moment in the portion of the first span near the support, and negative moment over the last interior support will generally be offset when the portion of the girder over interior support is prestressed, as shown in Fig.14.c.

Fig.4.21c shows the moments induced in the girder as a result of prestressing the region over the first interior support. Prestressing induces positive moment between the anchorages over the support and negative moment in the interior regions of the adjacent spans. These moments oppose moments induced by gravity loads. Due to the smaller eccentricity of tendons over the interior supports, usually a higher prestress force is required to achieve the same counteracting moment produced by prestressing the positive moment region. This large compressive, prestress force may cause compression stresses in the bottom flange of steel beam over the interial supports that are larger than the tension stresses induced by prestressing. If this is the case, prestressing will be detrimental.

Fig.4.21d shows the moments in the girder caused by prestressing the positive moment regions of the interior span. Prestressing induces large negative moments between the anchorages and smaller positive moments over the interior supports.

The moment diagrams due to prestressing of all tendons are superimposed to calculate the final stresses in the girder due to prestressing.

CHAPTER 5 — DESIGN EXAMPLES

Prestressed composite girders can be used in new constructions as well as for strengthening of existing structures. The following two examples illustrate how two existing highway bridges which were originally designed for H15 truck loading can be upgraded to HS20 truck loading by prestressing the structural steel section in the girders. It is assumed that the prestressing operation is carried out at a time when the old deck is removed and before the new deck is placed. Therefore, the steel beams are prestressed before the concrete deck is cast.

5.1 Strengthening of Single–Span Bridge (Bridge A)

Bridge A is simple–supported and is 18.3 m (60 ft) long. The bridge was designed for the maximum positive moment due to H15 truck loading. The design parameters for the bridge are summarized by the following.

1. 7.3 m (24 ft) wide roadway.
2. Composite construction; rolled beam with concrete deck.
3. AASHTO H15 loading, to be upgraded to HS20.
4. Steel beam: four $W755 \times 145$ ($W30 \times 99$) beams spaced 2.1 m (6 ft 11 in) on centers; yield stress of the steel beam F_y = 345 MPa (50 ksi).
5. Concrete deck: 165 mm (6–1/2 in) thick; concrete compressive strength f'_c = 27.6 MPa (4,000 psi).
6. Diaphragms: spaced at 3 m (10 ft) intervals.

The dead load, carried by the steel beam alone, consists of the weight of the concrete deck, steel beam, and tendon: DL_1 = 10.4 N/mm (0.71 k/ft) per girder. The superimposed dead load, carried by the composite section, consists of the weights of the curbs and railing and is assumed to be distributed equally to the four girders by the deck slab and the diaphragms: DL_2 = 2.5 N/mm (0.17 k/ft) per girder. The live load plus impact, $LL + I$, is carried by the composite section.

The bridge is strengthed by prestressing each steel beam with two 25 mm (1 in) diameter high–strength DYWIDAG bars ("DYWIDAG" 1984). The prestressing bars are located 25 mm (1 in) above the tension flange of the steel beam. For the purposes of illustration, straight as well as draped tendon profiles are used and the resulting stresses are compared. For the draped tendons, seven–wire strands with total area equal to that of the two high–strength bars are used.

The girders are strengthened in the regions where the moment due to HS20 truck loading exceeds the maximum moment due to H15 truck loading. The cut–off points for straight tendons and bend points for draped tendons are selected using the moment envelopes as shown in Fig.5.1. The envelopes are obtained by moving the truck along the span at every tenth point. Accordingly, the anchorages for the straight tendons and bend points for the draped tendons are located at 2.75 m (9 ft) from each support. Fig.5.2 shows the cross section of the upgraded bridge. Fig.5.3 shows the models of the girders that were used in the analysis with straight and draped tendons.

The initial eccentric prestressing force T_i is selected so as to approximately offset the additional moment due to HS20 truck loading (Saadatmanesh et al. 1987). This force is a trial value and can be modified in the design iterations to result in more favorable stresses. Accordingly, for bridge A, each steel beam is prestressed with a force of T_i = 623 kN (140 kip)

The girder, acting as a beam–column, is subjected to bending and axial compression at the same time. Lateral stability requirements of the AASHTO Specifications (Standard 1983) are satisfied during prestressing as well as after application of loads.

The allowable stresses, calculated from the AASHTO equations, are as follows: Allowable stress of steel beam before the deck is compositely connected to the steel beam F_s = 183.4 MPa (26.6 ksi); after the deck is compositely connected to the beam F_s = 190.3 MPa (27.6 ksi); allowable tensile stress of concrete deck F_c = 2.6 MPa (0.4 ksi), allowable compressive stress of concrete deck F_c = 11.0 MPa (1.6 ksi); and allowable stress of steel bar F_t = 723.9 MPa (105 ksi), F_y = 1030 (150 ksi).

Table 5.1 summarizes the stresses and deflections in the bridge before and after strengthening.

5.2 Results (Bridge A)

It is seen from Table 5.1 that prestressing reduced the maximum stress (in the tension flange) by about 40%, for both tendon profiles. It is also seen that by adding bars to the composite girder alone the maximum stresses due to the dead loads ($DL_1 + DL_2$) are reduced by more than 20%. Prestressing greatly reduced the total deflection due to the induced initial camber. However, it is not efficient in reducing the live load deflection. Shear stresses do not present a limitation in this strengthenning technique. In fact, adding bars slightly reduces the shear stresses. For the girder with the draped tendon, there is an additional reduction in the shear stresses due to the vertical component of the force in the tendon.

The stress and deflection ratings of bridge A are satisfactory for H15 truck loading as can be seen from Table 5.2. However, they are unacceptable for HS20 truck loading. Prestressing the girders greatly increased the stress rating from H14.7 to HS28.9 for the straight tendons and from H14.7 to HS26.6 for the draped tendons. The deflection rating is reduced from HS22.5 to HS16 by prestressing the girder with the straight or the draped tendons.

The following equations are used to calculate the stress and deflection ratings, respectively.

$$stress\ rating = \frac{F_b - f_{DL} - f_t}{f_{LL+I}} \times truck\ load \tag{5.1}$$

$$deflection\ rating = \frac{\Delta_a}{\Delta_c} \times truck\ load \tag{5.2}$$

where F_b = allowable stress of steel beam; f_{DL} = total dead load stresses; f_t = initial compression stress in steel beam induced by prestressing; and f_{LL+I} = live load plus impact stress due to H15 and/or HS20 truck loading; Δ_a = allowable live

load plus impact deflection (given in AASHTO Article 10.62) = L/800 = 23 mm (0.9 in); and Δ_c = calculated live load deflection.

Comparison of Straight vs. Draped Tendon Layout: The stresses in the prestressed girder for the two tendon profiles are shown in Table 5.1. As noted in Fig.5.3, the cut–off points and bend points in both cases are located in the same positions. Table 5.1 shows that the stresses and deflections in the case of straight tendon are slightly smaller than those of the drapped tendon, while the tendon force is slightly greater in the draped tendon than the one with straight tendon. In this bridge, the difference in stresses and deflections did not seem to be significant for the two tendon layout.

An advantage of the girder with draped tendons is that the eccentricity of the tendon can be varied for load balancing purposes. The load carrying capacity is almost the same in the both cases. Since the purpose of prestressing is to decrease stresses and/or increase the load carrying capacity, as such, the choice of the tendon profile depends on the constructional convenience and cost efficiency.

5.3 Strengthening of Two Span Bridge (Bridge B)

The two span, continuous, composite bridge B had the same design details as those of bridge A, except each span is 19.5 m (64 ft) long. The girders were originally designed for the maximum negative moment at the interior support due to H15 truck loading. The bridge is strengthened by prestressing each steel beam with two 35 mm (1–3/8 in) high–strength DYWIDAG bars before the concrete deck is cast. Precast, prestressed concrete deck panels are used in the negative moment region to prevent cracking and to increase the stiffness of the girder over the interior support under service loads. Each 2.1 m (6 ft 11 in) wide, 165 mm (6–1/2 in) thick concrete panel in the negative moment region is concentrically prestressed with a total of 2,450 mm^2 (3.8 in^2) of 9.5 mm (3/8 in) diameter high–strength, seven–wire strands (ASTM A–416 Grade 250), distributed at 192 mm (7.5 in) on centers. The allowable stress for strands is F_t = 1,207 MPa (175 ksi). The total prestress force for each panel is 2,760 kN (620 kip). The initial compression

stress induced in concrete is 8.3 MPa (1.2 ksi). The following equation is used to calculate the stress in concrete due to the concentric prestressing force.

$$f_{ci} = \frac{F_i}{A_c + nA_s} \tag{5.3}$$

where F_i = prestressing force; A_c = area of concrete deck; A_s = area of strands; n = modular ratio.

The prestressing bars are located 25 mm (1 in) below the tension flange of the steel beam in the negative moment region and 25 mm (1 in) above the tension flange in the positive moment regions. Two different tendon layouts are used in the design — straight and draped. The cut–off or bend points are located according to the moment envelopes, as shown in Figs.5.4. Fig.5.5 shows the model of a typical girder in bridge B with straight and draped tendons.

Each steel beam is prestressed with a force of 555 kN (125 kip) per tendon, both in the positive and the negative moment regions.

Table 5.3 summarizes the stresses and deflections in the bridge before and after strengthening, respectively. Table 5.4 summarizes the stress and deflection ratings of bridge B. The stresses given in Table 5.3 are calculated at the locations of the midspan and the maximum negative moment.

5.4 Results (Bridge B)

It is seen from Table 5.3 that the stresses in the bridge for H15 truck loading are below their allowable values. However, for HS20 truck loading, the stresses in the steel beam in the positive moment region as well as in the negative mement region are significantly above their allowable values.

Prestressing the steel girders reduced the stresses in the steel beam to their allowable values. For example, prestressing reduced the stress in the compression flange of the girder at the interior support from 260.6 MPa (37.8 ksi) to 188.9 MPa (27.4 ksi) — below the allowable value of F_s = 190.3 MPa (27.6 ksi). In the positive moment region, the bottom (tension) flange renames in compression after all loads have been applied. This can help increase fatigue strength of girders

because steel in compression is not prior (?) to brittle fracture. The shear stresses are well below their allowable value and do seem to present a limitation on this strengthening technique. The midspan live load deflections are also below the allowable values. Maximum deflections are not shown in the table but their values are very close to those at midspan.

A comparison of stresses and deflections resulting from the two tendon profiles indicate that these values are not significantly different. Only, higher shear stresses due to the initial prestress force were observed for the girder with draped tendon. This is due to larger reactions developed as a result of prestressing in the girder with draped tendon. Therefore, the choice of tendon profile will generally depend on the construction convenience and cost.

The stress rating is increased from H14.5 to HS20.2 with the straight tendons, and from H14.5 to HS19.8 for the draped tendons. The deflection rating is reduced from H50 to HS25.

CHAPTER 6 CONCLUSIONS

Based on the comparison of the analytical results with available experimental results, design examples and the parametric study conducted, the following conclusions can be drawn.

1. The methods of analysis of prestressed composite girders developed in this study gives a reasonable accuracy and can be used to demonstrate the behavior of these structures through the elastic range of a variety of loading conditions.
2. The elastic analysis of continuous prestressed composite girders indicates that prestressing significantly increases the working load of this type of girders.
3. Prestressing positive moment regions will result in beneficial moments both in the positive and negative moment regions. These moments oppose moments induced by gravity loads. Prestressing negative moment regions will also result in beneficial moments in positive moment regions.
4. The increase in allowable load, for a composite girder with discontinuous tendons, is affected linearly to a considerable extent by the prestressing force, eccentricity, and the tendon length. The practical range for the eccentricity and the length of the tendon are somewhat limited; consequently, the value of prestress force has the greatest effect on the yield moment. As noted in the parametric study on girders A and B in chapter 4, with the same prestress force, increasing the length of the tendon produces a larger increase in the allowable load than does variation of the eccentricity. With the same allowable load for a conventional composite girder, the increase in allowable load by prestressing decreases with the number of the spans.

5. Prestressing reduces the dead load deflection of composite girders, because of the induced initial camber. However, it does not significantly reduce the live load deflection. Therefore, if the design of a composite girder is controlled by the live load deflection, prestressing is not appropriate.
6. The increase in tendon force due to external load application can reach as high as 20.4% of the prestress force in the case of a three–span continuous girder with discontinuous tendons, whereas the increase is only 10.5% in the same composite girder with continuous tendons. The tendon force may also be reduced to some extent (depending on load pattern and the tendon configuration) for the case of a composite girder with discontinuous tendon.
7. Prestressing a composite girder before the concrete deck is casted greatly increases the load producing the allowable steel stress, but does not significantly increase the load producing the allowable concrete stress. Thus, for an allowable stress design, prestressed composite girders will be efficient only if the concrete slab in negative moment region is prestressed and an initial compressive stress in the concrete is induced.
8. If the locations of cut–off or bend points in a prestressed composite girder are preselected, the load carrying capacity is almost the same in both the cases. Such choice will generally depend on the constructional convenience and cost efficiency.

In this paper, the presentation has been limited to single to three–span composite girders. The application of prestressing to more than three–span continuous composite girders as well as problems such as lateral stability during and after prestressing need to be further studied.

Table 4.1 Summary of Change in Tendon Forces of Girders A and B with Straight Tendon

load pattern		$\Delta T/T_{max}$ (%) span 1	span 2	span 3
1	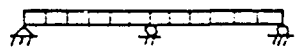	10.2	10.2	- - -
2	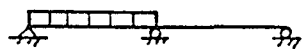	15.9	-5.6	- - -
1	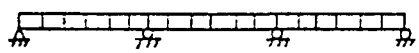	14.9	4.0	14.9
2		20.4	-11.0	20.4
3	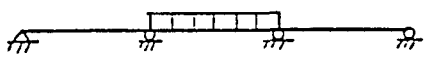	-5.5	14.9	-5.5
4	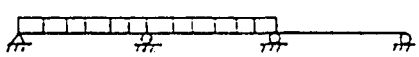	15.0	10.8	-4.2

Table 4.2 Summary of Change in Tendon Force of Girders A and B with Draped Tendons

load pattern		$\Delta T/T_{max}$ (%)
1		9.1
2	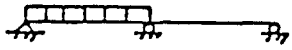	4.6
1	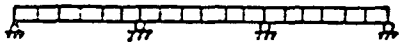	10.0
2	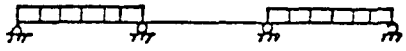	9.0
3	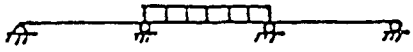	1.0
4	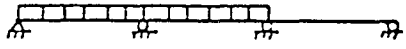	5.4

Table 5.1 Summary of Stresses and Deflections in Bridge A

Type of loading	Tension flange stress MPa(ksi)	Compression flange stress MPa(ksi)	Concrete deck stress MPa(ksi)	Tendon stress MPa(ksi)	Web shear stress MPa(ksi)	Maximum deflectioon mm(in)
Conventional Bridge A: H15						
DL_1	98.5 (14.3)	-98.5 (-14.3)	- - -	- - -	9.6(1.4)	45.5(1.79)
DL_2	17.3 (2.5)	-5.3 (-0.8)	-0.4(-0.1)	- - -	2.1(0.3)	5.3 (0.2)
$LL+I$	67.3 (9.8)	-5.1 (-0.7)	-2.8(-0.4)	- - -	12.4(1.8)	15.0(0.6)
TOTAL	183.1(26.6)	-108.9(-15.8)	-3.2(-0.5)	- - -	24.1(3.5)	65.8(2.6)
Conventional Bridge A: HS20						
DL_1	98.5 (14.3)	-98.5 (-14.3)	- - -	- - -	9.6(1.4)	45.5(1.79)
DL_2	17.3 (2.5)	-5.3 (-0.8)	-0.4(-0.1)	- - -	2.1(0.3)	5.3 (0.2)
$LL+I$	131.8(19.1)	-10.1 (-1.46)	-5.4(-0.8)	- - -	24.8(3.6)	30.1(1.2)
TOTAL	248.0(35.9)	-113.9(-16.5)	-5.8(-0.9)	- - -	36.5(5.3)	80.9(3.2)
Prestressed Bridge A: HS20; Straight Tendon						
T_i	-64.8(-9.5)	1.1 (0.2)	- - -	547.1(79.3)	0.0(0.0)	-17.3(-0.7)*
DL_1	75.3 (10.9)	-82.0(-11.9)	- - -	56.8 (8.2)	9.6(1.4)	29.0 (1.1)
DL_2	15.7 (2.3)	-5.4 (-0.8)	-0.5(-0.1)	12.3 (1.8)	2.1(0.3)	4.8 (0.2)
$LL+I$	120.7(17.5)	-10.9(-1.6)	-5.0(-0.7)	107.3(15.6)	24.8(3.6)	27.4 (1.1)
TOTAL	146.9(21.3)	-97.2(-14.1)	-5.5(-0.8)	723.5(104.9)	36.5(5.3)	43.9 (1.7)
Prestressed Bridge A: HS20; Continuous Tendon						
T_i	-64.0(-9.4)	0.8 (0.1)	- - -	549.0(79.6)	-8.3(-1.2)	-17.5(-0.7)*
DL_1	77.0 (11.2)	-82.3(-11.9)	- - -	45.4 (6.6)	10.3(1.5)	36.6 (1.4)
DL_2	13.9 (2.0)	-4.6 (-0.7)	-0.3(-0.1)	8.1 (1.2)	2.8(0.4)	4.3 (0.2)
$LL+I$	123.1(17.9)	-10.7(-1.6)	-5.0(-0.7)	82.6 (12.0)	26.2(3.8)	27.8 (1.1)
TOTAL	150.0(21.6)	-98.4(-14.3)	-5.3(-0.8)	685.1(99.4)	31.0(4.5)	51.2 (2.0)

* Negtive sign indicates upward deflection

Table 5.2 Summary of Stress and Deflection Ratings (Bridge A)

Type of girder	Truck loading	Stress rating	Deflection rating
Conventional	H15 HS20	H14.7 HS10.3	H22.5 HS15
Prestessed (straight)	HS20	HS28.9	HS16 HS16
Prestessed (draped)	HS20	HS26.6	

Table 5.4 Summary of Stress and Deflection Ratings (Bridge B)

Type of girder	Truck loading	Stress rating	Deflection rating
Conventional	H15 HS20	H14.5 HS8.9	H50 HS25
Prestessed (straight)	HS20	HS20.2	HS25 HS25
Prestessed (draped)	HS20	HS19.8	

Table 5.3 Summary of Stresses and Deflections in Bridge B

Type of loading	Tension flange stress MPa(ksi)	Compression flange stress MPa(ksi)	Concrete deck stress MPa(ksi)	Tendon stress MPa(ksi)	Web shear stress MPa(ksi)	Midspan deflectioon mm(in)
Conventional Bridge: H15 Truck						
DL_1	114.5(16.6)	-114.5(-16.6)	- - -	- - -	11.0(1.6)	20.8(0.8)
DL_2	20.1 (2.9)	-20.1 (-2.9)	-0.7(-0.1)	- - -	5.5(0.8)	2.5 (0.1)
$LL+I$	43.5 (6.3)	-57.7 (-8.4)	-2.1(-0.3)	- - -	11.7(1.7)	10.1 (0.4)
TOTAL	178.1(25.8)	-192.2(-27.9)	-2.8(-0.4)	- - -	28.2(4.1)	33.5(1.4)
Conventional Bridge: HS20 Truck						
DL_1	114.5(16.6)	-114.5(-16.6)	- - -	- - -	11.0(1.6)	20.8(0.8)
DL_2	20.1 (2.9)	-20.1 (-2.9)	-0.7(-0.1)	- - -	5.5(0.8)	2.5 (0.1)
$LL+I$	80.1 (11.6)	-126.1(-18.3)	-4.4(-0.6)	- - -	23.3(3.4)	20.1(0.8)
TOTAL	214.7(31.1)	-260.6(-37.8)	-5.1(-0.7)	- - -	39.8(5.8)	43.6(1.7)
Prestressed Bridge: HS20 Truck; Straight Tendon						
T_i	-142.0(-20.6)	41.4 (6.0)	- - -	584.1(84.7)	0.1(0.01)	-35.6(-1.4)*
DL_1	55.2 (8.0)	-88.3(-12.8)	- - -	89.7 (4.4)	10.8(1.6)	16.3 (0.6)
DL_2	11.7 (1.7)	-16.3(-2.4)	-0.6(-0.1)	6.9 (1.0)	5.3(0.8)	2.3 (0.1)
$LL+I$	71.7 (10.4)	-127.7(-18.2)	-4.2(-0.6)	61.4 (8.9)	23.0(3.3)	19.3 (0.8)
TOTAL	-3.4(-0.5)	-188.9(-27.4)	-4.8(-0.7)	683.0(99.0)	39.2(5.7)	2.3 (0.1)
Prestressed Bridge: HS20 Truck; Draped Tendon						
T_i	-141.4(-20.5)	40.7 (5.9)	- - -	578.6(83.9)	10.3(1.5)	-32.9(-1.3)*
DL_1	54.5 (7.9)	-86.9(-12.6)	- - -	24.2 (3.5)	10.9(1.6)	16.5 (0.7)
DL_2	11.7 (1.7)	-15.9(-2.3)	-0.6(-0.1)	4.2 (0.6)	5.5(0.8)	2.3 (0.1)
$LL+I$	71.0 (10.3)	-129.7(-18.8)	-4.1(-0.6)	37.0 (5.4)	23.4(3.4)	19.8 (0.8)
TOTAL	-4.15(-0.6)	-191.8(-27.8)	-4.7(-0.7)	644.0(93.4)	50.1(7.3)	5.7 (0.3)

* Negtive sign indicates upward deflection

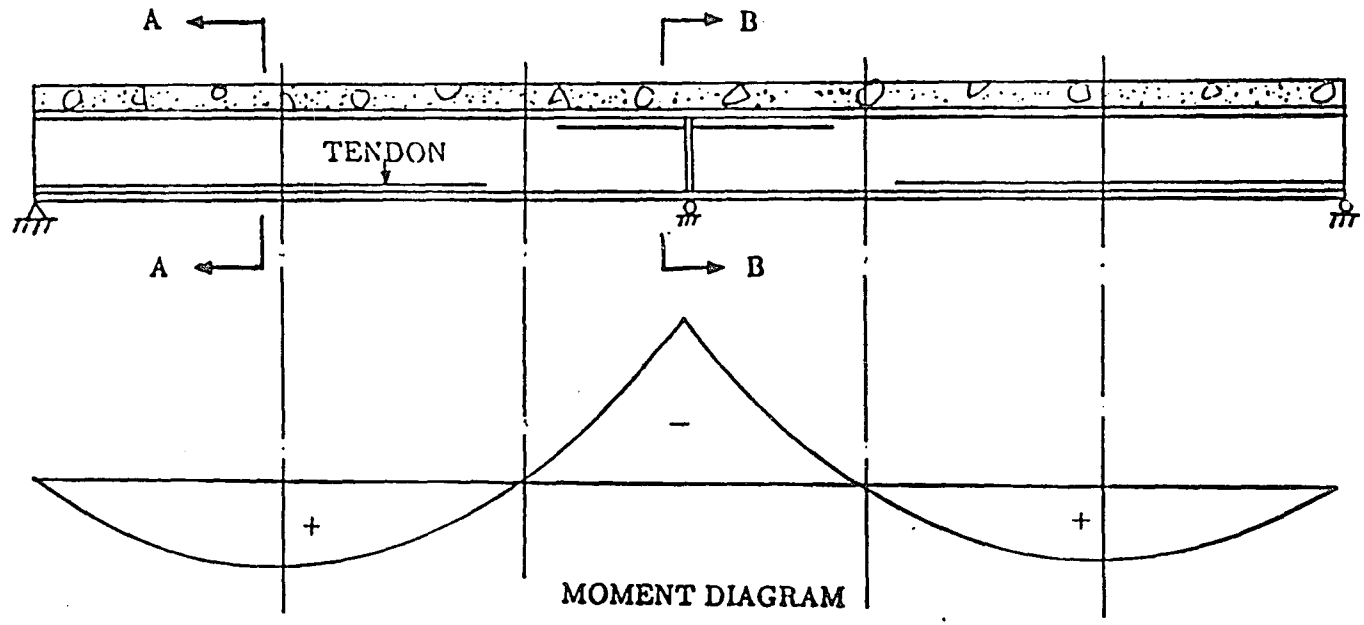

SECTION A—A SECTION B—B

Fig.1.1 Two Span Continuous Girder with Straight Tendon

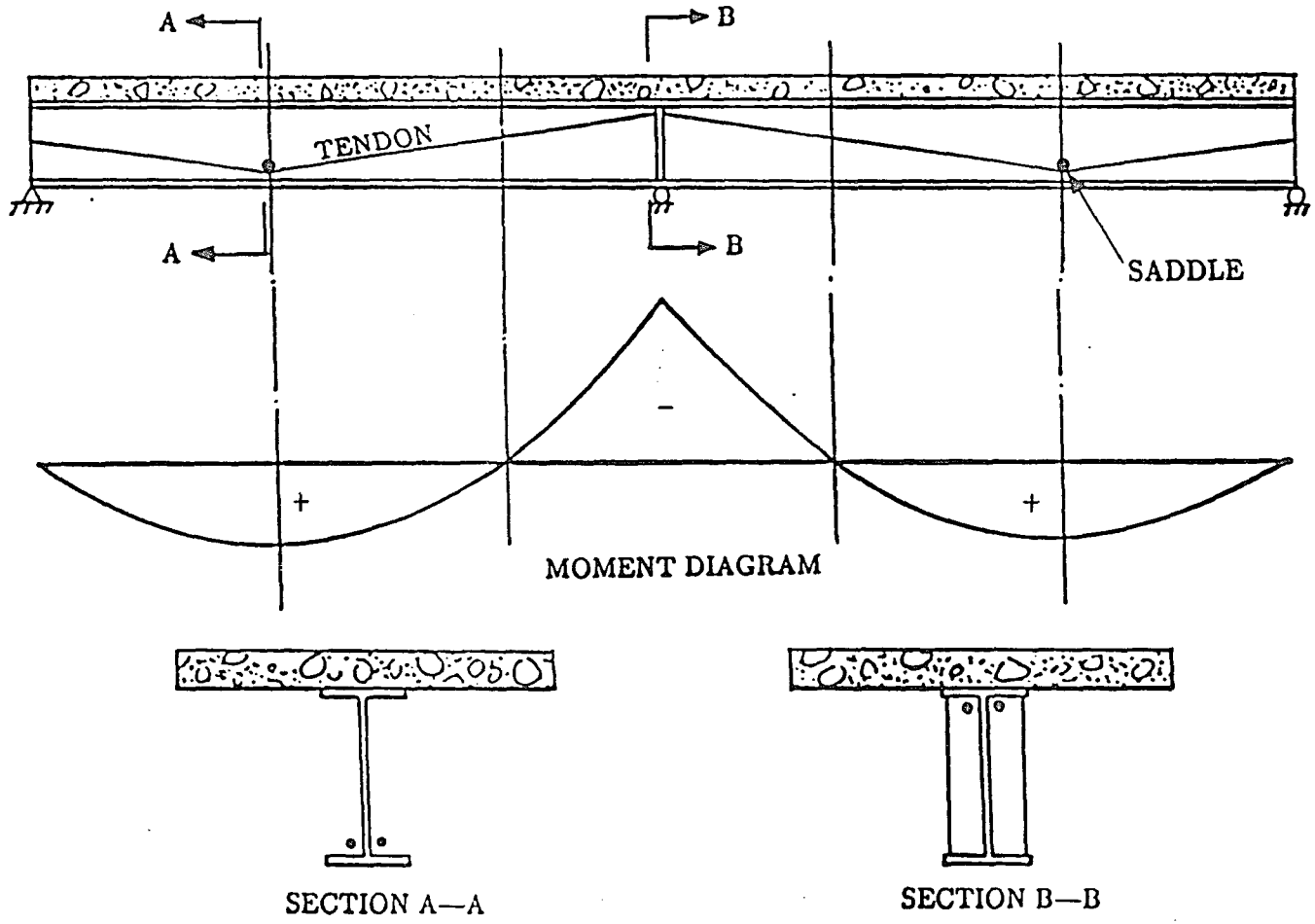

Fig.1.2 Two Span Continuous Girder with Draped Tendon

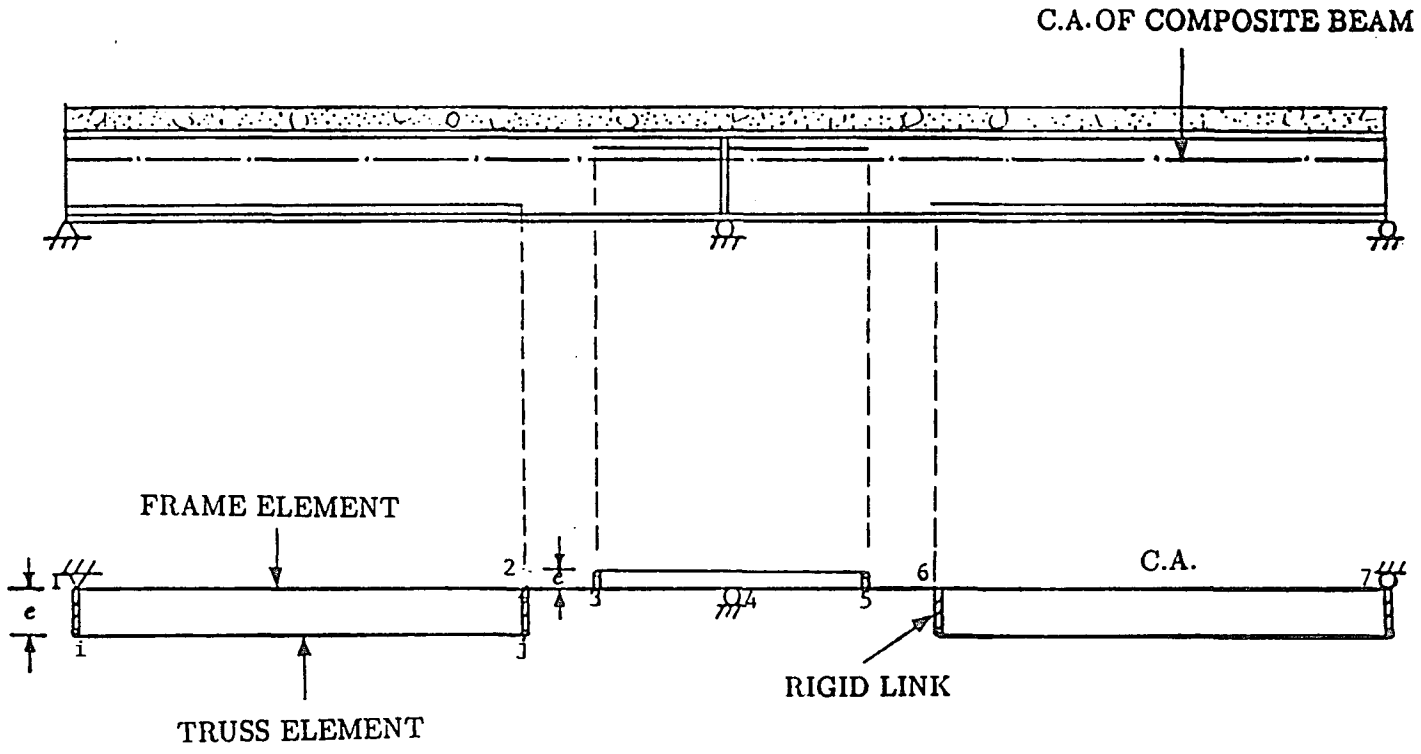

Fig.2.1 Model of Prestressed Composite Girder with Straight Discontinuous Tendon

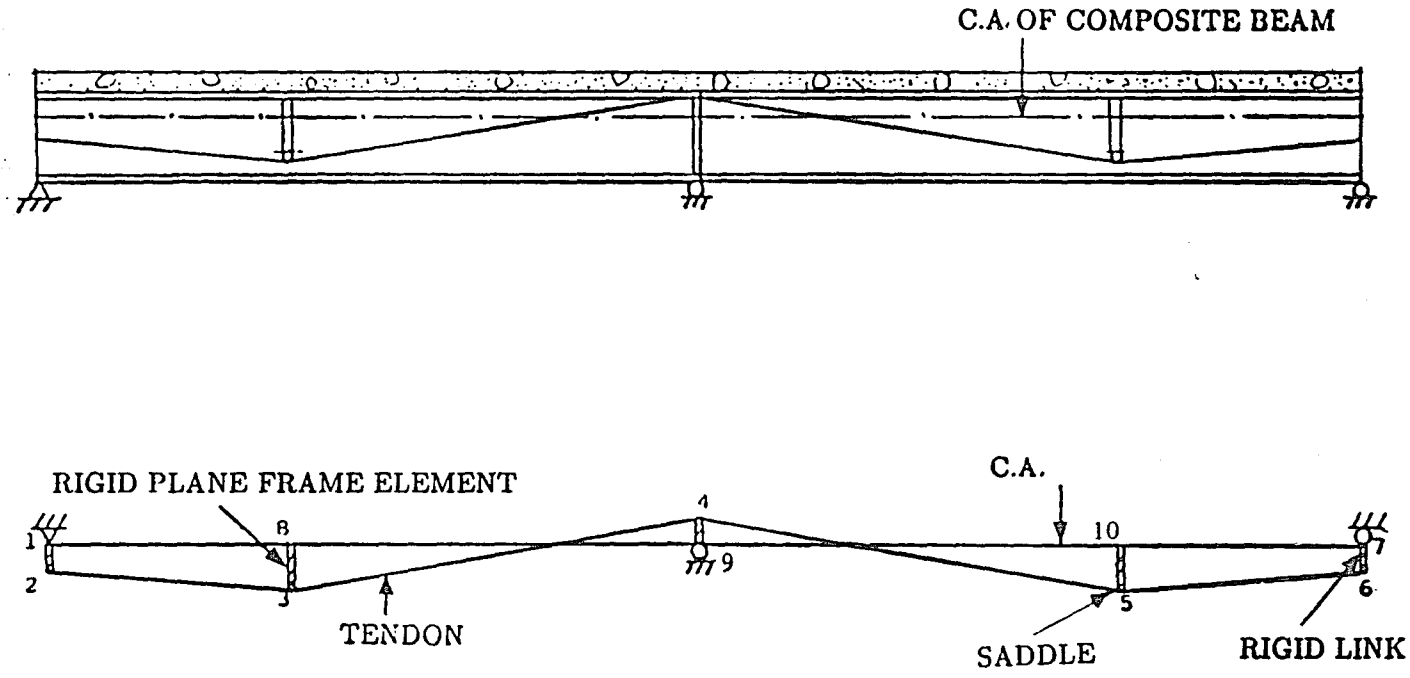

Fig.2.2 Model of Prestressed Composite Girder with Draped Continuous Tendon

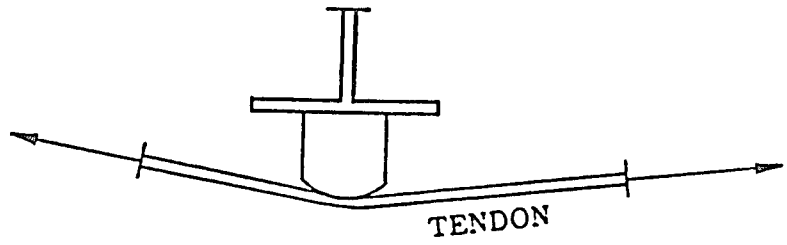

(a) TENDON SADDLE

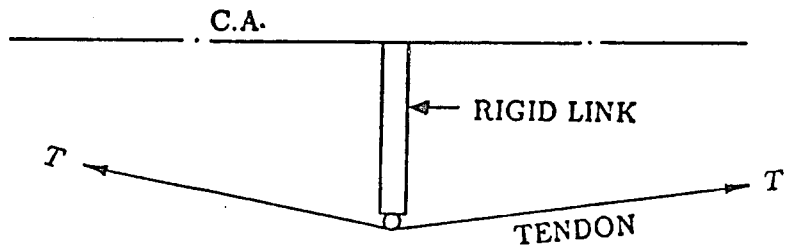

(b) CONNECTION OF TENDON AND GIRDER AT SADDLE

Fig.2.3 Tendon Saddle Detail

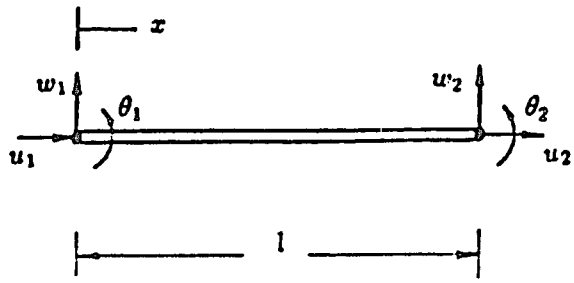

(a) FRAME ELEMENT WITH D.O.F. $\{d\} = \{u_1, w_1, \theta_1, u_2, w_2, \theta_2, \}$

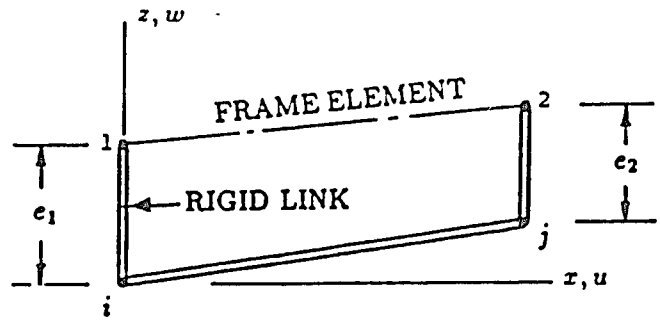

(b) NODES i AND j OF TRUSS ELEMENT ARE MADE SLAVE TO NODES 1 AND 2 OF FRAME ELEMENT BY RIGID LINKS $i1$ AND $j2$

Fig.2.4 Plane Frame and Truss Elements

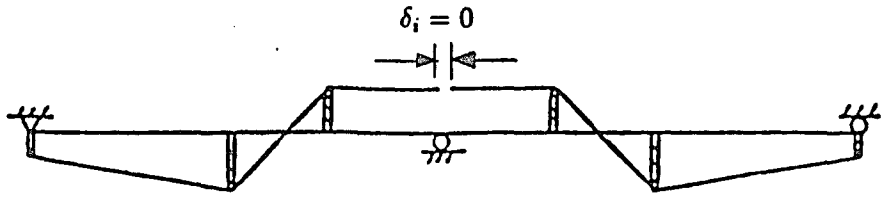

(a) CUT BARS TO MAKE CONVENTIONAL CONTINUOUS GIRDER

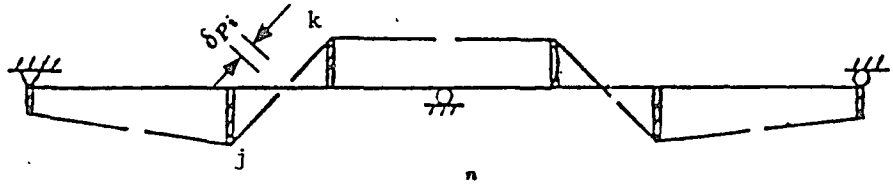

$$\delta_P = \sum_{i=1}^{n} \delta_{Pi}$$

(b) CALCULATE ELONGATION CAUSED BY APPLIED LOADS

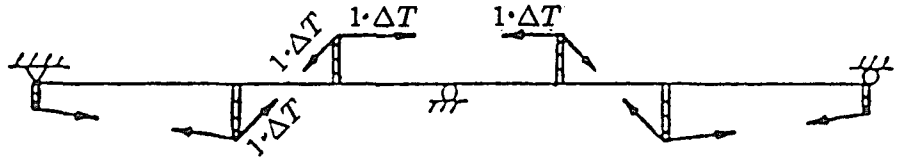

$$\delta_1 \Delta T = \Delta T \sum_{i=1}^{n} \delta_{1i}$$

(c) CLOSE GAP BY APPLYING A FORCE INCREMENT

$$\delta_P - \delta_1 \Delta T - \frac{L}{EA} \Delta T = 0$$

Fig.2.5 Increase in Tendon Force

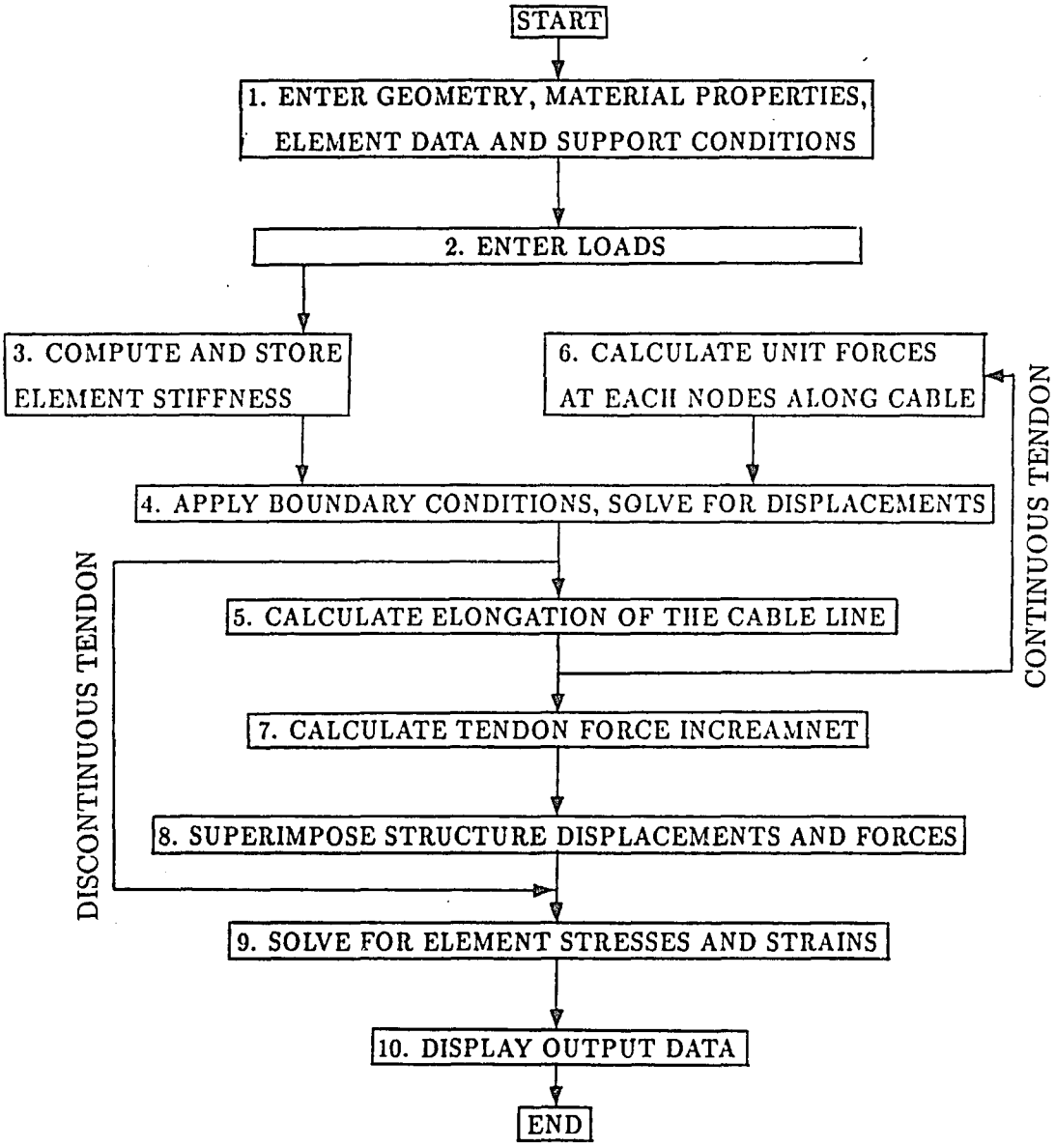

Fig.3.1 Main Flow Chart of Program BRIDGE

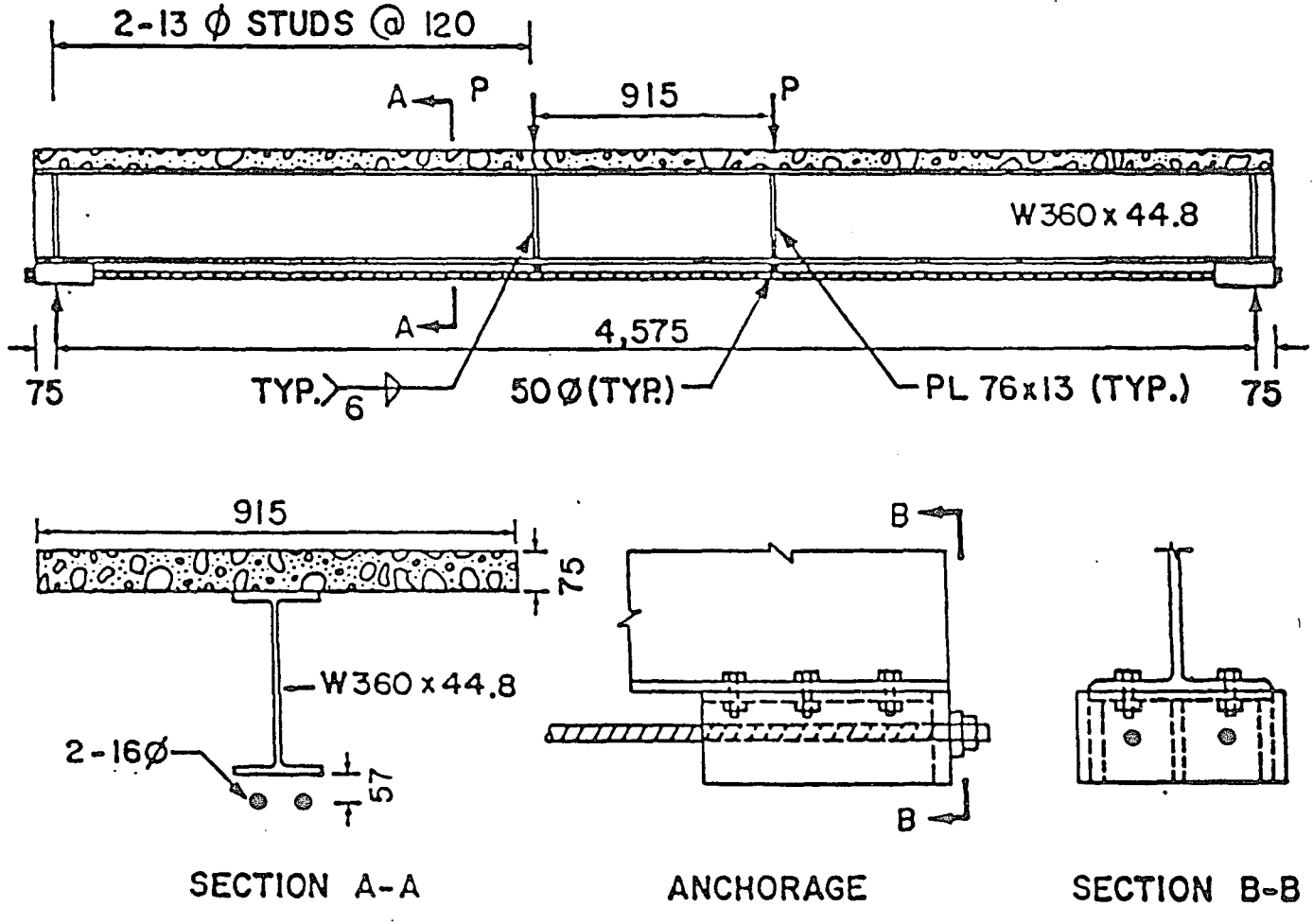

Fig.3.2 Test Girder with Straight Tendon

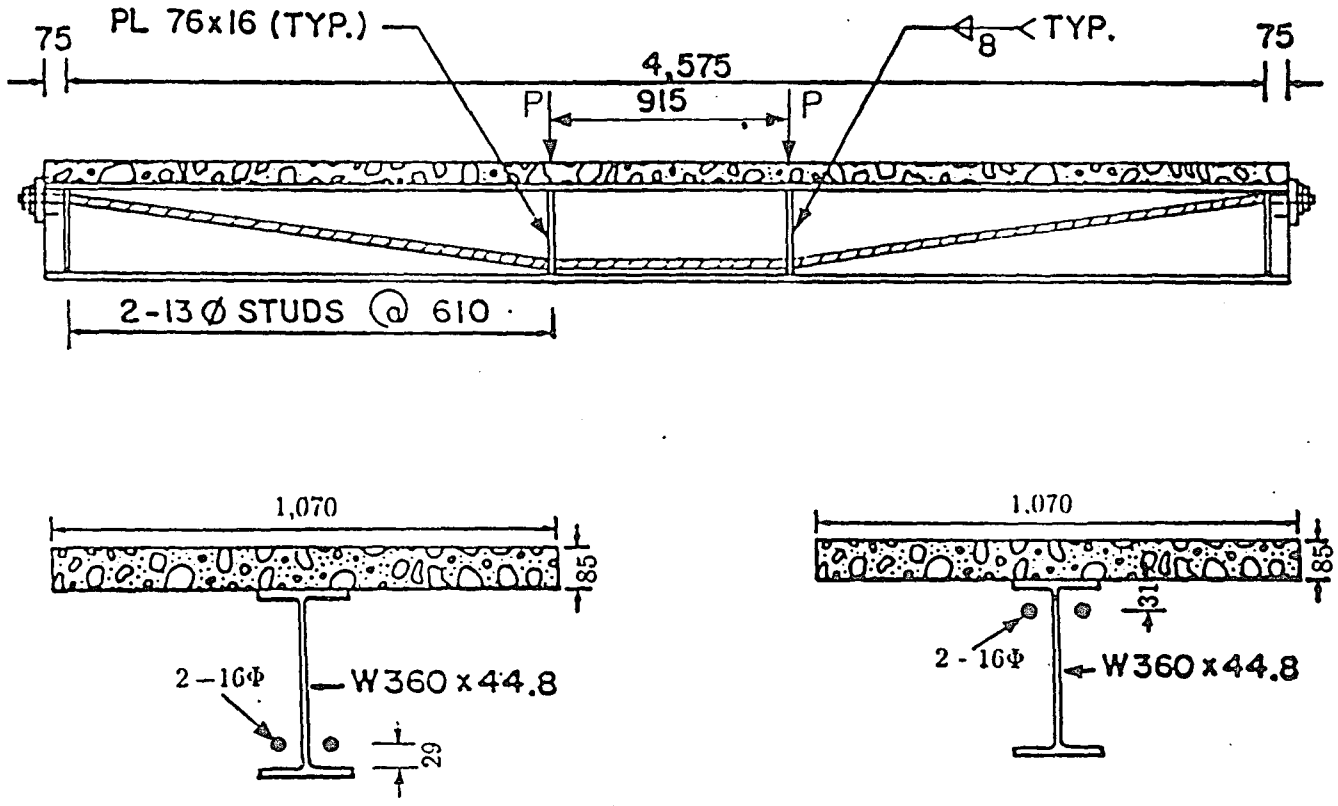

Fig.3.3 Test Girder with Draped Tendon

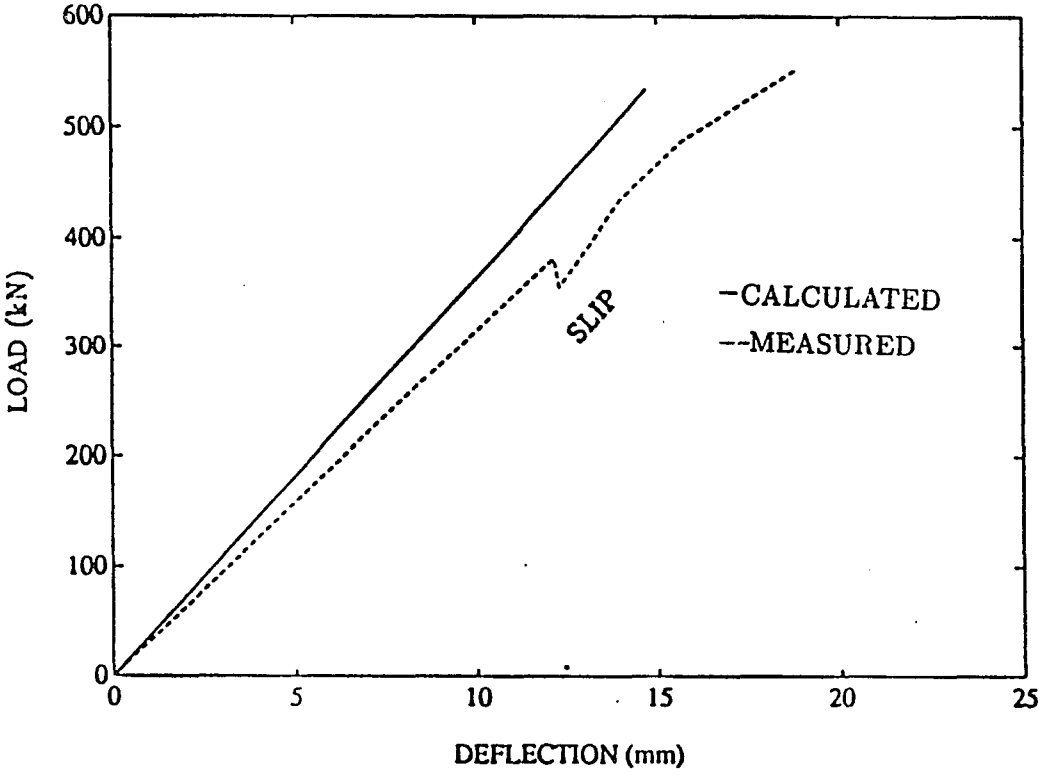

Fig.3.4 Measured and Calculated Load vs. Deflection at Midspan of Girder with Straight Tendon

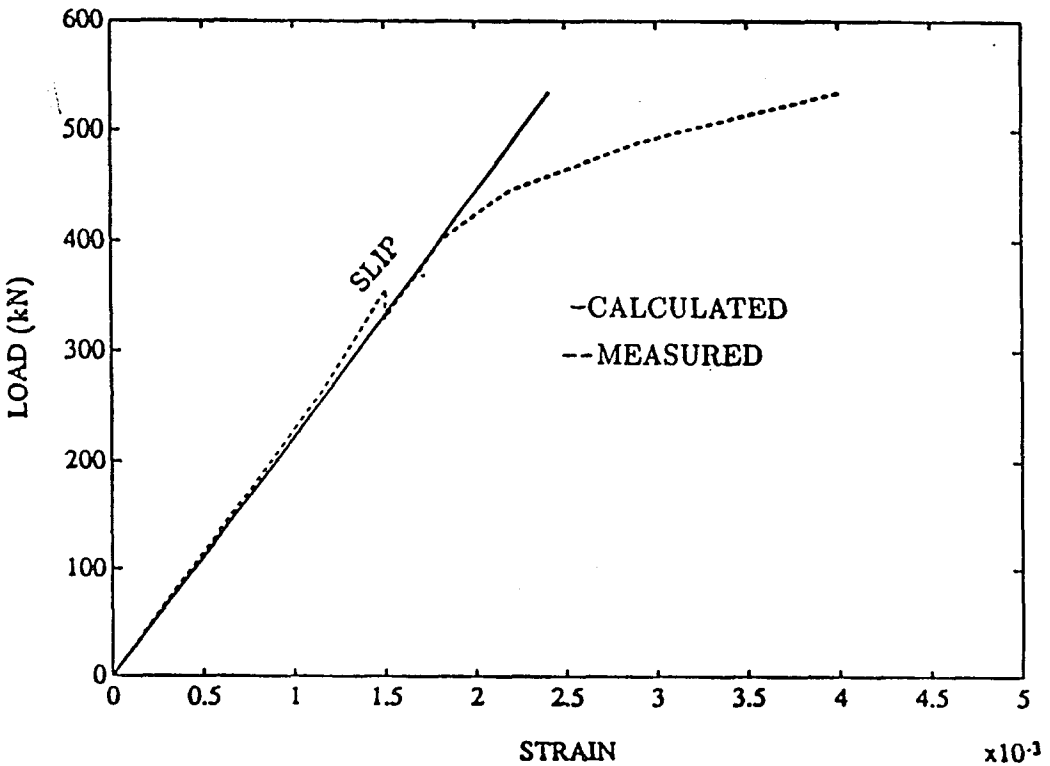

Fig.3.5 Measured and Calculated Load vs. Strain in Tension Flange at Midspan of Girder with Straight Tendon

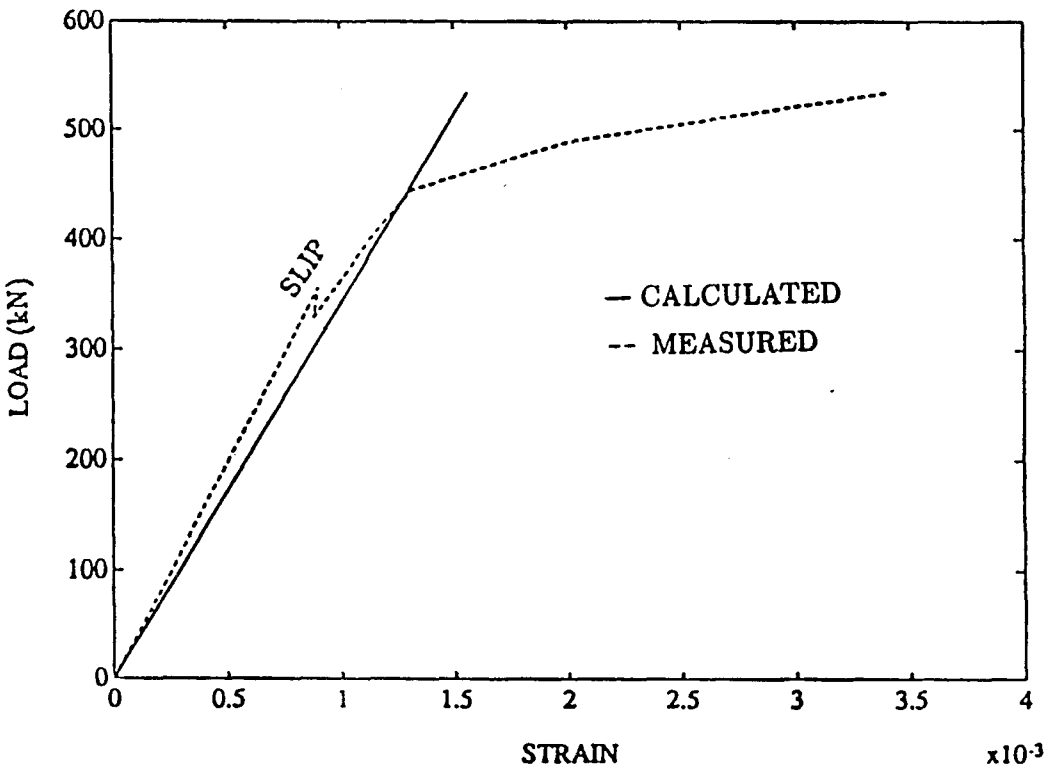

Fig.3.6 Measured and Calculated Load vs. Strain in Prestress Bar of Girder with Straight Tendon

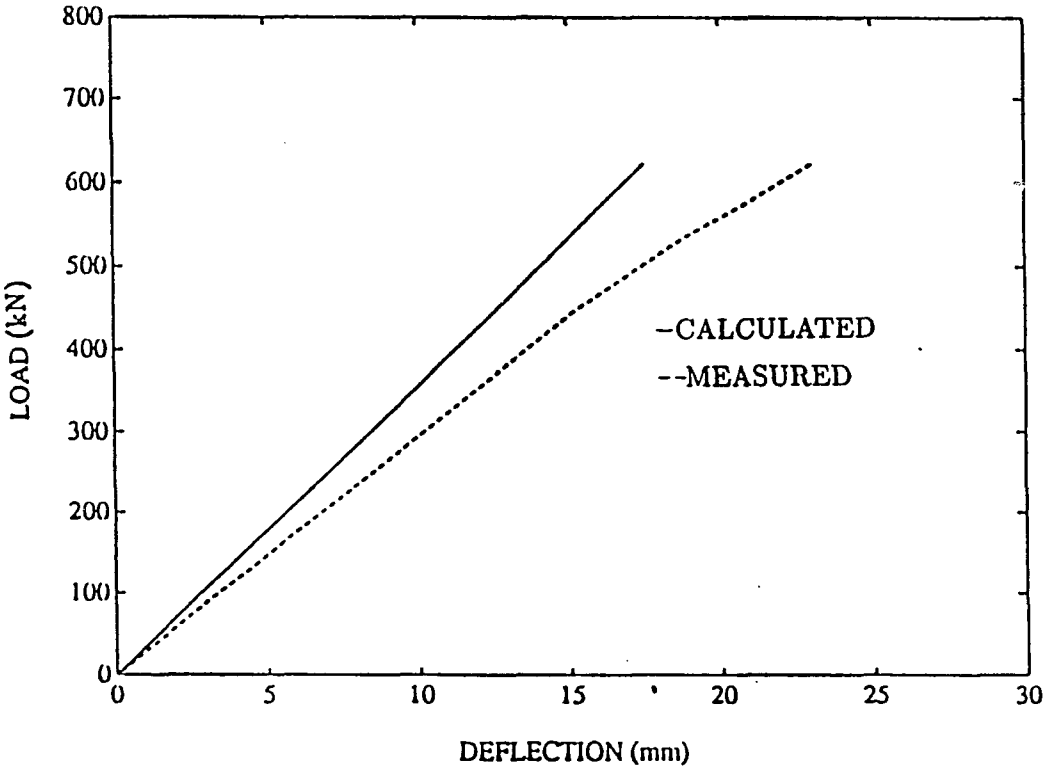

Fig.3.7 Measured and Calculated Load vs. Deflection at Midspan of Girder with Draped Tendon

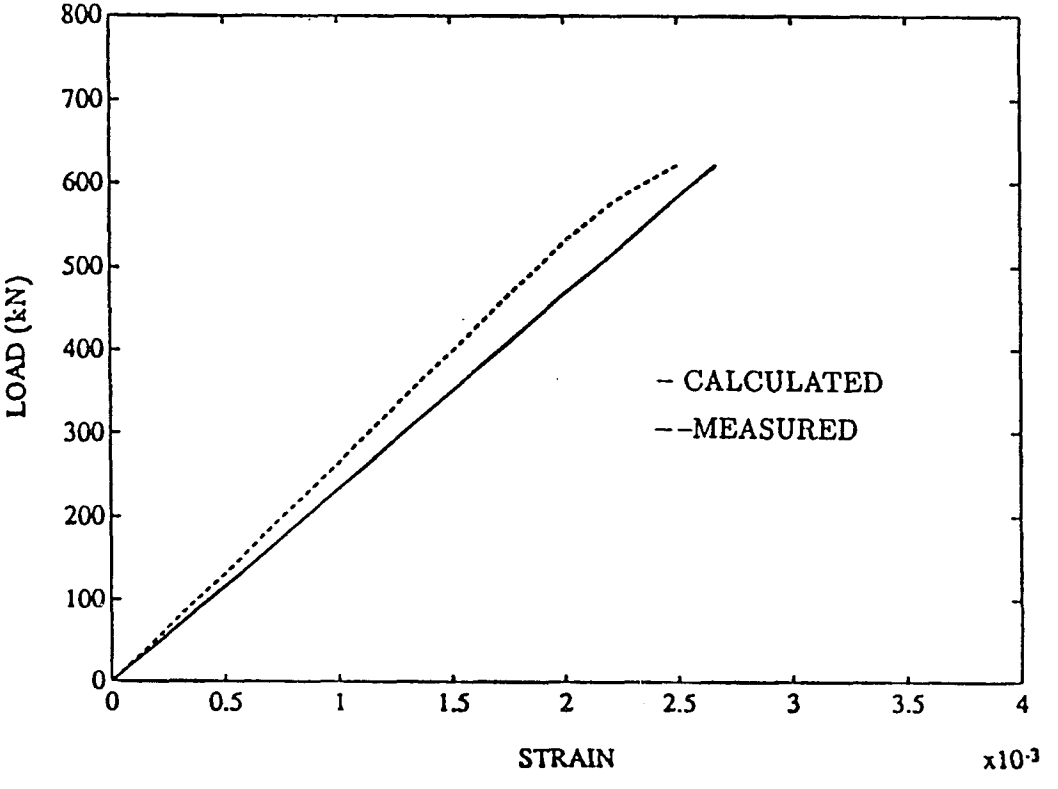

Fig.3.8 Measured and Calculated Load vs. Strain in Tension Flange at Midspan of Girder with Draped Tendon

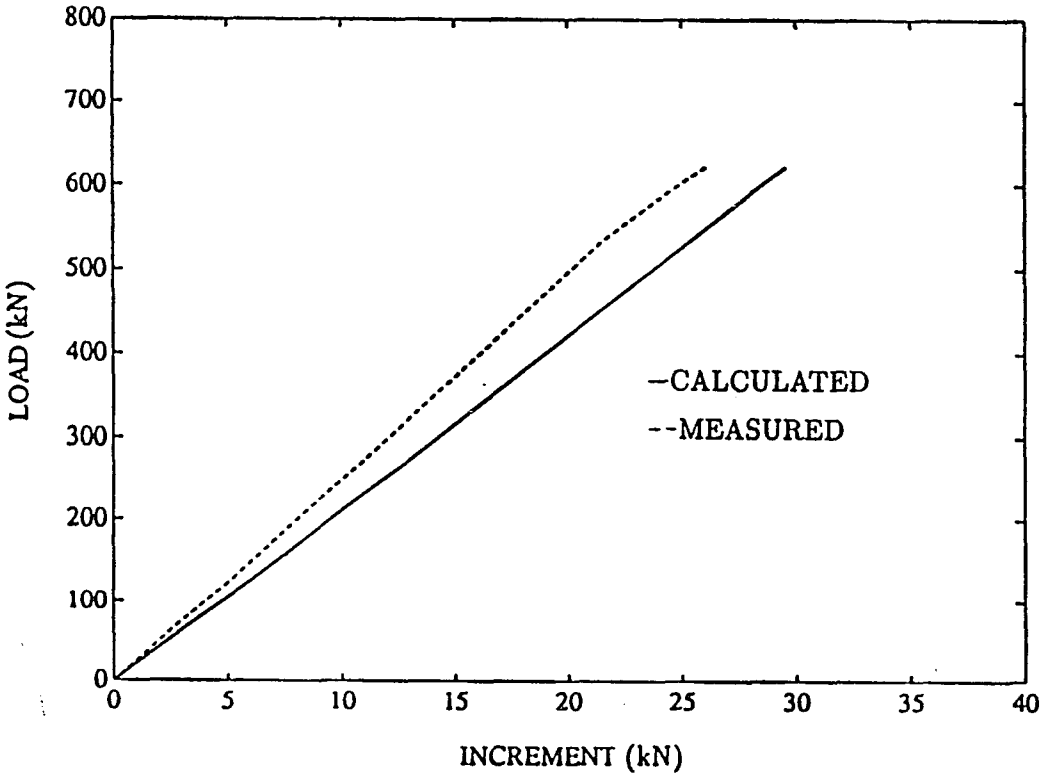

Fig.3.9 Measured and Calculated Load vs. Increase in Cable Force of Girder with Draped Tendon

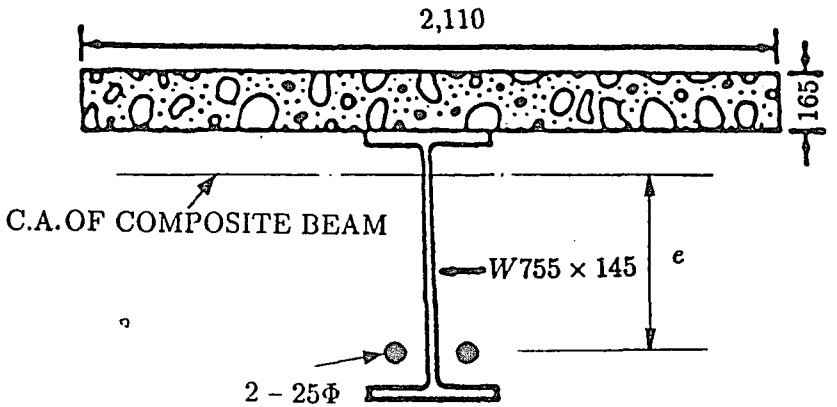

Fig.4.1 Cross Section of Girder A

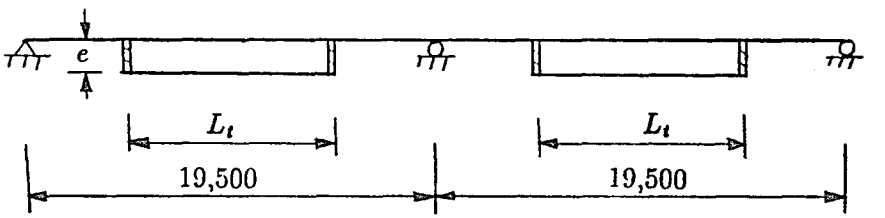

(a) GIRDER A

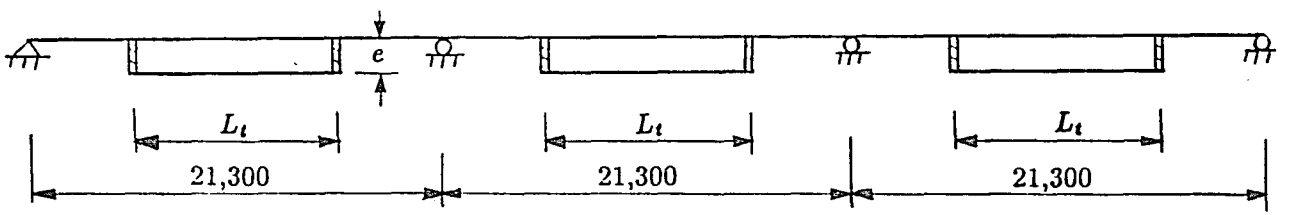

(b) GIRDER B

Fig.4.2 Model of Girders A and B with Straight Discontinuous Tendons

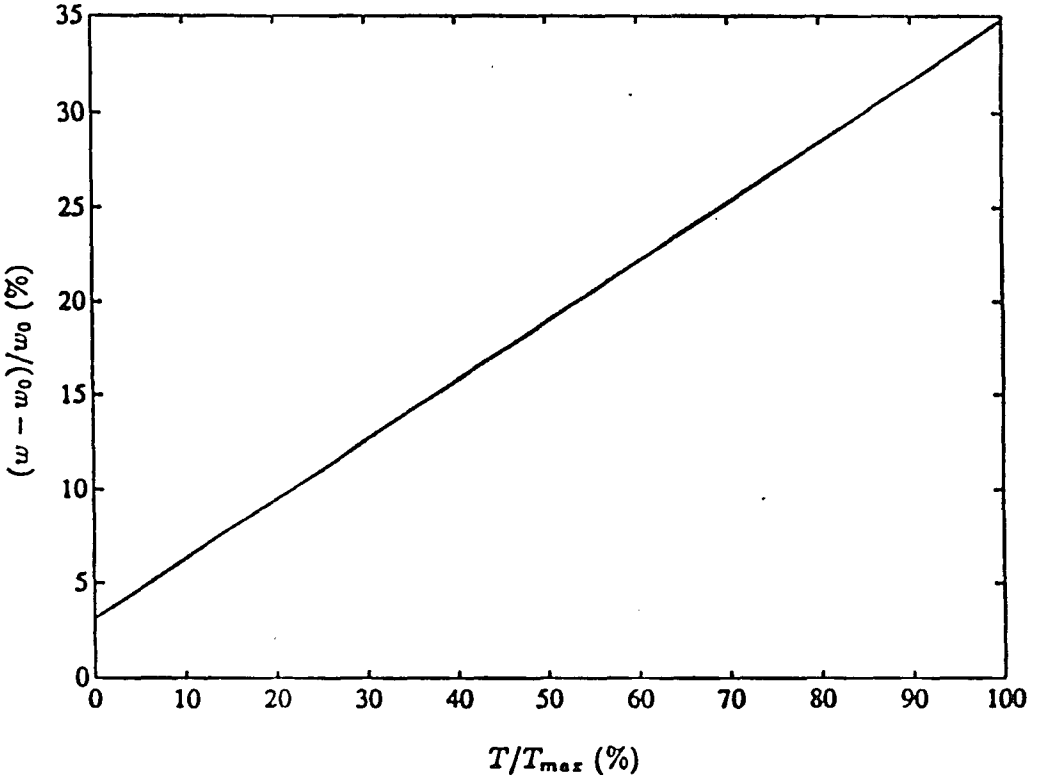

Fig.4.3 Prestress Force vs. Increase in Allowable Load (Girder A)

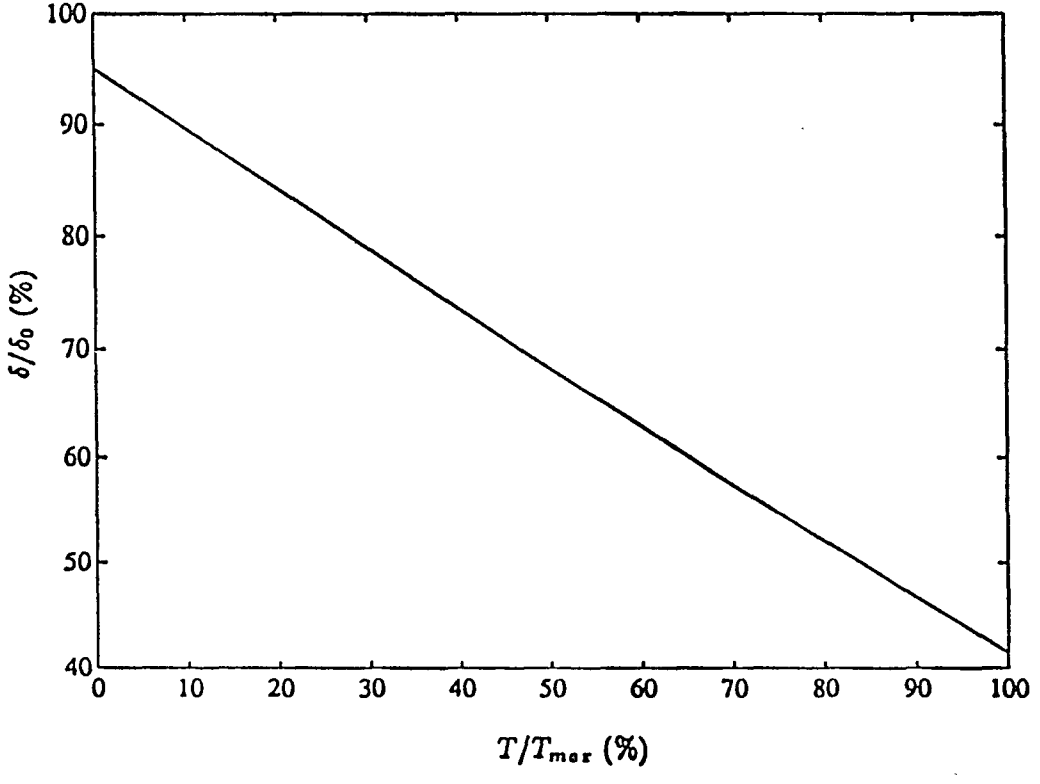

Fig.4.4 Prestress Force vs. Deflection (Girder A)

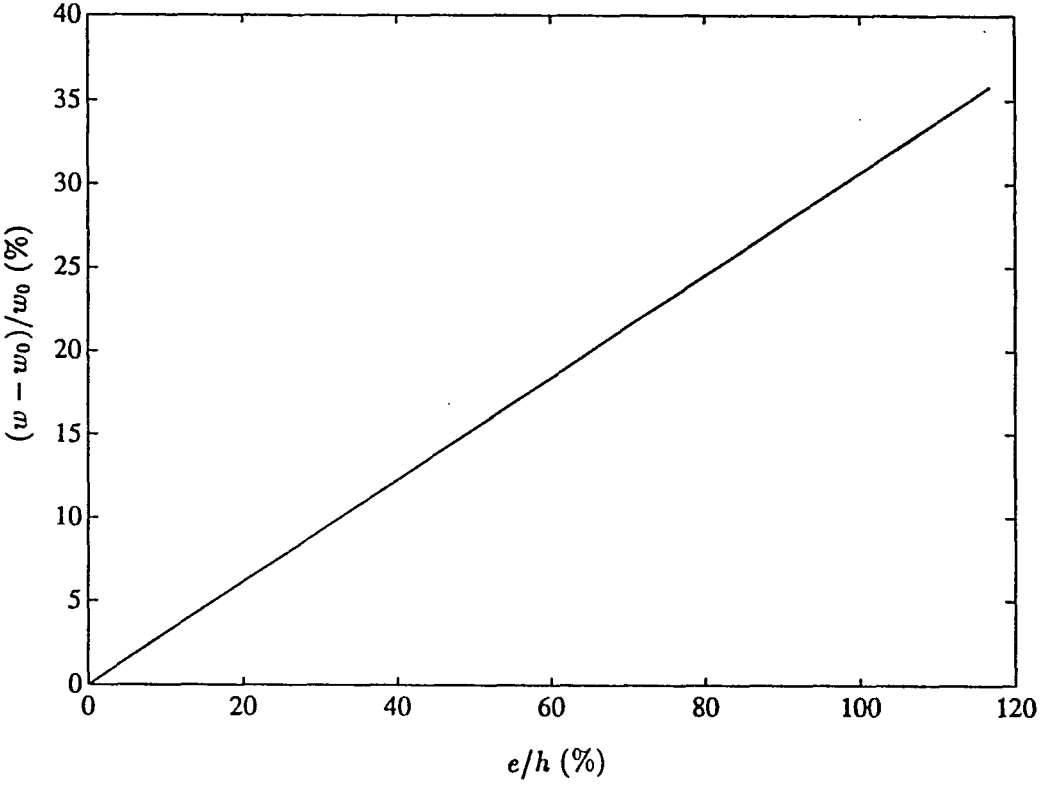

Fig.4.5 Eccentricity vs. Increase in Allowable Load (Girder A)

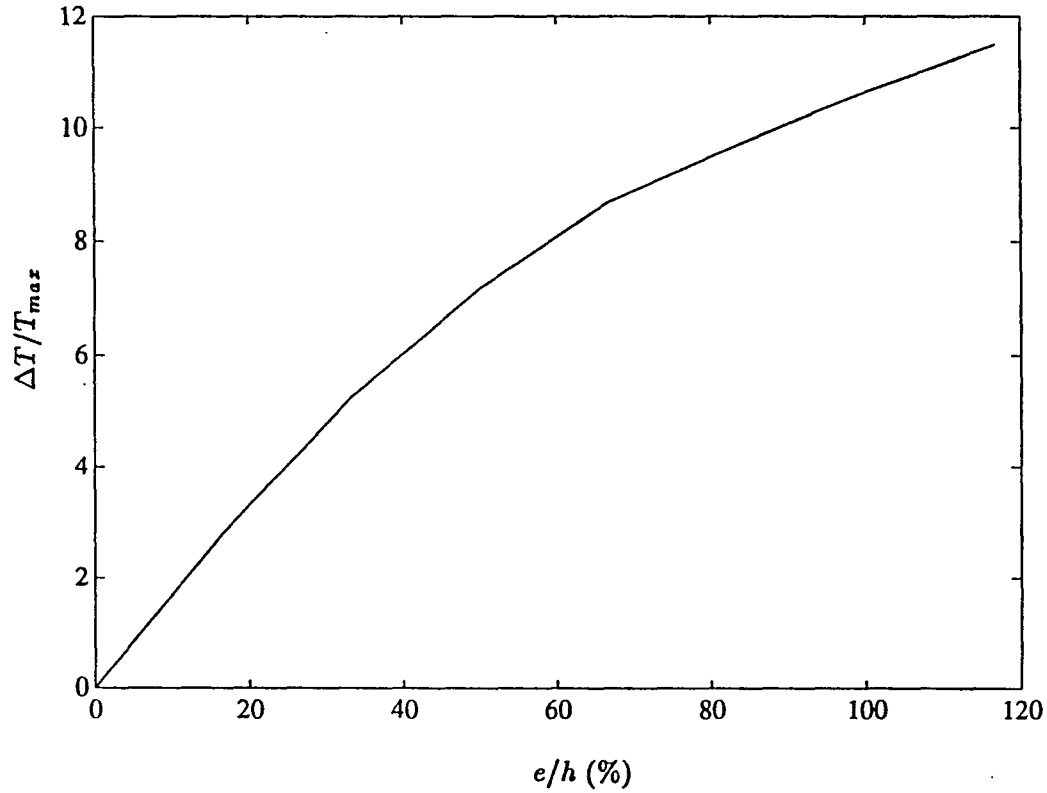

Fig.4.6 Eccentricity vs. Increase in Tendon Force (Girder A)

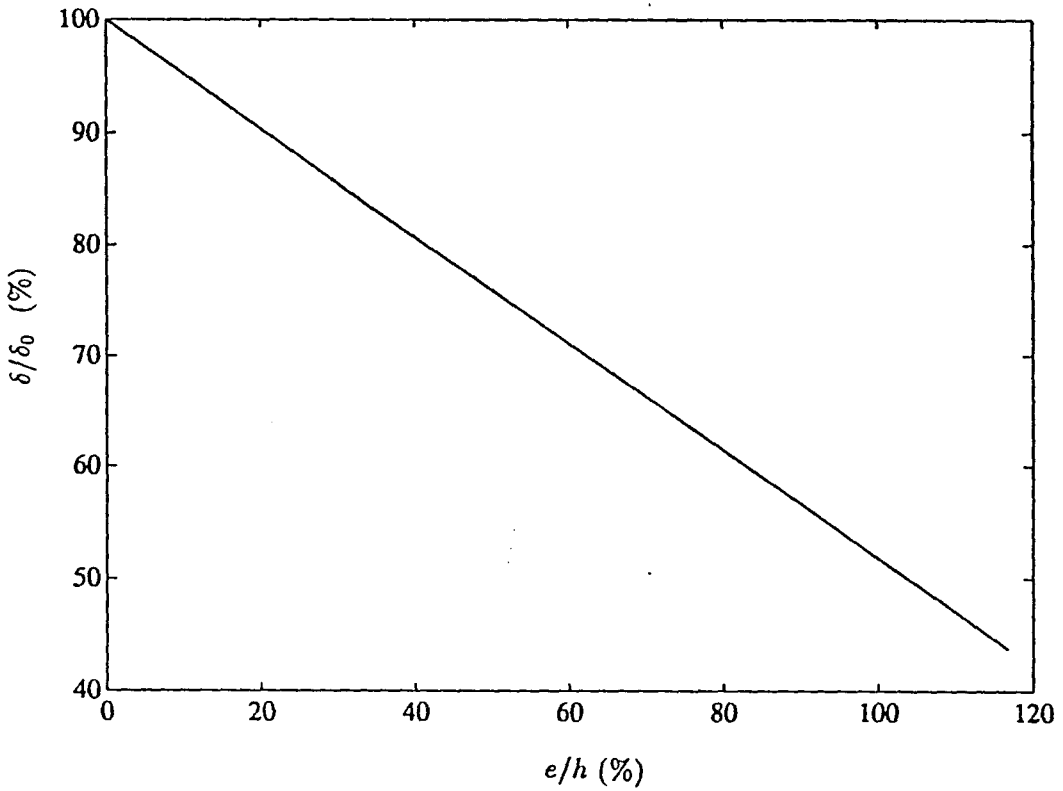

Fig.4.7 Eccentricity vs. Deflection (Girder A)

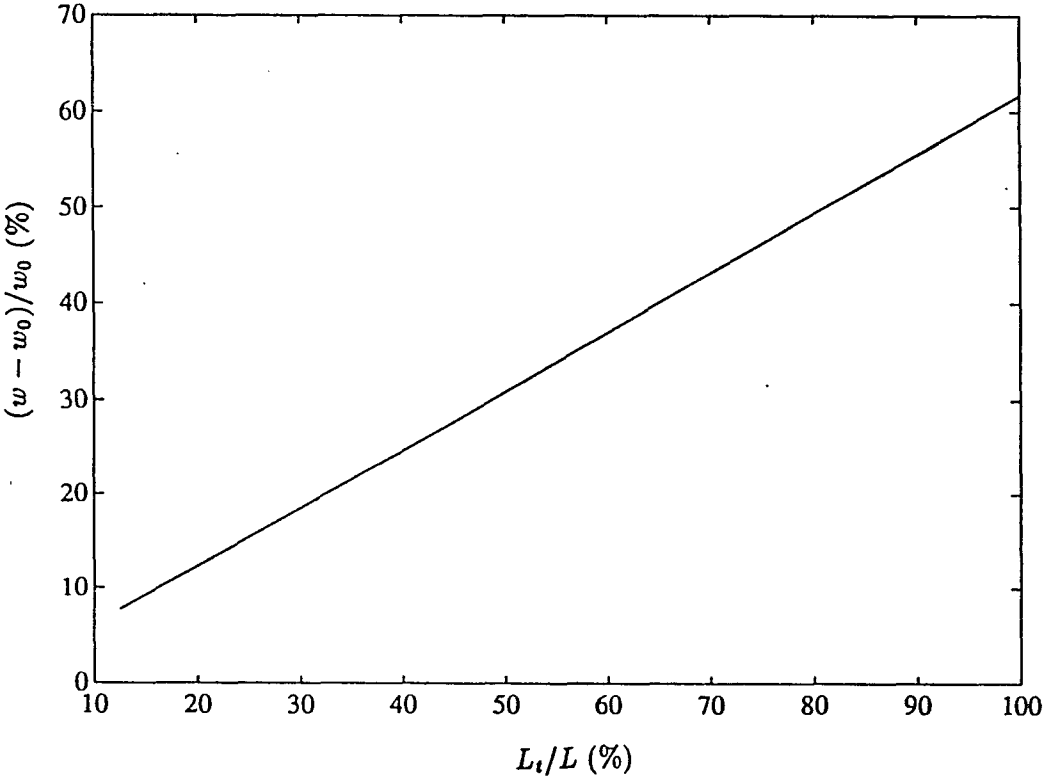

Fig.4.8 Tendon Length vs. Increase in Allowable Load (Girder A)

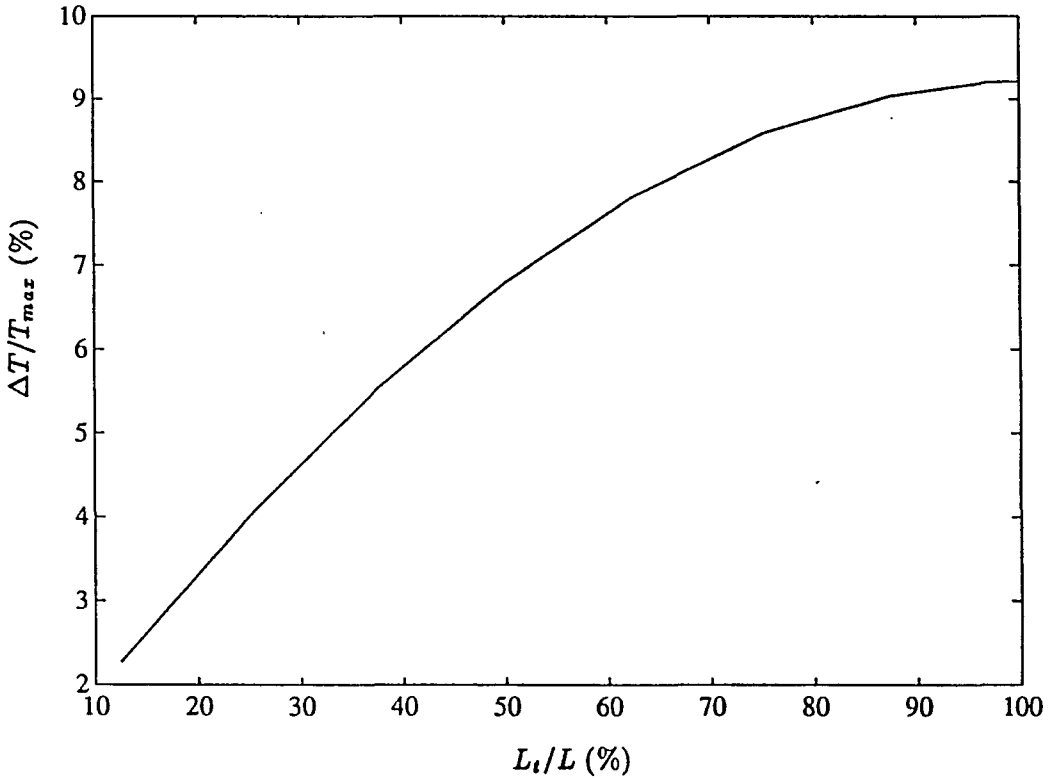

Fig.4.9 Tendon Length vs. Increase in Tendon Force (Girder A)

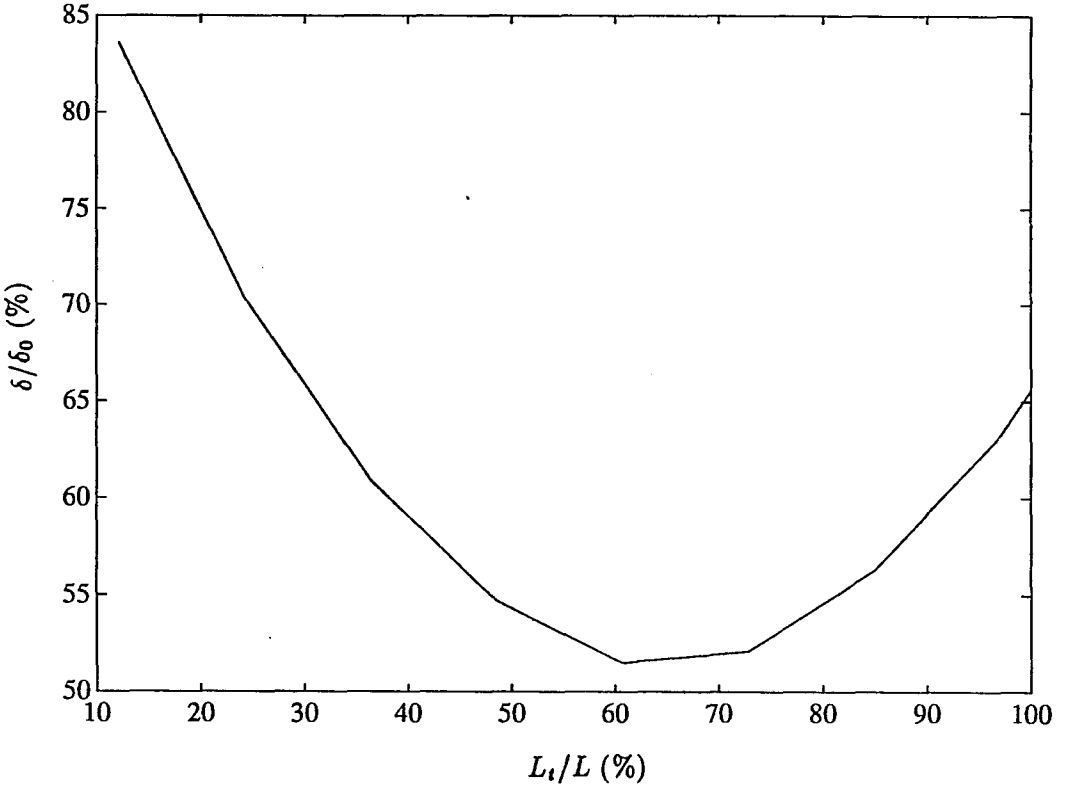

Fig.4.10 Tendon Length vs. Deflection (Girder A)

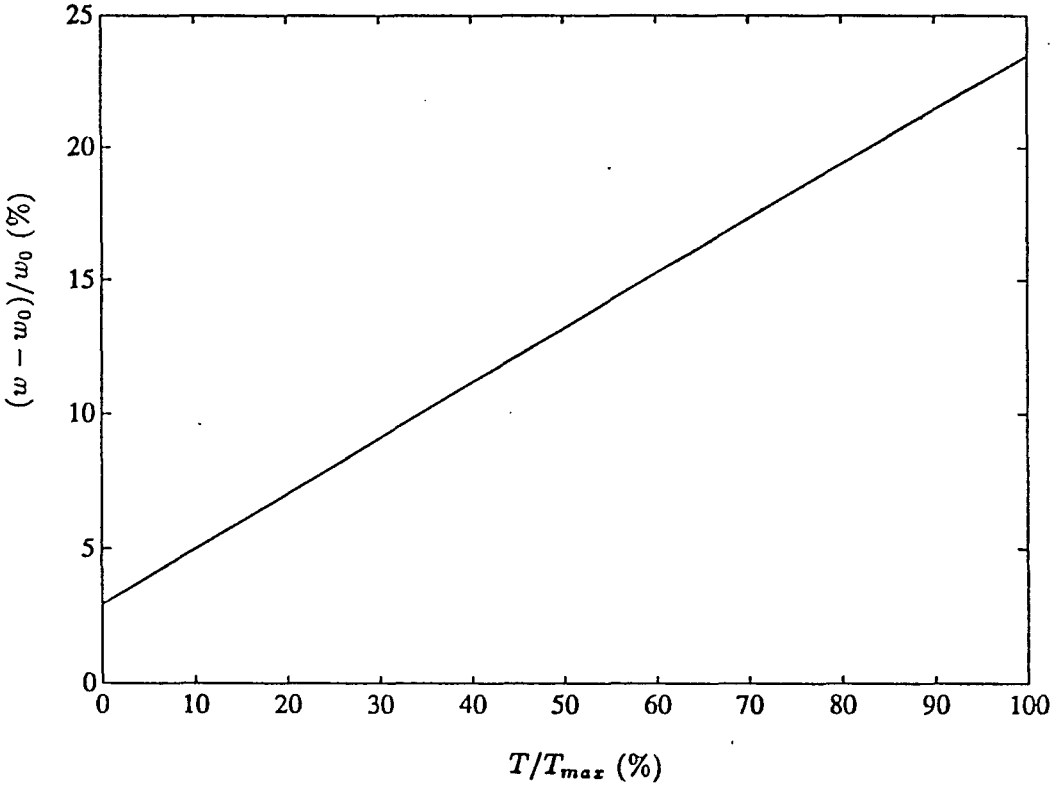

Fig.4.11 Pretress Force vs. Increase in Allowable Load (Girder B)

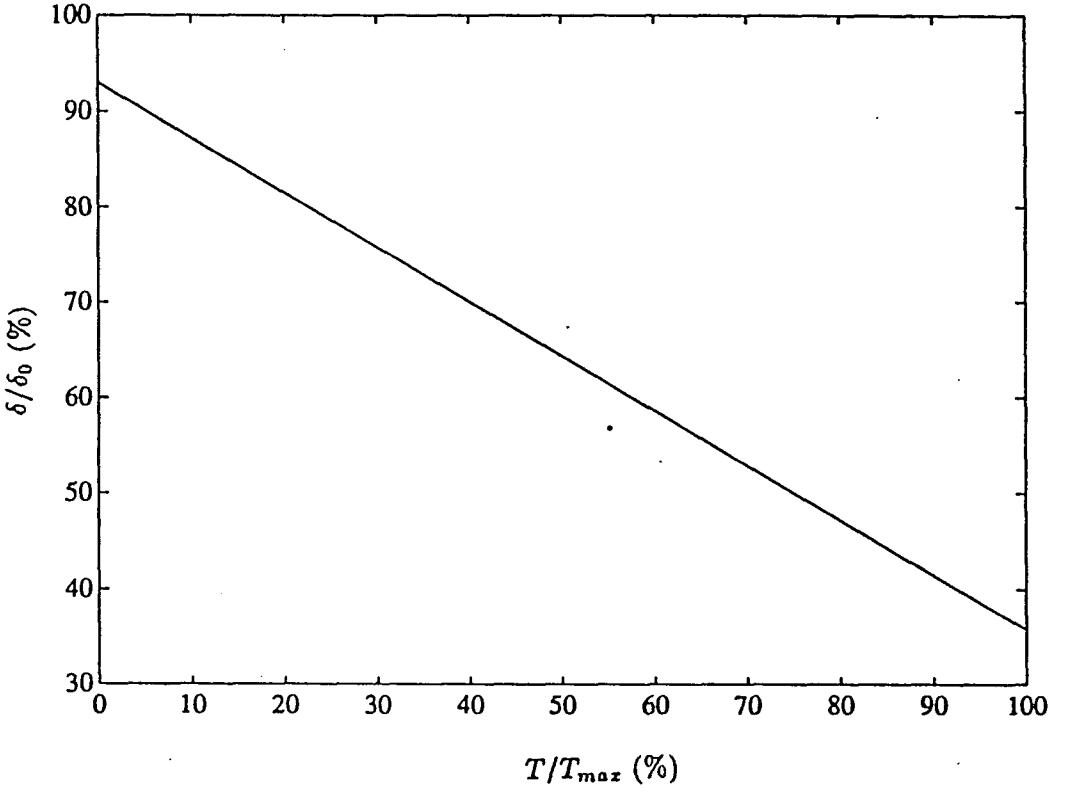

Fig.4.12 Pretress Force vs. Deflection (Girder B)

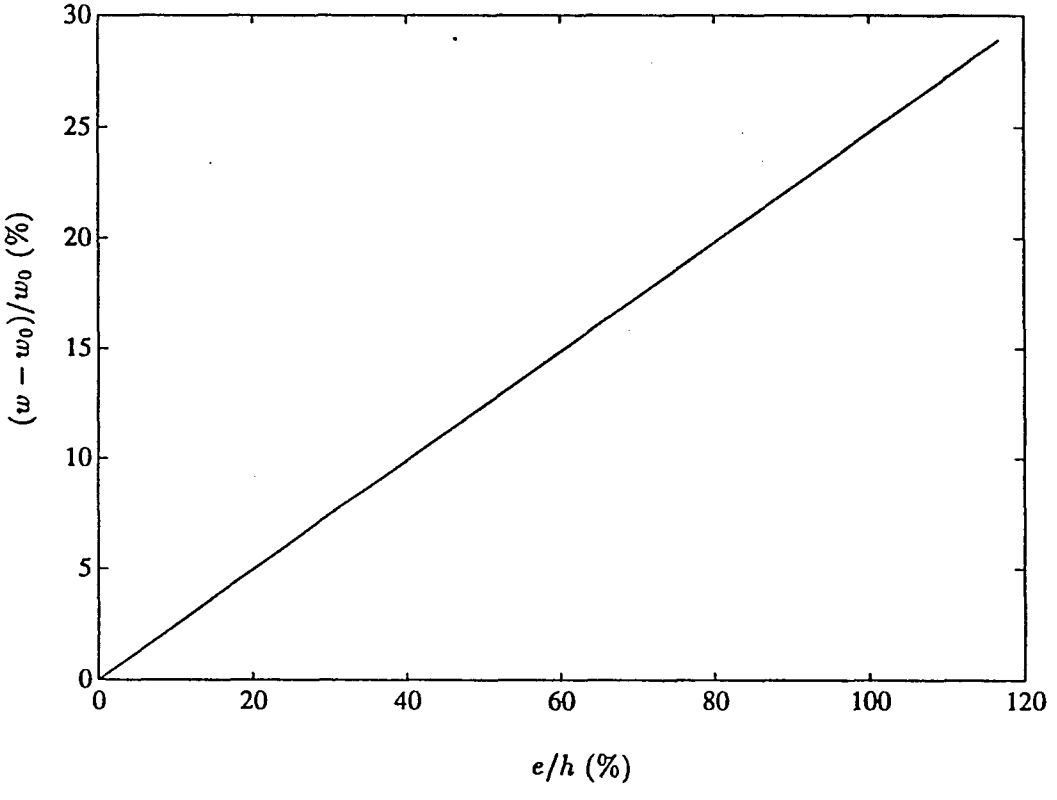

Fig.4.13 Eccentricity vs. Increase in Allowable Load (Girder B)

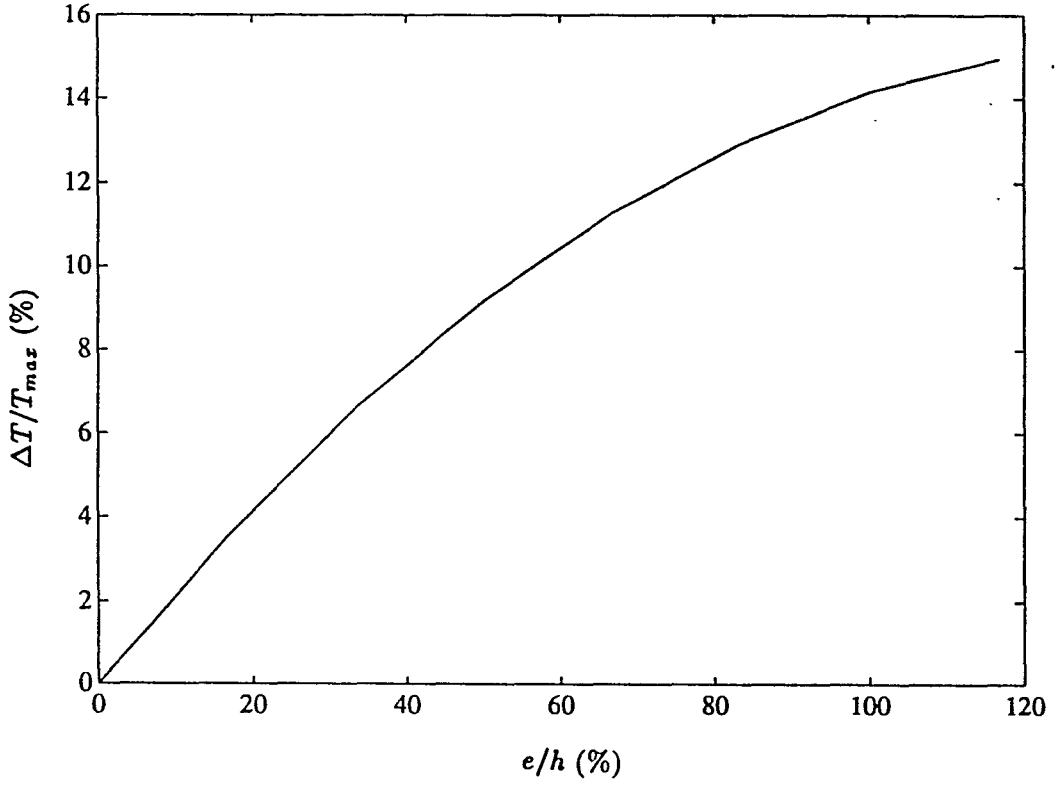

Fig.4.14 Eccentricity vs. Increase in Tendon Force (Girder B)

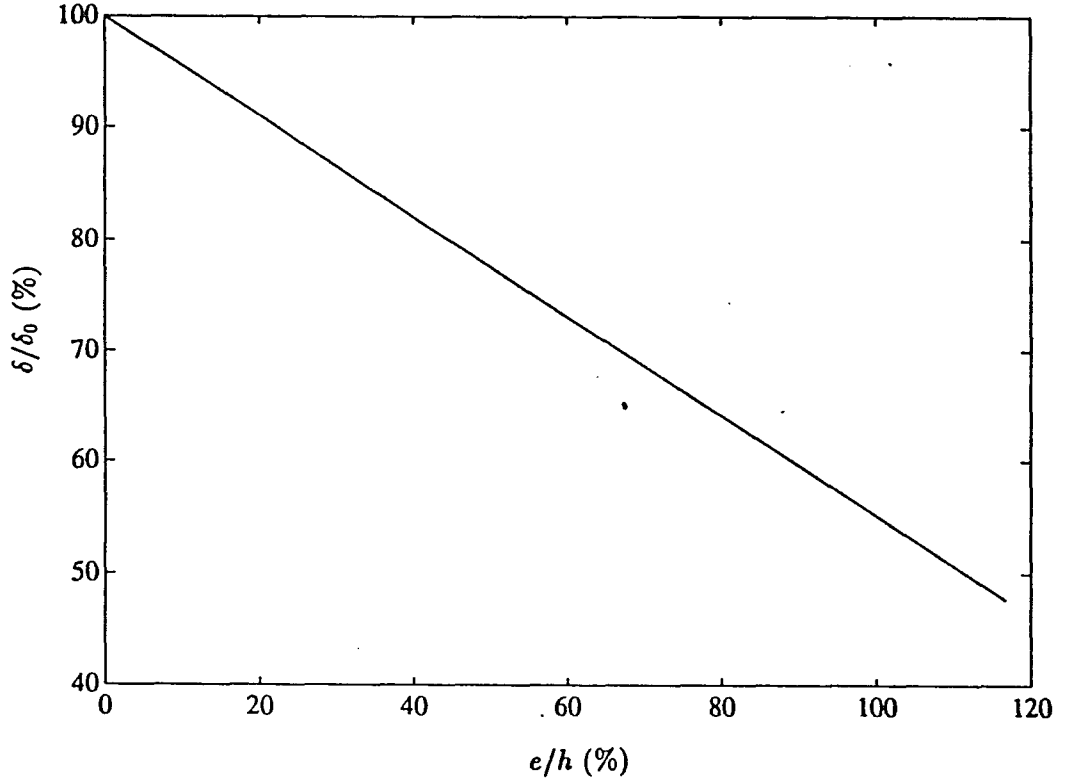

Fig.4.15 Eccentricity vs. Deflection (Girder B)

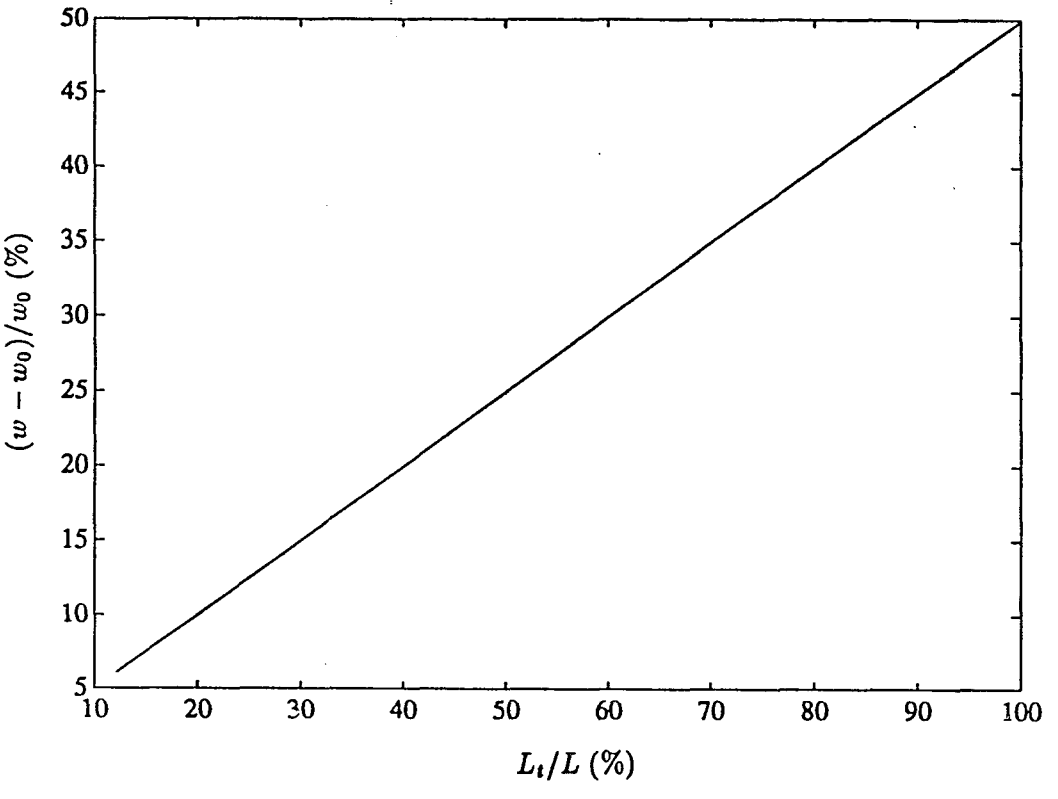

Fig.4.16 Tendon Length vs. Increase in Allowable Load (Girder B)

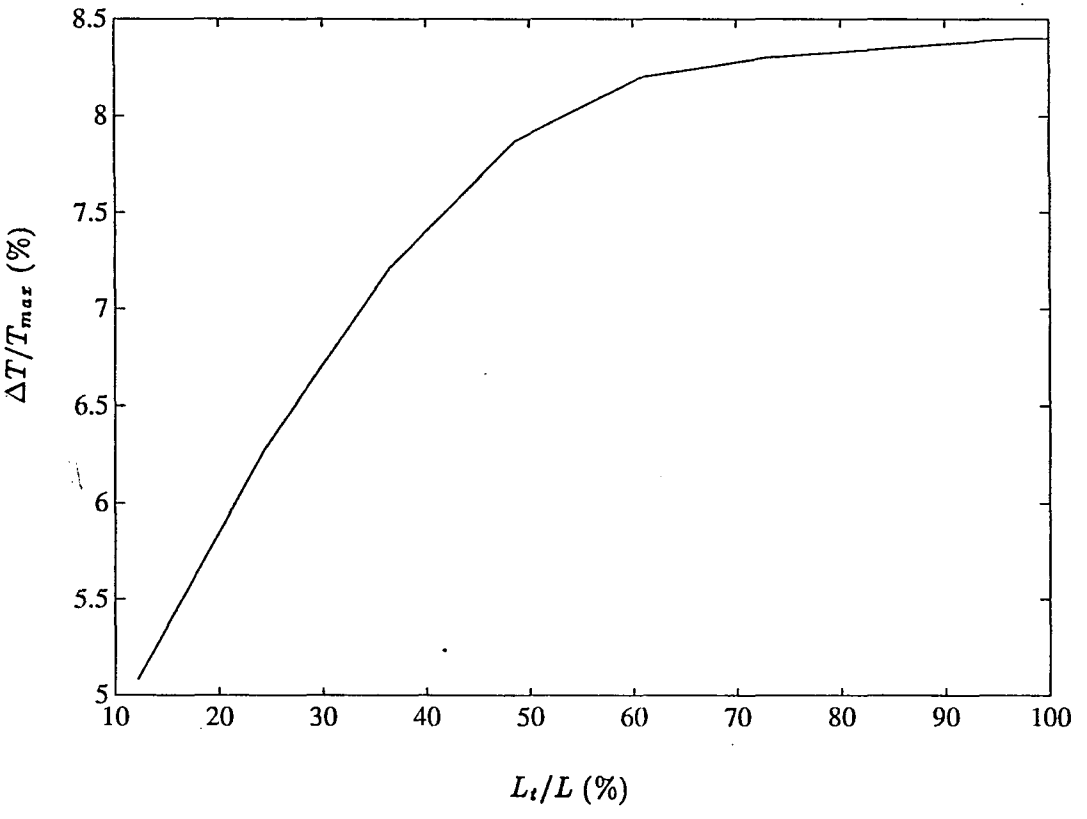

Fig.4.17 Tendon Length vs. Increase in Tendon Force (Girder B)

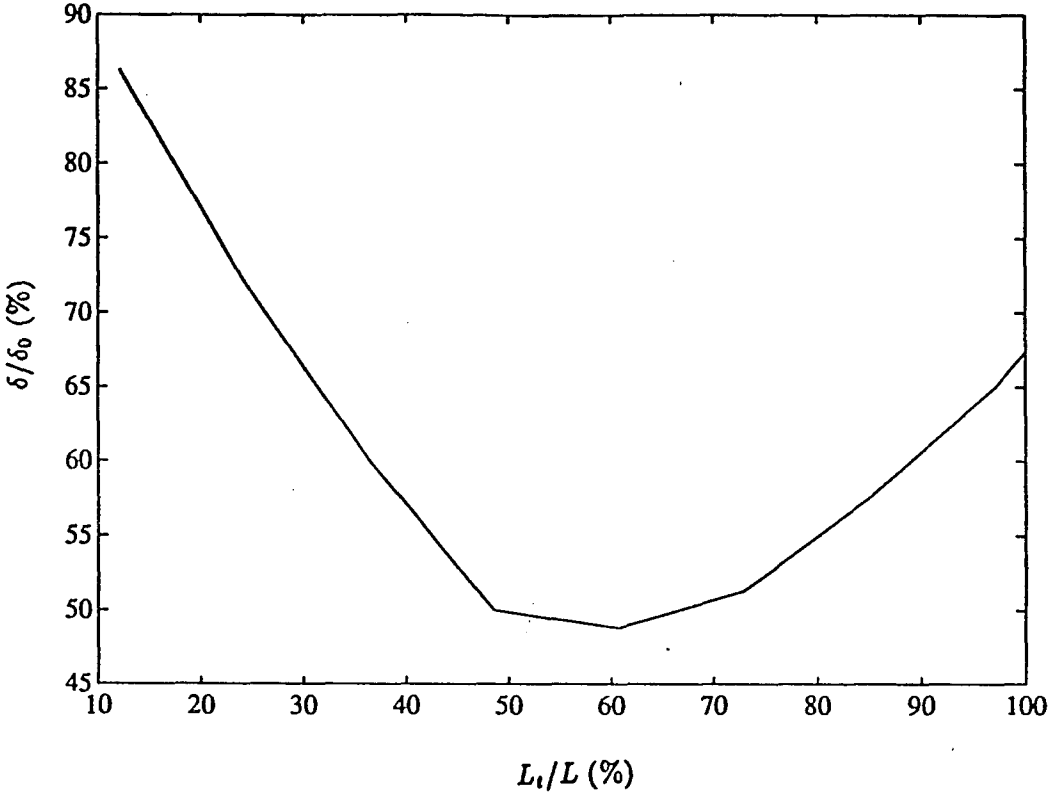

Fig.4.18 Tendon Length vs. Deflection (Girder B)

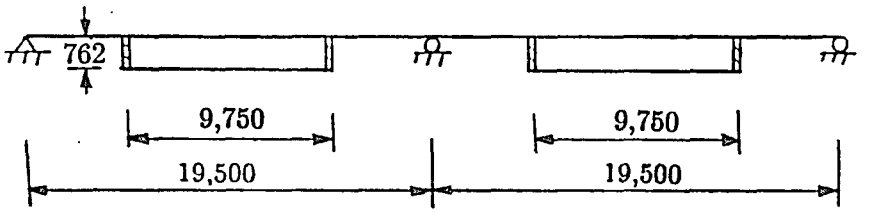

(a) GIRDER A

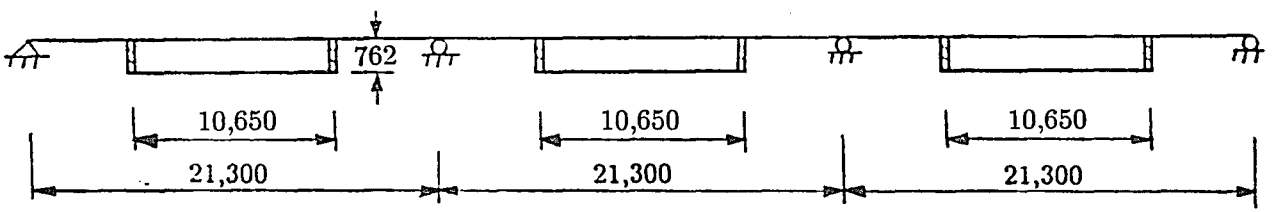

(b) GIRDER B

Fig.4.19 Models of Girders A and B Straight Discontinuous Tendons

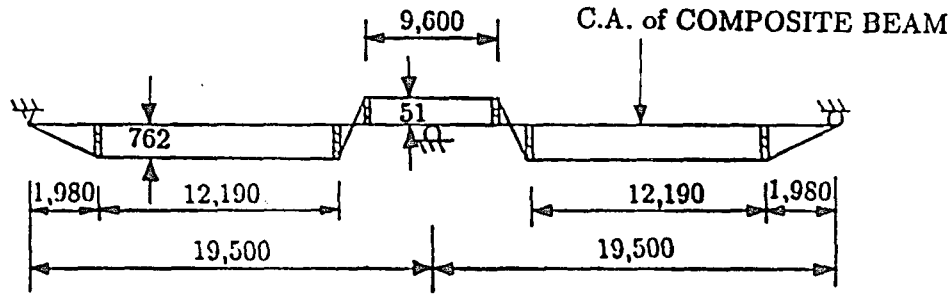

(a) GIRDER A

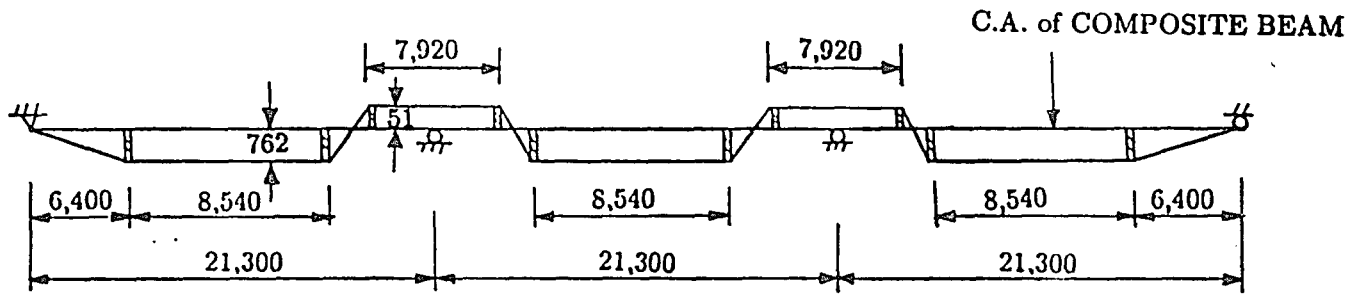

(b) GIRDER B

Fig.4.20 Models of Girders A and B with Draped Continuous Tendons

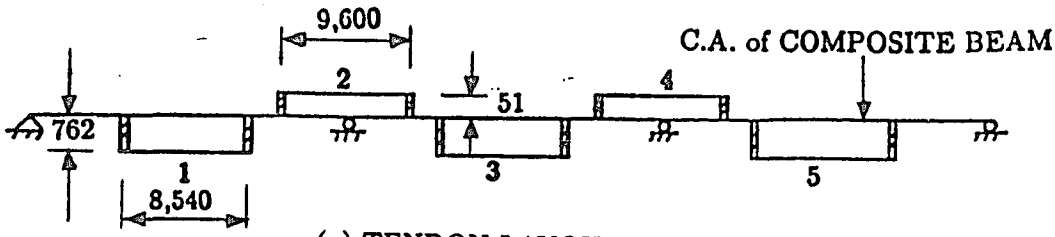

(a) TENDON LAYOUT

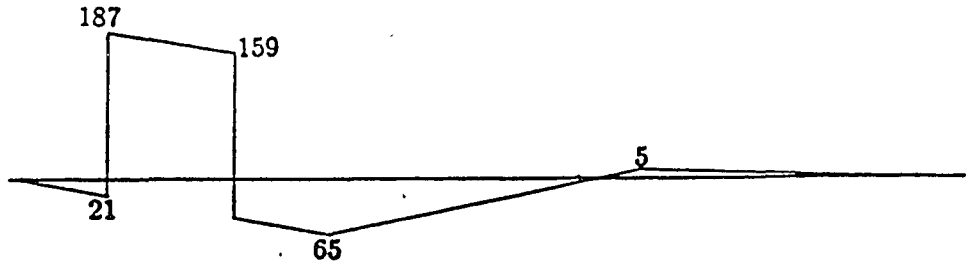

(b) MOMENT DUE TO PRESTRESS FORCE IN TENDON 1

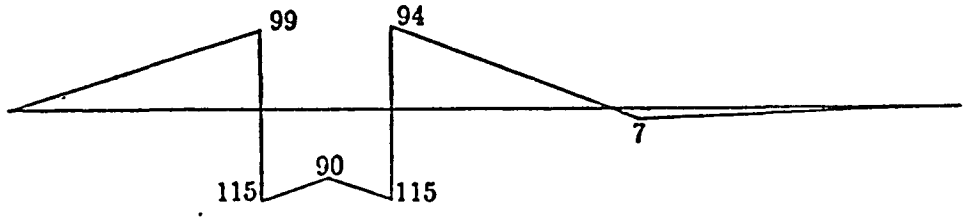

(c) MOMENT DUE TO PRESTRESS FORCE IN TENDON 2

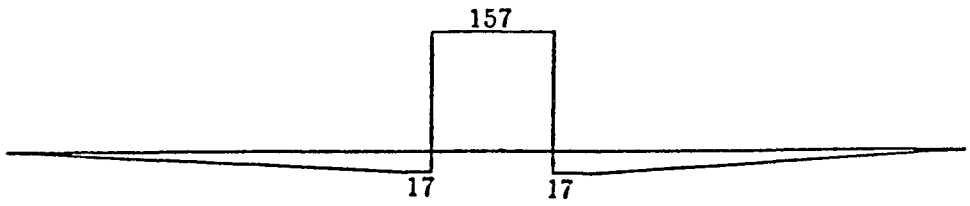

(d) MOMENT DUE TO PRESTRESS FORCE IN TENDON 3

Fig.4.21 Moment Diagrams Due to Prestress Force(kN-m)

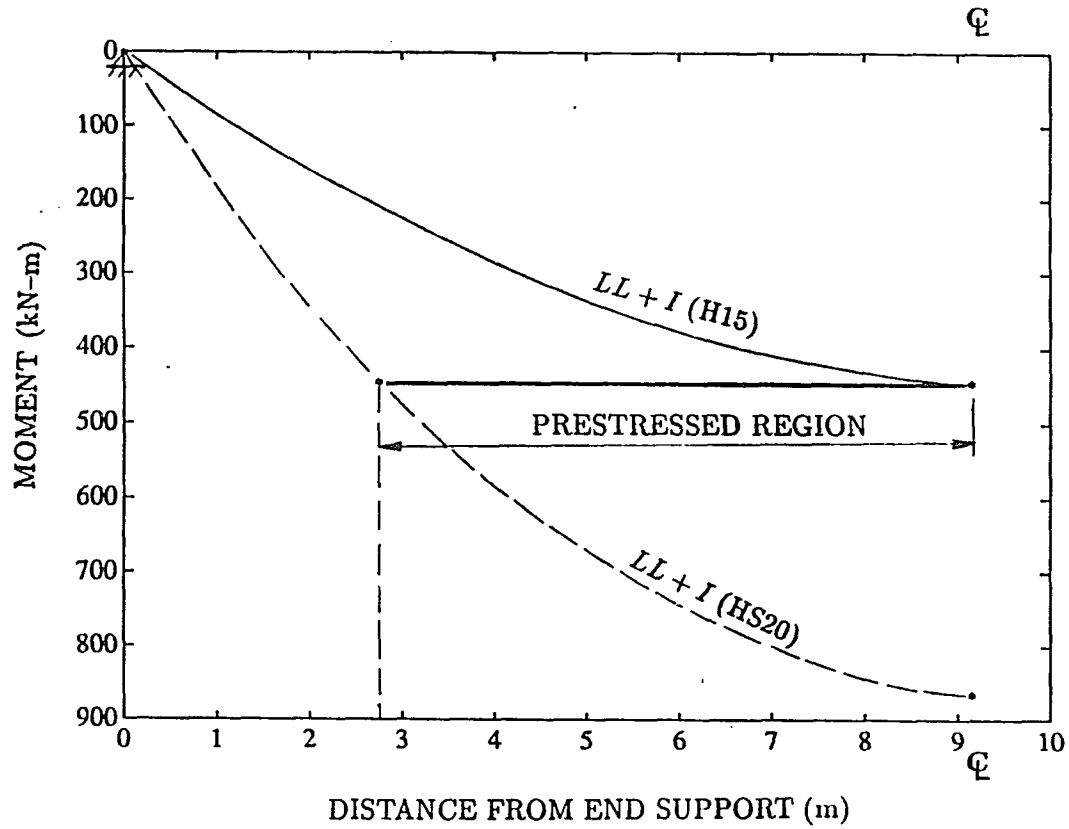

Fig.5.1 Curves of Maximum Moment for Live Load Plus Impact (Bridge A)

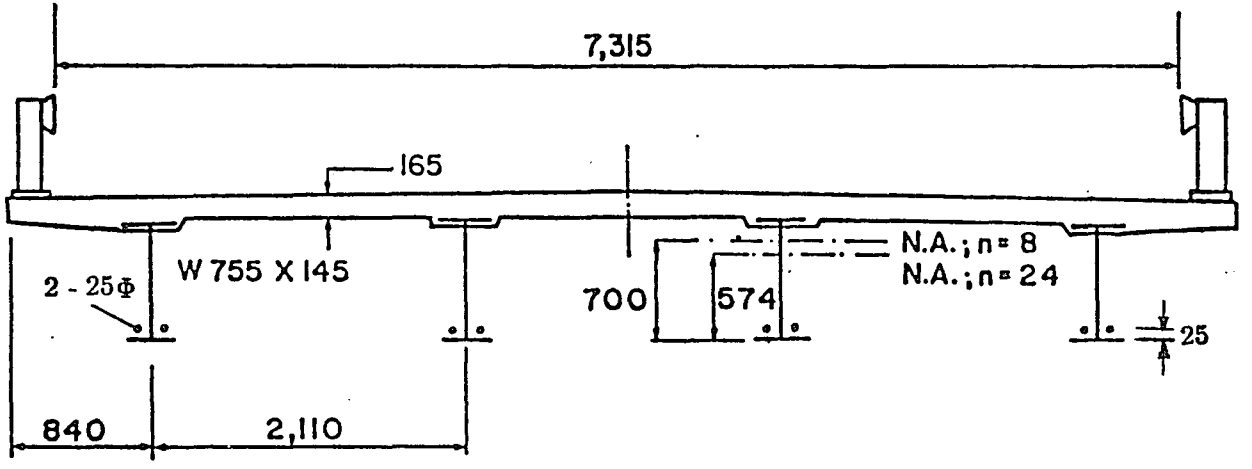

Fig.5.2 Cross Section of Upgraded Bridge A

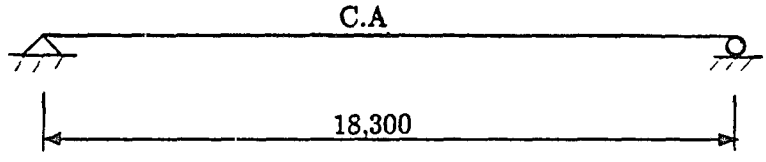

(a) CONVENTIONAL BRIDGE

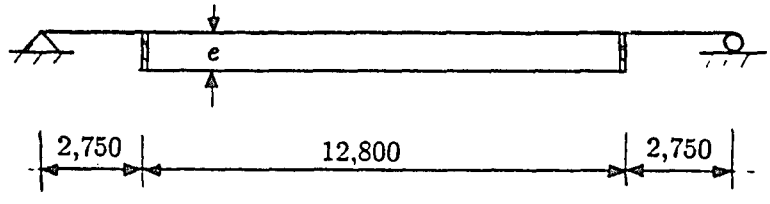

(b) PRESTRESSED WITH STRAIGHT TENDON

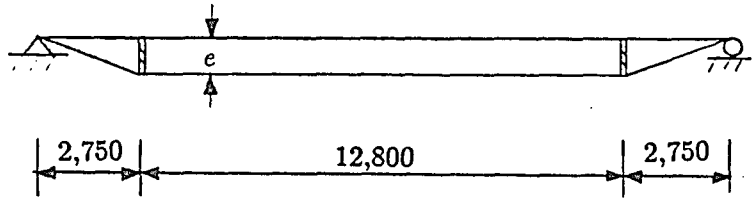

(c) PRESTRESSED WITH DRAPED TENDON

Fig.5.3 Tendon Layout for Bridge A

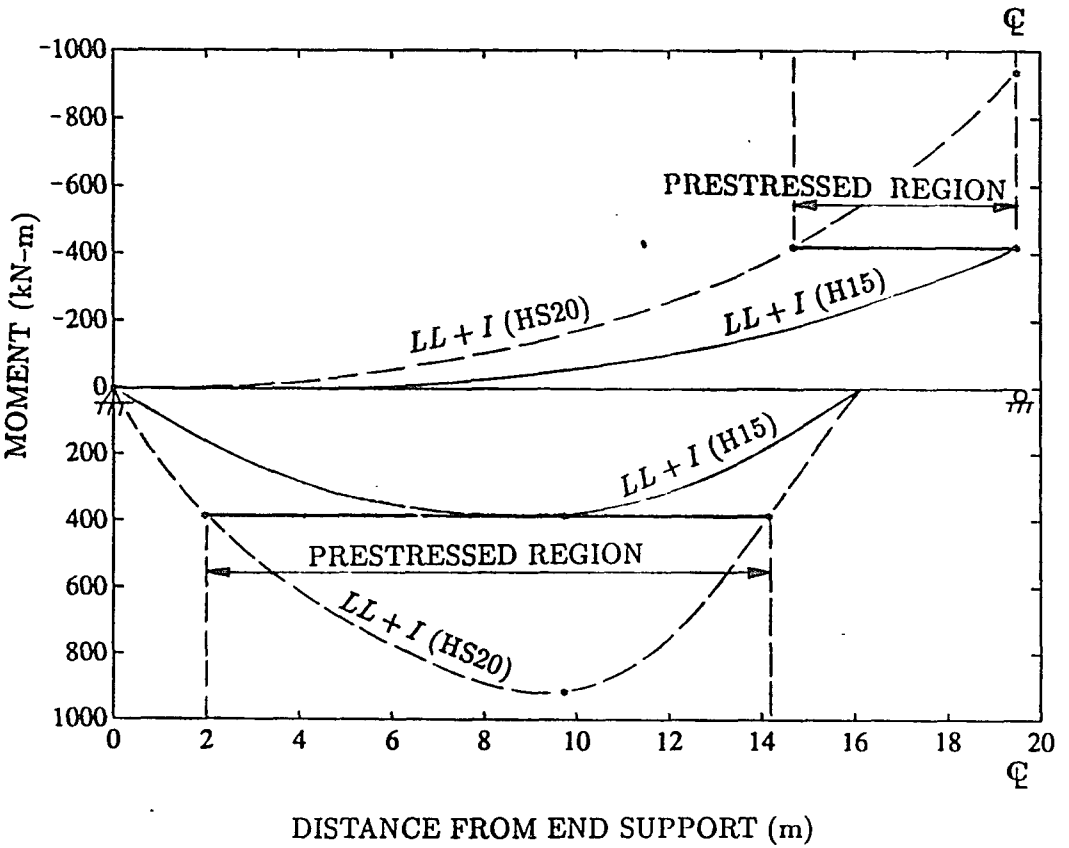

Fig.5.4 Curves of Maximum Moment for Live Load Plus Impact (Bridge B)

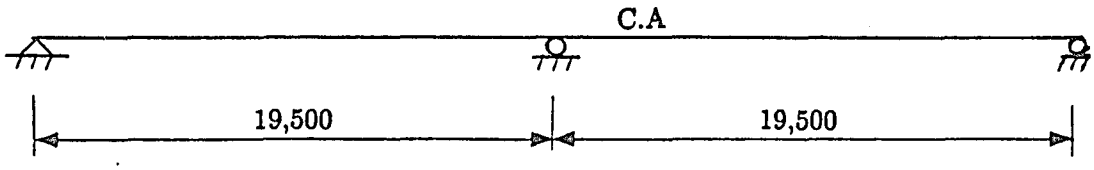

(a) CONVENTIONAL BRIDGE

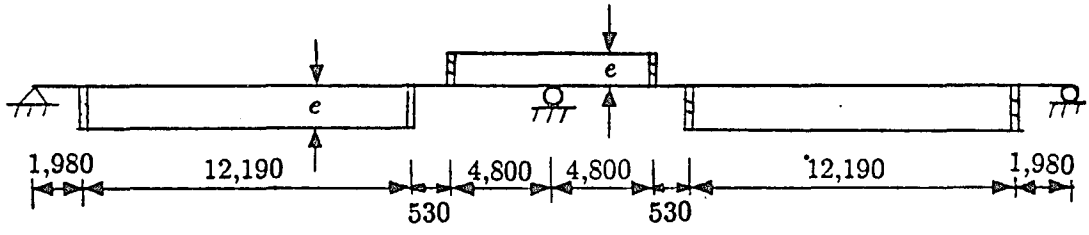

(b) PRESTRESSED WITH DISCONTINUOUS TENDON

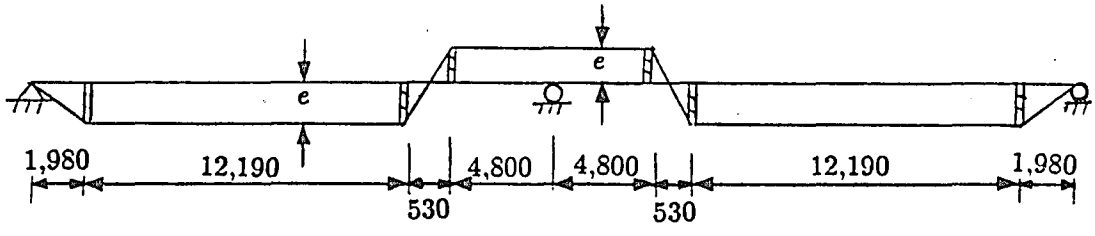

(c) PRESTRESSED WITH CONTINUOUS TENDON

Fig.5.5 Tendon Layout for Bridge B

APPENDIX

LIST OF PROGRAM

```
*************************************************************************
*                                                                       *
*      PROGRAMMER: WENXIA TONG                                          *
*                                                JULY 19, 1989          *
*                                                                       *
*************************************************************************


C-------------------------------------------------------------
C      1          MAIN PROGRAM
C-------------------------------------------------------------

      PROGRAM BRIDGE
      INCLUDE 'COM.FIL'
      CHARACTER*30 INNAME,OUTNAME
      WRITE(5,*,ERR=1101)'               ENTER INPUT FILE NAME'
 1101 ACCEPT 1103,INNAME
      OPEN(11,FILE=INNAME,STATUS='OLD',READ ONLY)
      WRITE(5,*,ERR=1102)'               ENTER OUTPUT FILE NAME'
 1102 ACCEPT 1103,OUTNAME
      OPEN(12,FILE=OUTNAME,STATUS='NEW')
 1103 FORMAT(A)
      OPEN(9,FILE='SCRTCH.07',STATUS='SCRATCH',FORM='UNFORMATTED')
      OPEN(10,FILE='SCRTCH.08',STATUS='SCRATCH',FORM='UNFORMATTED')
      WRITE(12,1000)
 1000 FORMAT(2X,80('*'))
      READ(11,1100)TITLE
 1100 FORMAT(80A)
      WRITE(12,1200)TITLE
 1200 FORMAT(5X,75A)
      WRITE(12,1000)
      READ(11,*)NN
      IF(NN .NE. 1)GOTO 300

C*****READ INPUT DATA
C
      CALL INPUT

C*****GET GENERATION OF STIFFNESS MATRIX

      NDOF=3
      CALL BANDWIDTH
      DO 200 IE=1,NELE
      IF(NTYPE(IE).EQ.1)CALL BAR(IE)
      IF(NTYPE(IE).EQ.2)CALL BEAM(IE)
 200  CONTINUE
      REWIND(9)
      NEQ=NDOF*NNODE
      NMBAND=NEQ*MBAND
      WRITE(9) (S(I),I=1,NMBAND)

C*****APPLYING BOUNDARY CONDITIONS
```

```
      CALL BOUDCOND

C******SOLVE EQUATIONS FOR DISPLACEMENT

      CALL EQSOLV(NEQ,MBAND,S,R)

C******CACULATE REACTIONS, STRAINS AND STRESSES

      CALL FORCE
      GOTO 600

C******READ INPUT DATA

 300  CALL IINPUT
      DO 500 N=1,2
      IF(N.NE.1) GOTO 250

C******READ APPLIED LOADS

      CALL LOAD
      GOTO 450

C******READ UNIT LOADS AT CABLE NODES

 250  CALL UNITG
      GOTO 490

C******GET GENERATION OF STIFFNESS MATRIX

 450  NDOF=3
      CALL BANDWIDTH
      DO 480 IE=1,NELE
      IF(NTYPE(IE).EQ.2)CALL BBEAM(IE)
 480  CONTINUE
      REWIND(9)
      NEQ=NDOF*NNODE
      NMBAND=NEQ*MBAND
      WRITE(9) (S(I),I=1,NMBAND)

C******APPLYING BOUNDARY CONDITIONS

  490 REWIND(9)
      READ(9) (S(I),I=1,NMBAND)
      CALL BOUDCOND

C******SOLVE EQUATIONS FOR DISPLACEMENT

      CALL EQSOLV(NEQ,MBAND,S,R)

C******CACULATE ELONGATION AND CABLE FORCE

      CALL ELONGATE
      IF(N.EQ.1) THEN
      DATAP=DATA
      DO 499 I=1,NEQ
```

```
      RP(I)=R(I)
      PP(I)=P(I)
 499  CONTINUE
      END IF
 500  CONTINUE
      TCA=DATAP/((TL/(EA))-DATA)

C******SUPERPOSITION OF TWO LOADS CONDITIONS

      DO 520 I=1,NEQ
      R1(I)=R(I)*TCA
      P1(I)=P(I)*TCA
 520  CONTINUE
 530  DO 540 I=1,NEQ
      R(I)=R1(I)+RP(I)
      P(I)=P1(I)+PP(I)
 540  CONTINUE

C******TOTAL DISPLACEMENT

      CALL DISPL

C******CALCULATE STRESSES

      DO 550 IE=1,NELE
      IF(NTYPE(IE).EQ.2) CALL BBEAMFOR(IE)
 550  CONTINUE

 600  STOP
      END


C-------------------------------------------------------------
C     2  SUBROUTINES FOR CALCULATIONS WITH DISCONTINOUS CABLES
C-------------------------------------------------------------

      SUBROUTINE INPUT
      INCLUDE 'COM.FIL'

      WRITE(12,80)
 80   FORMAT(/18X,44('*')/)
      WRITE(12,100)
 100  FORMAT(18X,'*              INPUT QUANTITIES             *')
      WRITE(12,80)
      WRITE(12,150)
 150  FORMAT(////2X,'INPUT TABLE 1  STRUCTURE PARAMETERS: ')
      WRITE(12,90)
 90   FORMAT(2X,'-----------------------------------')
      WRITE(12,120)
 120  FORMAT(/2X,'NO.NODE',6X,'NO.ELEM',5X,'NO.SECT',5X,'NO.MATE')
      READ(11,*)NNODE,NELE,NSEC,NMAT
      WRITE(12,110)NNODE,NELE,NSEC,NMAT
 110  FORMAT(/2X,I5,3(8X,I4)/)

C******READ NODAL POINT DATA
```

```
      READ(11,*)NNODE
      WRITE(12,200)
 200  FORMAT(///2X,'INPUT TABLE 2    NODAL  POINT DATA:')
      WRITE(12,90)
      WRITE(12,210)
 210  FORMAT(/2X,'NODE NO',4X,'X-COORDINATE',2x,'Y-COORDINATE',3X,
     1      'RESTRAIN-X   RESTRAIN-Y   RESTRAIN-XY')
      DO 250 N=1,NNODE
      READ(11,*)NPT,X(NPT),y(npt),NSP(3*NPT-2)
     1           ,NSP(3*NPT-1),NSP(3*NPT)
      WRITE(12,240)NPT,X(NPT),Y(NPT),NSP(3*NPT-2)
     1           ,NSP(3*NPT-1),NSP(3*NPT)
 240  FORMAT(2X,I4,8X,D10.4,4x,D10.4,1X,I8,2(5X,I8))
 250  CONTINUE

C******READ ELEMENT DATA

      READ(11,*)NELE
      WRITE(12,300)
 300  FORMAT(////2X,'INPUT TABLE 3       ELEMENT   DATA:')
      WRITE(12,90)
      WRITE(12,350)
 350  FORMAT(/2X,'ELEM NO',3X,'NODE 1  NODE 2',2X,
     1       'ELEM TYPE',4X,'SECT NO',3X,'MATE NO'/)
      DO 390 N=1,NELE
 360  READ(11,*)IE,(IN(IE,I),I=1,2),NTYPE(IE),ISEC(IE),
     2          MAT(IE)
      WRITE(12,372)IE,(IN(IE,I),I=1,2),NTYPE(IE),
     1             ISEC(IE),MAT(IE)
 372  FORMAT(2X,I4,2X,2I8,6X,I5,5X,I6,4X,I6)
 390  CONTINUE


C******READ SECTION DATA

      READ(11,*)NSEC
      WRITE(12,400)NSEC
 400  FORMAT(////2X,'INPUT TABLE 4   SECTION DATA:',
     1       I5,2X,'DIFFERENT SECTIONS')
      WRITE(12,90)
      WRITE(12,410)
 410  FORMAT(/2X,'SECT NO',4X,'AREA',7X,'INERTIA X',
     1       6X,'NA YST',6X,'NA YSB',8X,'NA YCT',7X,'WEB',/)
      DO 470 L=1,NSEC
      READ(11,*)I,AOT(I),AIZZ(I),YST(I),YSB(I),YCT(I),AW(I)
      WRITE(12,480)I,AOT(I),AIZZ(I),YST(I),YSB(I),YCT(I),AW(I)
 480  FORMAT(2X,I5,6(3X,D10.3))
 470  CONTINUE

C******READ MATERIAL DATA

      READ(11,*)NMAT
      WRITE(12,500)NMAT
 500  FORMAT(////2X,'INPUT TABLE 5   MATERIAL DATA:',
```

```
 100  T(I,J)=0.0D0
      XL=X(IN(IE,2))-X(IN(IE,1))
      EL=DSQRT(XL*XL)
      T(1,1)=1.
      T(1,3)=Y(IN(IE,1))
      T(2,2)=1.
      T(3,3)=1.
      T(4,4)=T(1,1)
      T(4,6)=Y(IN(IE,2))
      T(5,5)=T(2,2)
      T(6,6)=T(3,3)
      DO 200 I=1,6
      DO 200 J=1,6
 200  SL(I,J)=0.0D0
      SL(1,1)=AOT(ISEC(IE))*E(MAT(IE))/EL
      SL(1,4)=-SL(1,1)
      SL(4,1)=SL(1,4)
      SL(4,4)=SL(1,1)
      END


C******SUBROUTINE BAR ELEMENT FORCES

      SUBROUTINE BARFOR(IE)
      INCLUDE 'COM.FIL'
      DIMENSION SL(6,6),UL(6),FORL(6),UGE(6),UG(1),T(6,6)
      EQUIVALENCE (UG(1),R(1))

C******ELEMENT GLOBAL DISPLACEMENTS

      DO 100 I=1,6
      K=I/4+1
      L=NDOF-I+3*(K-1)
      UGE(I)=UG(IN(IE,K)*3-L)
 100  CONTINUE

C******ELEMENT LOCAL DISPLACEMENTS AND FORCES

      CALL BARSL(IE,SL,T)
      CALL MULT(T,UGE,UL,6,6,1)
      CALL MULT(SL,UL,FORL,6,6,1)
      XL=X(IN(IE,2))-X(IN(IE,1))
      EL=DSQRT(XL*XL)
      DEFOR=UL(4)-UL(1)
      FORCE=FORL(4)
      WRITE(12,400)
 400  FORMAT(///2X,'TENDEN ',2X,'DEFORMATION',5X,'FORCE',7X,
     1       'STRAIN',7X,'STRESS')
      STRAIN=(UL(4)-UL(1))/EL
      STRESS=E(MAT(IE))*STRAIN
      WRITE(12,410)IE,DEFOR,FORCE,STRAIN,STRESS
 410  FORMAT(/2X,I3,6X,4(D10.4,3X))

      END
```

```
     1       I5,2X,'DIFFERENT TYPES')
      WRITE(12,90)
      WRITE(12,510)
 510  FORMAT(/2X,'MATE NO',7X,'  E'/)
      DO 530 L=1,NMAT
      READ(11,*)M,E(M)
      WRITE(12,550)M,E(M)
 550  FORMAT(2X,I5,5X,D10.3)
 530  CONTINUE


C******READ LOAD CONDITION

      READ(11,*)NLOAD
      WRITE(12,600)NLOAD
 600  FORMAT(////2X,'TABLE 6  LOAD CONDITIONS:  ','TOTAL',I5)
      WRITE(12,90)
      WRITE(12,608)
 608  FORMAT(/2X,'NODE NO',6X,'HORIZOTAL', 4X,'VERTICAL',5X,'ROTATION'/)
      DO 610 J=1,NEQ
 610  R(J)=0.0
      DO 620 I=1,NLOAD
      READ(11,*)NPT,R(3*NPT-2),R(3*NPT-1),R(3*NPT)
      WRITE(12,650)NPT,R(3*NPT-2),R(3*NPT-1),R(3*NPT)
 650  FORMAT(2X,I5,5X,3(D10.4,3X))
 620  CONTINUE
      READ(11,*)W,DIN
      WRITE(12,660)W
 660  FORMAT(/2X,'DISTRIBUTION LOAD:',5X,D10.4)
      WRITE(12,670)DIN
 670  FORMAT(/2X,'LIVE LOAD DEDUCTION FACTOR:',5X,D10.2////)
      END



C******GET GLOBAL STIFFNESS MATRIX

      SUBROUTINE BAR(IE)
      INCLUDE 'COM.FIL'
      DIMENSION TSE(6,6),SE(6,6),SL(6,6),TTR(6,6),T(6,6)
      CALL BARSL(IE,SL,T)
      CALL TRANSPOSE(T,TTR,6,6)
      CALL MULT(TTR,SL,TSE,6,6,6)
      CALL MULT(TSE,T,SE,6,6,6)
      NPE=2
      CALL STORE(IN,SE,S,NDOF,NPE,MBAND,IE,6)
      END

C******GET LOCAL STIFFNESS AND TRANSFORMATION  MATRIX

      SUBROUTINE BARSL(IE,SL,T)
      INCLUDE 'COM.FIL'
      DIMENSION SL(6,6),T(6,6),TT(6,6),TTR(6,6),SLT(6,6)
      DO 100 I=1,6
      DO 100 J=1,6
```

```
C******GET GLOBAL STIFFNESS MATRIX

      SUBROUTINE BEAM(IE)
      INCLUDE 'COM.FIL'
      DIMENSION SL(6,6),T(6,6),TTR(6,6),TSE(6,6),SE(6,6)
      CALL BEAMSL(IE,SL,T)
      CALL TRANSPOSE(T,TTR,6,6)
      CALL MULT(TTR,SL,TSE,6,6,6)
      CALL MULT(TSE,T,SE,6,6,6)
      NPE=2
      CALL STORE(IN,SE,S,NDOF,NPE,MBAND,IE,6)
      END



      SUBROUTINE BEAMSL(IE,SL,T)
      INCLUDE 'COM.FIL'
      DIMENSION SL(6,6),T(6,6)
      DO 100 I=1,6
      DO 100 J=1,6
100   T(I,J)=0.0D0
      XL=X(IN(IE,2))-X(IN(IE,1))
      EL=DSQRT(XL*XL)
      T(1,1)=XL/EL
      T(2,2)=T(1,1)
      T(3,3)=1
      DO 150 I=1,3
      DO 150 J=1,3
150   T(I+3,J+3)=T(I,J)
      DO 200 M=1,6
      DO 200 N=1,6
200   SL(M,N)=0.0D0
      SL(1,1)=AOT(ISEC(IE))*E(MAT(IE))/EL
      SL(1,4)=-SL(1,1)
      SL(4,1)=SL(1,4)
      SL(4,4)=SL(1,1)
      SL(2,2)=(12*AIZZ(ISEC(IE))*E(MAT(IE)))/(EL*EL*EL)
      SL(2,3)=(SL(2,2)*EL)/2.0D0
      SL(2,5)=-SL(2,2)
      SL(2,6)=SL(2,3)
      SL(3,2)=SL(2,3)
      SL(3,3)=(SL(2,2)*EL*EL)/3.0D0
      SL(3,5)=-SL(3,2)
      SL(3,6)=SL(3,3)/2.0D0
      SL(5,2)=SL(2,5)
      SL(5,3)=SL(3,5)
      SL(5,5)=SL(2,2)
      SL(5,6)=SL(3,5)
      SL(6,2)=SL(2,6)
      SL(6,3)=SL(3,6)
      SL(6,5)=SL(5,6)
      SL(6,6)=SL(3,3)
      END
```

```
      SUBROUTINE FORCE
      INCLUDE 'COM.FIL'
      DIMENSION UG(3,MNODE),FOR(3,MNODE)
      EQUIVALENCE (R(1),UG(1,1)),(P(1),FOR(1,1))

C*****CALCULATE REACTIONS (P)

      REWIND(9)
      NMBAND=NEQ*MBAND
      READ(9)(S(I),I=1,NMBAND)
      CALL VBMUL(S,R,P,NEQ,MBAND)
      WRITE(12,100)
  100 FORMAT(/18X,45('*')/)
      WRITE(12,110)
  110 FORMAT(18X,'*              OUTPUT QUANTITIES              *')
      WRITE(12,100)
      WRITE(12,150)
  150 FORMAT(///2X,'NODE',T19,'NODAL DISPLACEMENTE',20X,
     1      'NODAL REACTION')
      WRITE(12,160)
  160 FORMAT(2X,'----',6X,28('-'),12X,28('-'))
      WRITE(12,200)
  200 FORMAT(/2X,' NO.',1X,2(5X,'AXIAL',8X,'SHEAR',7X,'ROTATION',2X)/)
      WRITE(12,250)(I,(UG(J,I),J=1,3),(FOR(K,I),K=1,3),I=1,NNODE)
  250 FORMAT(2X,I3,2X,6D13.4)

C*****MAXIMUM DISPLACEMNT
      DISP=0
      DO 252 I=1,NNODE
      DISP=DMAX1(DISP,DABS(UG(2,I)))
  252 CONTINUE
      WRITE(12,254)DISP
  254 FORMAT(/2X,'MAXIMUM DISPLACMENT:',5X,D10.4)

C*****CALCULATE ELEMENT DEFORMATION AND FORCES

      WRITE(12,260)
  260 FORMAT(///18X,'******** ELEMENT DEFORMATION AND FORCE ********')
      DO 300 IE=1,NELE
      IF(NTYPE(IE).EQ.1)CALL BARFOR(IE)
      IF(NTYPE(IE).EQ.2)CALL BEAMFOR(IE)
  300 CONTINUE
      END


      SUBROUTINE BEAMFOR(IE)
      INCLUDE 'COM.FIL'
      DIMENSION SL(6,6),UL(6),UGE(6),UG(1),T(6,6),FORL(6)
      EQUIVALENCE (UG(1),R(1))

C*****ELEMENT GLOBAL DISPLACEMENT

      DO 100 I=1,6
      K=I/4+1
```

```
      L=NDOF-I+3*(K-1)
      UGE(I)=UG(IN(IE,K)*3-L)
  100 CONTINUE

C*****ELEMENT LOCAL DISPLACEMENT AND FORCE

      CALL BEAMSL(IE,SL,T)
      CALL MULT(T,UGE,UL,6,6,1)
      CALL MULT(SL,UL,FORL,6,6,1)
      XL=X(IN(IE,2))-X(IN(IE,1))
      XL1=X(IN(1,2))-X(IN(1,1))
      SUPO=W*XL/24
      FORL(2)=FORL(2)+SUPO
      FORL(5)=FORL(5)-SUPO
      FIXM=DIN*W*XL*XL/144
      FORL(3)=DIN*FORL(3)+FIXM
      FORL(6)=DIN*FORL(6)-FIXM
      WRITE(12,270)
  270 FORMAT(//2X,'BEAM',2X,'NODE',T25,'DEFORMATION',
     1            T60,'ELEMENT  FORCE')
      WRITE(12,282)
      WRITE(12,272)
  272 FORMAT(/3X,'NO.',2X,'NO.',5X,'AXIAL ',4X,'SHEAR ',6X,'ROTATION'
     1       6X,'AXIAL ',5X,'SHEAR ',7X,'MOMENT')
  282 FORMAT(2X,'----',2X,'----',T18,28('-'),T50,30('-'))
      WRITE(12,190)IE,IN(IE,1),(UL(I),I=1,3),(FORL(I),I=1,3)
      WRITE(12,190)IE,IN(IE,2),(UL(I),I=4,6),(FORL(I),I=4,6)
  190 FORMAT(/2X,I3,I4,4X,6(D10.4,2X))

C*****CACULATE ELEMENT  STRESSES IN STEEL, CONCRET AND CABLE

      IF((ISEC(IE)).NE.1)GOTO 199
      AM1=FORL(3)
      AM2=FORL(6)
      AF=DIN*FORL(1)
      FSTOP1=(AM1*YST(ISEC(IE))/AIZZ(ISEC(IE)))-(AF/AOT(ISEC(IE)))
      FSBOT1=(-AM1*YSB(ISEC(IE))/AIZZ(ISEC(IE)))-(AF/AOT(ISEC(IE)))
      FCTOP1=(AM1*YCT(ISEC(IE))/AIZZ(ISEC(IE)))-(AF/AOT(ISEC(IE)))
      FSTOP2=(-AM2*YST(ISEC(IE))/AIZZ(ISEC(IE)))-(AF/AOT(ISEC(IE)))
      FSBOT2=(AM2*YSB(ISEC(IE))/AIZZ(ISEC(IE)))-(AF/AOT(ISEC(IE)))
      FCTOP2=(-AM2*YCT(ISEC(IE))/AIZZ(ISEC(IE)))-(AF/AOT(ISEC(IE)))
      SHEAR1=FORL(2)/AW(ISEC(IE))
      SHEAR2=FORL(5)/AW(ISEC(IE))
      WRITE(12,300)
  300 FORMAT(//2X,' STRESS IN BEAM  SECTION ')
      WRITE(12,302)
  302 FORMAT(2X,34('-'))
      WRITE(12,310)
  310 FORMAT(/2X,'BEAM ',1X,'NODE ',T15,'STEEL TOP',3X,'STEEL BOT',
     1       3X,'CONC. TOP',5X,'SHEAR')
      WRITE(12,200)IE,IN(IE,1),FSTOP1,FSBOT1,FCTOP1,SHEAR1
      WRITE(12,200)IE,IN(IE,2),FSTOP2,FSBOT2,FCTOP2,SHEAR2
  200 FORMAT(/2X,I3,I4,4X,4(D10.4,2X))
  199 CONTINUE
      END
```

```
C-------------------------------------------------------------
C     3   SUBROUTINES FOR CALCULATIONS WITH CONTINOUS CABLES
C-------------------------------------------------------------

      SUBROUTINE IINPUT
      INCLUDE 'COM.FIL'

      WRITE(12,80)
 80   FORMAT(/18X,44('*')/)
      WRITE(12,100)
 100  FORMAT(18X,'*              INPUT QUANTITIES              *')
      WRITE(12,80)
      WRITE(12,150)
 150  FORMAT(////2X,'INPUT TABLE 1  STRUCTURE PARAMETERS: ')
      WRITE(12,90)
 90   FORMAT(2X,'-----------------------------------')
      WRITE(12,120)
 120  FORMAT(/2X,'NO.NODE',6X,'NO.ELEM',5X,'NO.SECT',5X,'NO.MATE')
      READ(11,*)NNODE,NELE,NSEC,NMAT
      WRITE(12,110)NNODE,NELE,NSEC,NMAT
 110  FORMAT(/2X,I5,3(8X,I4)/)

C*****READ NODAL POINT DATA

      READ(11,*)NNODE
      WRITE(12,200)
 200  FORMAT(///2X,'INPUT TABLE 2    NODAL  POINT DATA:')
      WRITE(12,90)
      WRITE(12,210)
 210  FORMAT(/2X,'NODE NO',4X,'X-COORDINATE',2x,'Y-COORDINATE',3X,
     1      'RESTRAIN-X   RESTRAIN-Y   RESTRAIN-XY')
      DO 250 N=1,NNODE
      READ(11,*)NPT,X(NPT),y(npt),NSP(3*NPT-2)
     1           ,NSP(3*NPT-1),NSP(3*NPT)
      WRITE(12,240)NPT,X(NPT),Y(NPT),NSP(3*NPT-2)
     1           ,NSP(3*NPT-1),NSP(3*NPT)
 240  FORMAT(2X,I4,8X,D10.4,4x,D10.4,1X,I8,2(5X,I8))
 250  CONTINUE

C*****READ ELEMENT DATA

      READ(11,*)NELE
      WRITE(12,300)
 300  FORMAT(////2X,'INPUT TABLE 3       ELEMENT   DATA:')
      WRITE(12,90)
      WRITE(12,350)
 350  FORMAT(/2X,'ELEM NO',3X,'NODE 1  NODE 2',2X,
     1       'ELEM TYPE',4X,'SECT NO',3X,'MATE NO'/)
      DO 390 N=1,NELE
 360  READ(11,*)IE,(IN(IE,I),I=1,2),NTYPE(IE),ISEC(IE),
     2          MAT(IE)
      WRITE(12,372)IE,(IN(IE,I),I=1,2),NTYPE(IE),
```

```
     1              ISEC(IE),MAT(IE)
 372  FORMAT(2X,I4,2X,2I8,6X,I5,5X,I6,4X,I6)                          108
 390  CONTINUE


C******READ SECTION DATA

      READ(11,*)NSEC
      WRITE(12,400)NSEC
 400  FORMAT(////2X,'INPUT TABLE 4   SECTION DATA:',
     1       I5,2X,'DIFFERENT SECTIONS')
      WRITE(12,90)
      WRITE(12,410)
 410  FORMAT(/2X,'SECT NO',4X,'AREA',7X,'INERTIA X',
     1       6X,'NA YST',6X,'NA YSB',8X,'NA YCT',7X,'WEB',/)
      DO 470 L=1,NSEC
      READ(11,*)I,AOT(I),AIZZ(I),YST(I),YSB(I),YCT(I),AW(I)
      WRITE(12,480)I,AOT(I),AIZZ(I),YST(I),YSB(I),YCT(I),AW(I)
 480  FORMAT(2X,I5,6(3X,D10.3))
 470  CONTINUE

C******READ MATERIAL DATA

      READ(11,*)NMAT
      WRITE(12,500)NMAT
 500  FORMAT(////2X,'INPUT TABLE 5   MATERIAL DATA:',
     1       I5,2X,'DIFFERENT TYPES')
      WRITE(12,90)
      WRITE(12,510)
 510  FORMAT(/2X,'MATE NO',7X,'  E'/)
      DO 530 L=1,NMAT
      READ(11,*)M,E(M)
      WRITE(12,550)M,E(M)
 550  FORMAT(2X,I5,5X,D10.3)
 530  CONTINUE
      END

      SUBROUTINE LOAD
      INCLUDE 'COM.FIL'

      READ(11,*)NLOAD
      WRITE(12,100)NLOAD
 100  FORMAT(////2X,'TABLE 6  LOAD CONDITIONS:  ','TOTAL',I5)
      WRITE(12,110)
 110  FORMAT(2X,'---------------------------------')
      WRITE(12,120)
 120  FORMAT(/2X,'NODE NO',6X,'HORIZOTAL', 4X,'VERTICAL',5X,'ROTATION'/)
      DO 150 J=1,NEQ
 150  R(J)=0.0
      DO 220 I=1,NLOAD
      READ(11,*)NPT,R(3*NPT-2),R(3*NPT-1),R(3*NPT)
      WRITE(12,200)NPT,R(3*NPT-2),R(3*NPT-1),R(3*NPT)
 200  FORMAT(2X,I5,7X,3(D10.4,3X))
 220  CONTINUE
      READ(11,*)W,DIN
```

```
      WRITE(12,240)W
      WRITE(12,245)DIN
  240 FORMAT(/2X,'DISTRIBUTION LOAD:',5X,D10.4/)
  245 FORMAT(/2X,'LIVE LOAD PRODUCTION FACTOR:',5X,D8.2////)
      END

      SUBROUTINE UNITG
      INCLUDE 'COM.FIL'

  250 READ(11,*)NLOAD
      WRITE(12,300)NLOAD
  300 FORMAT(////2X,'TABLE 7    UNIT FORCES :  ','TOTAL',I5)
      WRITE(12,110)
  110 FORMAT(2X,'----------------------------------')
      WRITE(12,320)
  320 FORMAT(/2X,'NODE NO',6X,'HORIZOTAL', 4X,'VERTICAL',5X,'ROTATION'/)
      DO 310 J=1,NEQ
  310 R(J)=0.0
      I=1
      DO 330 IE=1,NELE
      IF(NTYPE(IE).NE.1)GOTO 330
      CALL UNIT(IE,I)
      I=I+1
  330 CONTINUE
      R(3*NPT1(1)-2)=RX1(1)
      R(3*NPT1(1)-1)=RY1(1)
      R(3*NPT1(1))=0.
      NBAR=NLOAD-1
      DO 340 I=2,NBAR-1
      IF(NPT2(I).EQ.NPT1(I+1))R(3*NPT1(I)-2)=-(RX2(I)+RX1(I-1))
      R(3*NPT1(I)-1)=-(RY2(I)+RY1(I-1))
      R(3*NPT2(I)-2)=(RX2(I)+RX1(I+1))
      R(3*NPT2(I)-1)=(RY2(I)+RY1(I+1))
      R(3*NPT1(I))=0.
      R(3*NPT1(I))=0.
  340 CONTINUE
      R(3*NPT2(NBAR)-2)=RX2(NBAR)
      R(3*NPT2(NBAR)-1)=RY2(NBAR)
      R(3*NPT2(NBAR-1))=0.
      R(3*NPT2(NBAR))=0.
      WRITE(12,345) NPT1(1),R(3*NPT1(1)-2),R(3*NPT1(1)-1)
     1            ,R(3*NPT1(1))
      WRITE(12,345)(NPT2(I), R(3*NPT2(I)-2),R(3*NPT2(I)-1),
     1             R(3*NPT2(I)),I=1,NBAR)
  345 FORMAT(2X,I5,4X,3D13.4)
C*****READ NUMBER SUPPORTS
      READ(11,*)NSUP
      DO 360 I=1,NSUP
      READ(11,*)NPT,R(3*NPT-2),R(3*NPT-1),R(3*NPT)
      WRITE(12,350)NPT,R(3*NPT-2),R(3*NPT-1),R(3*NPT)
  360 CONTINUE
  350 FORMAT(2X,I5,7X,3(D10.4,3X))
      END

      SUBROUTINE UNIT(IE,I)
```

```
      INCLUDE 'COM.FIL'

      XL=X(IN(IE,2))-X(IN(IE,1))
      YL=Y(IN(IE,2))-Y(IN(IE,1))
      EL=DSQRT(XL*XL+YL*YL)
      NPT1(I)=IN(IE,1)
      RX1(I)=XL/EL
      RX2(I)= -XL/EL
      RY1(I)=YL/EL
      RY2(I)=-RY1(I)
      NPT2(I)=IN(IE,2)
      END


C******SUBROUTINE ELEMENT ELONATION

      SUBROUTINE BBARFOR(IE,EL,ELON)
      INCLUDE 'COM.FIL'
      DIMENSION UGE(6),UG(1)
      EQUIVALENCE (UG(1),R(1))

C******ELEMENT GLOBAL DISPLACEMENTS

      DO 100 I=1,6
      K=I/4+1
      L=NDOF-I+3*(K-1)
      UGE(I)=UG(IN(IE,K)*3-L)
  100 CONTINUE
  105 FORMAT(2X,I3,2X,6D13.4)

C******ELEMENT ELONGATION

      XL=X(IN(IE,2))-X(IN(IE,1))
      YL=Y(IN(IE,2))-Y(IN(IE,1))
      EL=DSQRT(XL*XL+YL*YL)
      XLL=XL-UGE(1)+UGE(4)
      YLL=YL-UGE(2)+UGE(5)
      ELL=DSQRT(XLL*XLL+YLL*YLL)
      ELON=ELL-EL
      END


C******GET GLOBAL STIFFNESS MATRIX

      SUBROUTINE BBEAM(IE)
      INCLUDE 'COM.FIL'
      DIMENSION SL(6,6),T(6,6),TTR(6,6),TSE(6,6),SE(6,6)
      CALL BBEAMSL(IE,SL,T)
      CALL TRANSPOSE(T,TTR,6,6)
      CALL MULT(TTR,SL,TSE,6,6,6)
      CALL MULT(TSE,T,SE,6,6,6)
      NPE=2
      CALL STORE(IN,SE,S,NDOF,NPE,MBAND,IE,6)
      END
```

```
      SUBROUTINE BBEAMSL(IE,SL,T)
      INCLUDE 'COM.FIL'
      DIMENSION SL(6,6),T(6,6)
      DO 100 I=1,6
      DO 100 J=1,6
  100 T(I,J)=0.0D0
      XL=X(IN(IE,2))-X(IN(IE,1))
      YL=Y(IN(IE,2))-Y(IN(IE,1))
      EL=DSQRT(XL*XL+YL*YL)
      T(1,1)=XL/EL
      T(1,2)=YL/EL
      T(2,1)=-T(1,2)
      T(2,2)=T(1,1)
      T(3,3)=1
      DO 150 I=1,3
      DO 150 J=1,3
  150 T(I+3,J+3)=T(I,J)
      DO 200 M=1,6
      DO 200 N=1,6
  200 SL(M,N)=0.0D0
      SL(1,1)=AOT(ISEC(IE))*E(MAT(IE))/EL
      SL(1,4)=-SL(1,1)
      SL(4,1)=SL(1,4)
      SL(4,4)=SL(1,1)
      SL(2,2)=(12*AIZZ(ISEC(IE))*E(MAT(IE)))/(EL*EL*EL)
      SL(2,3)=(SL(2,2)*EL)/2.0D0
      SL(2,5)=-SL(2,2)
      SL(2,6)=SL(2,3)
      SL(3,2)=SL(2,3)
      SL(3,3)=(SL(2,2)*EL*EL)/3.0D0
      SL(3,5)=-SL(3,2)
      SL(3,6)=SL(3,3)/2.0D0
      SL(5,2)=SL(2,5)
      SL(5,3)=SL(3,5)
      SL(5,5)=SL(2,2)
      SL(5,6)=SL(3,5)
      SL(6,2)=SL(2,6)
      SL(6,3)=SL(3,6)
      SL(6,5)=SL(5,6)
      SL(6,6)=SL(3,3)
      END


      SUBROUTINE BBEAMFOR(IE)
      INCLUDE 'COM.FIL'
      DIMENSION SL(6,6),UL(6),UGE(6),UG(1),T(6,6),FORL(6)
      EQUIVALENCE (UG(1),R(1))

C*****ELEMENT GLOBAL DISPLACEMENT

      DO 100 I=1,6
      K=I/4+1
```

```
      L=NDOF-I+3*(K-1)
      UGE(I)=UG(IN(IE,K)*3-L)                                          112
  100 CONTINUE

C******ELEMENT LOCAL DISPLACEMENT AND FORCE

      CALL BBEAMSL(IE,SL,T)
      CALL MULT(T,UGE,UL,6,6,1)
      CALL MULT(SL,UL,FORL,6,6,1)
      XL=X(IN(IE,2))-X(IN(IE,1))
      XL1=X(IN(1,2))-X(IN(1,1))
      SUPO=W*XL/24
      FORL(2)=FORL(2)+SUPO
      FORL(5)=FORL(5)-SUPO
      FIXM=DIN*W*XL*XL/144
      FORL(3)=DIN*FORL(3)+FIXM
      FORL(6)=DIN*FORL(6)-FIXM
      WRITE(12,270)
  270 FORMAT(//2X,'BEAM',2X,'NODE',T25,'DEFORMATION',
     1            T60,'ELEMENT  FORCE')
      WRITE(12,282)
      WRITE(12,272)
  272 FORMAT(/3X,'NO.',2X,'NO.',5X,'AXIAL ',4X,'SHEAR ',6X,'ROTATION'
     1       6X,'AXIAL ',5X,'SHEAR ',7X,'MOMENT')
  282 FORMAT(2X,'----',2X,'----',T18,28('-'),T50,30('-'))
      WRITE(12,190)IE,IN(IE,1),(UL(I),I=1,3),(FORL(I),I=1,3)
      WRITE(12,190)IE,IN(IE,2),(UL(I),I=4,6),(FORL(I),I=4,6)
  190 FORMAT(/2X,I3,I4,4X,6(D10.4,2X))

C******CACULATE ELEMENT  STRESSES IN STEEL, CONCRET AND CABLE

      IF((ISEC(IE)).NE.1)GOTO 199
      AM1=FORL(3)
      AM2=FORL(6)
      AF=DIN*FORL(1)
      FSTOP1=(AM1*YST(ISEC(IE))/AIZZ(ISEC(IE)))-(AF/AOT(ISEC(IE)))
      FSBOT1=(-AM1*YSB(ISEC(IE))/AIZZ(ISEC(IE)))-(AF/AOT(ISEC(IE)))
      FCTOP1=(AM1*YCT(ISEC(IE))/AIZZ(ISEC(IE)))-(AF/AOT(ISEC(IE)))
      FSTOP2=(-AM2*YST(ISEC(IE))/AIZZ(ISEC(IE)))-(AF/AOT(ISEC(IE)))
      FSBOT2=(AM2*YSB(ISEC(IE))/AIZZ(ISEC(IE)))-(AF/AOT(ISEC(IE)))
      FCTOP2=(-AM2*YCT(ISEC(IE))/AIZZ(ISEC(IE)))-(AF/AOT(ISEC(IE)))
      SHEAR1=FORL(2)/AW(ISEC(IE))
      SHEAR2=FORL(5)/AW(ISEC(IE))
      WRITE(12,300)
  300 FORMAT(//2X,' STRESS IN BEAM  SECTION ')
      WRITE(12,302)
  302 FORMAT(2X,34('-'))
      WRITE(12,310)
  310 FORMAT(/2X,'BEAM ',1X,'NODE ',T15,'STEEL TOP',3X,'STEEL BOT',
     1       3X,'CONC. TOP',5X,'SHEAR')
      WRITE(12,200)IE,IN(IE,1),FSTOP1,FSBOT1,FCTOP1,SHEAR1
      WRITE(12,200)IE,IN(IE,2),FSTOP2,FSBOT2,FCTOP2,SHEAR2
  200 FORMAT(/2X,I3,I4,4X,4(D10.4,2X))
  199 CONTINUE
      END
```

```
      SUBROUTINE ELONGATE
      INCLUDE 'COM.FIL'

C*****CALCULATE REACTIONS (P)

      REWIND(9)
      NMBAND=NEQ*MBAND
      READ(9)(S(I),I=1,NMBAND)
      CALL VBMUL(S,R,P,NEQ,MBAND)
      KOUNT=0.
      DATA=0.
      TL=0.
      DO 300 IE=1,NELE
      IF(NTYPE(IE).EQ.1)then
      CALL BBARFOR(IE,EL,elon)
      DATA=DATA+ELON
      TL=TL+EL
      KOUNT=KOUNT+1
      END IF
  300 CONTINUE
      END

      SUBROUTINE DISPL

      INCLUDE 'COM.FIL'
      DIMENSION UG(3,MNODE),FOR(3,MNODE)
      EQUIVALENCE (R(1),UG(1,1)),(P(1),FOR(1,1))

      WRITE(12,100)
  100 FORMAT(/18X,45('*')/)
      WRITE(12,110)
  110 FORMAT(18X,'*              OUTPUT QUANTITIES              *')
      WRITE(12,100)
      WRITE(12,150)
  150 FORMAT(///2X,'NODE',T19,'NODAL DISPLACEMENTE',20X,
     1       'NODAL REACTION')
      WRITE(12,160)
  160 FORMAT(2X,'----',6X,28('-'),12X,28('-'))
      WRITE(12,200)
  200 FORMAT(/2X,' NO.',1X,2(5X,'AXIAL',8X,'SHEAR',7X,'ROTATION',2X)/)
      WRITE(12,250)(I,(UG(J,I),J=1,3),(FOR(K,I),K=1,3),I=1,NNODE)
  250 FORMAT(2X,I3,2X,6D13.4)

C*****MAXIMUM DISPLACEMNT

      DISP=0
      DO 252 I=1,NNODE
      DISP=DMAX1(DISP,DABS(UG(2,I)))
  252 CONTINUE
      WRITE(12,254)DISP
  254 FORMAT(/2X,'MAXIMUM DISPLACMENT:',5X,D10.4)
      WRITE(12,256)TCA
  256 FORMAT(/2X,'INCREAMENT IN CABLE:',5X,D10.4)
```

```
C******CALCULATE ELEMENT DEFORMATION AND FORCES
      WRITE(12,260)
 260  FORMAT(///18X,'******** ELEMENT DEFORMATION AND FORCE ********')
      END

C-------------------------------------------------------------
C     4   SUBROUTINES COMMONLY USED
C-------------------------------------------------------------

      SUBROUTINE BANDWIDTH
      INCLUDE 'COM.FIL'
      NODSEP=0
      DO 200 I=1,NELE
      NODSEP=MAX0(NODSEP,(IABS(IN(I,1)-IN(I,2))))
 200  CONTINUE
      MBAND=(NODSEP+1)*NDOF
      END

C******TRANSPOSE MATRIX

      SUBROUTINE TRANSPOSE(A,AT,NR,NC)
      IMPLICIT DOUBLE PRECISION(A-H,O-Z)
      DIMENSION A(NR,NC),AT(NC,NR)
      DO 100 I=1,NR
      DO 100 J=1,NC
      AT(J,I)=A(I,J)
 100  CONTINUE
      END

C******TWO MATRIXES MULTIPLY

      SUBROUTINE MULT(A,B,C,L,M,N)
      IMPLICIT DOUBLE PRECISION(A-H,O-Z)
      DIMENSION A(L,M),B(M,N),C(L,N)
      DO 10 I=1,L
      DO 20 J=1,N
      C(I,J)=0.0D0
      DO 30 K=1,M
 30   C(I,J)=C(I,J)+A(I,K)*B(K,J)
 20   CONTINUE
 10   CONTINUE
      RETURN
      END



      SUBROUTINE BOUDCOND
      INCLUDE 'COM.FIL'
      DO 100 I=1,NEQ
      IF (NSP(I).EQ.0)GO TO 100
```

```
      II=MBAND*(I-1)+1
      S(II)=(S(II)+1)*1.0D8
      R(I)=R(I)*1.0D8
  100 CONTINUE
      END


       SUBROUTINE EQSOLV (NSIZE,MBAND,S,R)

C*******SUBROUTINE EQSOLV REDUCES AN NEQ * NSIZE BANDED SYSMETRIC
C*******MATRIX.STORED IN VECTOR FORM

       IMPLICIT DOUBLE PRECISION(A-H,O-Z)
       DIMENSION S(1),R(1)

C*******FORWARD REDUCTION OF SYSMETRIC MATRIC

       DO 20 N=1,NSIZE
       DO 20 L=2,MBAND
       NV=(N-1)*MBAND
       IF(S(NV+L).EQ.0) GO TO 20
       I=N+L-1
       IV=(I-1)*MBAND
       C=S(NV+L)/S(NV+1)
       J=0

C*******SUBTRACT C*ROW(N) FROM ROW(I)

       DO 10 K=L,MBAND
       J=J+1
  10   S(IV+J)=S(IV+J)-C*S(NV+K)
       S(NV+L)=C
  20   CONTINUE

C*******FORWARD REDSUCTION OF CONSTANTS

       DO 40 N=1,NSIZE
       DO 30 L=2,MBAND
       NV=(N-1)*MBAND
       IF(S(NV+L).EQ.0.) GO TO 30
       I=N+L-1
       R(I)=R(I)-S(NV+L)*R(N)
  30   CONTINUE
  40   R(N)=R(N)/S(NV+1)

C*******BACK SUBSTITUTION OF R(1) AND STORE IN R(1)

       DO 50 M=2,NSIZE
       N=NSIZE-M+1
       NV=(N-1)*MBAND
       DO 50 L=2,MBAND
       IF(S(NV+L).EQ.0.) GO TO 50
       K=N+L-1
       R(N)=R(N)-S(NV+L)*R(K)
  50   CONTINUE
```

```
      RETURN
      END


      SUBROUTINE STORE(IN,SE,S,NDOF,NPE,MBAND,IE,M)

C******SUBROUTINE STORE ASSEMBLIES THE ELEMENT STIFFNESS MATRIX
C     TO THE SYSTEM STIFFNESS MATRIX

C******IN IS THE ELEMENT CONNECTIVITY ARRAY
C******S IS THE STRUCTURE STIFFNESS ARRAY
C******N IS THE ELEMENT NUMBER

      IMPLICIT DOUBLE PRECISION(A-H,O-Z)
      DIMENSION IN(100,2),SE(M,M),S(1)

C******GO ROW BY ROW DOWN THE ELEMENT STIFFNESS MATRIX

      DO 10 I=1,NPE
      DO 10 J=1,NDOF

C******CALCULATE ELEMENT AND GLOBLE ROW NUMBERS

      IER=(I-1)*NDOF+J
      IGR=IN(IE,I)*NDOF-NDOF+J
      IGRV=(IGR-1)*MBAND

C******GO COLUMN BY COLUMN ACROSS THE ELEMENT MATRIX

      DO 10 K=1,NPE
      DO 10 L=1,NDOF

C******CALCULATE ELEMENT, GLOBAL AND SHIFTED GLOBAL
C     COLUMN NUMBERS


      IEC=(K-1)*NDOF+L
      IGC=IN(IE,K)*NDOF-NDOF+L
      IGCS=IGC-IGR+1
      IRCV=IGRV+IGCS

C******IF SE(IER,IEC) IS ABOVE THE MAIN DIAGONAL ADD
C     IT TO S(IRCV)

  10  IF(IGR.LE.IGC) S(IRCV)=S(IRCV)+SE(IER,IEC)

      RETURN
      END


      SUBROUTINE VBMUL (A,B,C,NEQ,MBAND)
      IMPLICIT DOUBLE PRECISION(A-H,O-Z)
      DIMENSION A(1),B(1),C(1)
      DO 20 I=1,NEQ
      C(I)=0
```

```
      DO 10 J=1,MINO(I,MBAND)
10    C(I)=C(I)+A((I-J)*MBAND+J)*B(I+1-J)
      DO 20 J=2,MINO(MBAND,NEQ-I+1)
20    C(I)=C(I)+A((I-1)*MBAND+J)*B(I+J-1)
      RETURN
      END
```

REFERENCES

1. Szilard, R., "Design of Prestressed Composite Steel Structure." Journal of The Structural Engineering, American Society of Civil Engineers, Volume 85, No. ST9, Proceedings Paper 2262, November, 1959, pp. 97-124.

2. Hoadley, P. G., "The Nature of Prestressed Steel Structures." paper sponsored by Committee on Construction Practices, National Research Council, Highway Research Board, Research Record No. 200, 1967, pp. 11-27.

3. Klaiber, F. W., Dunker, K. F., Sanders, W. W., "Strengthening of Single-Span Steel Beam Bridges." Journal of the Structural Engineering, American Society of Civil Engineers, Volume 108, No. ST12, December, 1982, pp. 2766-2780.

4. Regan, R. S., and Krahl, N. W., "Behavior of Prestressed Composite Beams." Journal of Structural Engineering, American Society of Civil Engineers, Volume 90, No. ST2, April 1964, pp. 131-151.

5. Saadatmanesh, B.M. H., Albrecht, P. and Ayyub, "Guidelines for Flexural Design of Prestressed Composite Beams." Journal of Structural Engineering, American Society of Civil Engineers, Volume 115, No. 11 November, 1989, pp. 2944-2961.

7. Saadatmanesh, H., Albrecht, P. and Ayyub, "Analytical Study of Prestressed Composite Composite Beams." Journal of Structural Engineering, American Society of Civil Engineers, Volume 115, No. 9 September, 1989, pp. 2364-2381.

8. Saadatmanesh, H., Albrecht, P. and Ayyub, "Experimental Study of Prestressed Composite Composite Beams." Journal of Structural Engineering, American Society of Civil Engineers, Volume 115, No. 9 September, 1989, pp. 2348-2363.

9. Sohn, G. S. "Static Strength of Prestressed Composite Steel Girders." Dissertation presented to the University of Maryland, College Park, Maryland, 1988.

10. Troitsky, M., Zielinski, Z., Rabbani, N., "Prestressed-Steel Continuous-Span Girders." Journal of Structural Engineering, American Society of Civil Engineers, Volume 115, No. 5, June 1989, pp. 1357-1370.

11. "DYWIDAG Threadbar Post Tensioning System." Brochure No. 2M DSI#4C, DYWIDAG Systems International, Lincoln Park, N.J. 1984